

INFORMATION TO USERS

This manuscript has been reproduced from the microfilm master. UMI films the text directly from the original or copy submitted. Thus, some thesis and dissertation copies are in typewriter face, while others may be from any type of computer printer.

The quality of this reproduction is dependent upon the quality of the copy submitted. Broken or indistinct print, colored or poor quality illustrations and photographs, print bleedthrough, substandard margins, and improper alignment can adversely affect reproduction.

In the unlikely event that the author did not send UMI a complete manuscript and there are missing pages, these will be noted. Also, if unauthorized copyright material had to be removed, a note will indicate the deletion.

Oversize materials (e.g., maps, drawings, charts) are reproduced by sectioning the original, beginning at the upper left-hand corner and continuing from left to right in equal sections with small overlaps. Each original is also photographed in one exposure and is included in reduced form at the back of the book.

Photographs included in the original manuscript have been reproduced xerographically in this copy. Higher quality 6" x 9" black and white photographic prints are available for any photographs or illustrations appearing in this copy for an additional charge. Contact UMI directly to order.

UMI[®]

Bell & Howell Information and Learning
300 North Zeeb Road, Ann Arbor, MI 48106-1346 USA
800-521-0600

NOTE TO USERS

Page(s) not included in the original manuscript are unavailable from the author or university. The manuscript was microfilmed as received.

ii

This reproduction is the best copy available.

UMI

A New Hybrid Acquisition Scheme for CDMA Systems Employing Short Concatenated Codes

Vijay Doradla

A Thesis
in
The Department
of
Electrical and Computer Engineering

Presented in Partial Fulfillment of the Requirements
for the Degree of Master of Applied Science at
Concordia University
Montréal, Québec, Canada

June 1997

© Vijay Doradla, 1997



National Library
of Canada

Acquisitions and
Bibliographic Services

395 Wellington Street
Ottawa ON K1A 0N4
Canada

Bibliothèque nationale
du Canada

Acquisitions et
services bibliographiques

395, rue Wellington
Ottawa ON K1A 0N4
Canada

Your file *Votre référence*

Our file *Notre référence*

The author has granted a non-exclusive licence allowing the National Library of Canada to reproduce, loan, distribute or sell copies of this thesis in microform, paper or electronic formats.

The author retains ownership of the copyright in this thesis. Neither the thesis nor substantial extracts from it may be printed or otherwise reproduced without the author's permission.

L'auteur a accordé une licence non exclusive permettant à la Bibliothèque nationale du Canada de reproduire, prêter, distribuer ou vendre des copies de cette thèse sous la forme de microfiche/film, de reproduction sur papier ou sur format électronique.

L'auteur conserve la propriété du droit d'auteur qui protège cette thèse. Ni la thèse ni des extraits substantiels de celle-ci ne doivent être imprimés ou autrement reproduits sans son autorisation.

0-612-40211-8

NOTE TO USERS

Page(s) not included in the original manuscript are unavailable from the author or university. The manuscript was microfilmed as received.

ii

This reproduction is the best copy available.

UMI

ABSTRACT

A New Hybrid Acquisition Scheme for CDMA Systems Employing Short Concatenated Codes

Vijay Doradla

With the rapid growth of Personal Wireless Communications in our times and the important role being played by Code Division Multiple Access (CDMA) in the realization of the goals of second generation wireless systems, there is an ever increasing need for the development of better acquisitions techniques along with the study of a variety of techniques. Noting the important role of synchronization in CDMA systems, active research is being carried out to develop synchronization (acquisition+tracking) schemes that suit particular applications.

In the first part of this thesis we propose a New Hybrid Acquisition Scheme for CDMA systems employing Short Concatenated Codes. A new coding scheme using short concatenated codes is presented along with a detailed description of a new hybrid acquisition scheme. Simulation studies of the scheme are performed in a multiple access and additive white gaussian noise environment.

In the second part of the thesis, a Simplified Analytical Model of the scheme is developed using the state transition flow diagram approach and standard signal flow graph reduction techniques. Expressions for the mean and variance of the acquisition along with the probability of detection are developed. Finally the simplified model is studied in a Rayleigh fading channel.

AUM SRI SAI RAM

**To Mom and Dad for their Love and
Encouragement**

and

Anil, my brother for all his Guidance and Support

ACKNOWLEDGEMENTS

At the outset I would like to express my most sincere gratitude to my thesis supervisor, Dr A. K. Elhakeem, for his guidance, support, patience and encouragement during the entire course of this thesis.

Among the others, I would like to thank Rocco with whom I had wonderful technical discussions that helped me broaden my knowledge of the wireless communication field.

My special thanks to the great group of friends I have in Montreal, Venu, Selva, Priya, Poonam, Reena, Vinu, Sriram, Rachit, Manijeh and many more who inspired me during the course of this work.

Finally I would like to express my thanks to my wonderful family, my parents, my brother, Anil and my sister-in-law, Aditi who have always stood besides me helping me with love and encouragement during the entire period of my Masters.

TABLE OF CONTENTS

TABLE OF CONTENTS	vi
LIST OF FIGURES	viii
LIST OF SYMBOLS	xiii
1 Introduction	1
1.1 Spread Spectrum Communications	1
1.2 Direct Sequence Systems (DS)	2
1.3 Frequency Hopping Systems (FH)	3
1.4 Time Hopping Systems (TH)	3
1.5 Chirp Systems	4
1.6 Code Division Multiple Access (CDMA)	4
1.7 Thesis Outline	6
2 Pseudorandom Code Acquisition in Direct Sequence Spread Spectrum Systems	11
2.1 Introduction	12
2.2 Historical Perspective	12
2.2.1 Classification of Detectors for PN code Acquisition	12
2.2.2 Classification of Acquisition Schemes	14
2.3 Serial PN Acquisition System: Single-Dwell	19
2.3.1 Markov Chain Acquisition Model	21
2.3.2 Single Dwell Acquisition Time Performance	23
2.3.3 Evaluation of P_D (Detection probability) and P_{FA} (False alarm probability) in terms of system parameters	26
2.4 Serial PN Acquisition System: Multi-Dwell	30
2.5 PN Synchronization procedures for Non Uniformly Distributed Signal Location	33

2.6	PN Synchronization Using Sequential Detection	35
3	A New Hybrid Acquisition Scheme for CDMA Systems employing Short Concatenated Codes	39
3.1	Introduction	39
3.1.1	Coding for Spread Spectrum Systems	40
3.1.2	Maximal-Length Sequences	40
3.1.3	Gold Codes	43
3.2	A New Hybrid Acquisition Scheme for CDMA Systems	45
3.2.1	Proposed Concatenated Signature Coding Scheme	45
3.2.2	Hybrid Acquisition Scheme for CDMA Systems	47
3.2.3	Simulation Procedure and Performance in a Multiple Access Environment	57
3.2.4	Simulation Results	61
4	Simplified Analytical Model and Performance in a Non Selective Rayleigh Fading Channel	75
4.1	Simplified Analytical Model	75
4.1.1	Mean and Variance of the Acquisition Time	83
4.2	Performance in a Rayleigh Fading Channel	86
4.2.1	Numerical Results and Discussion	89
5	Summary and Conclusions	104
	BIBLIOGRAPHY	108

LIST OF FIGURES

1.1	BPSK Direct Sequence Spread Spectrum transmitter/receiver	8
1.2	Coherent Frequency Hop Spread Spectrum modem	9
1.3	Time Hopping System (a)Transmitter, (b)Receiver	10
2.1	Block Diagram of Detectors for Acquisition Purposes.	15
2.2	A rapid acquisition by sequential estimation (RASE) technique.	17
2.3	Block diagram of Acquisition Schemes.	20
2.4	Block Diagram a of a single dwell PN acquisition system with Non-Coherent detection.	21
2.5	Markov chain model for Single Dwell System	24
2.6	The N-dwell serial synchronization system with half chip search.	31
2.7	Block diagram of an N-dwell time PN acquisition system with Non-Coherent detection.	31
2.8	Non Uniformly distributed signal location and possible sweep strategy.	37
2.9	Serial Sequential Detection PN acquisition systeme with timeout feature	37
2.10	(a): Integrator output with bias voltage absent	38
2.11	(b): Integrator output with bias voltage present.	38
2.12	(c): Integrator outputs with threshold dismissal and test truncation	38
3.1	Linear and Nonlinear code generator configurations	41
3.2	Autocorrelation function of Maximal length sequences	41
3.3	Power Spectral Density of Maximal length sequences	43
3.4	Gold Code Generator	44
3.5	Coding Scheme Structure	47
3.6	Block Diagram of the Proposed Acquisition Scheme	48
3.7	Structure of the Acquisition scheme comprising many Search Scenarios	53

3.8	Processing of the received signal for $CLIMIT=5$	56
3.9	(a) The Shift Register used to generate the Maximal Length Sequences. (b) The Gold Code generator of length 127 ($n=7$)	60
3.10	Mean Acquisition Time versus Number of Users for $\zeta(ZHI)=6$, $CLIMIT=6$ for Hard Decision and Soft Decision Cases and Signal to Noise Ratio's of 0dB, 4dB and 8dB. Chip rate is 1M chips/sec, processing gain = 127.	65
3.11	Probability of Acquisition versus Number of Users for $\zeta(ZHI)=6$, $CLIMIT=6$, SNR's: 0dB and 4dB for Hard Decision Case and SNR's 0dB, 4dB and 8dB for Soft Decision Case. Chip rate is 1M chips/sec, processing gain = 127.	66
3.12	Mean Acquisition Time versus Number of Users for $\zeta(ZHI)=8$, $CLIMIT=6$ for SNR's: 0dB and 4dB for Hard Decision Case, SNR's 0dB, 4dB and 8dB for Soft Decision Case. Chip rate is 1M chips/sec, processing gain = 127.	67
3.13	Probability of Acquisition versus Number of Users for $\zeta(ZHI)=8$, $CLIMIT=6$, SNR's: 4dB and 8dB for Hard Decision and SNR's: 0dB, 4dB and 8dB for Soft Decision Case. Chip rate is 1M chips/sec, processing gain = 127.	68
3.14	Mean Acquisition versus Number of Users for $ZHI=10$, $CLIMIT=6$, SNR's: 0dB, 4dB and 8dB for Hard Decision Case and SNR's: 0dB and 4dB for the Soft Decision Case. Chip rate is 1M chips/sec, processing gain = 127.	69
3.15	Probability of Acquisition versus Number of Users for $\zeta(ZHI)=10$, $CLIMIT=6$, SNR's: 4dB and 8dB for Hard Decision Case and SNR's 0dB, 4dB and 8dB for the Soft Decision Case. Chip rate is 1M chips/sec, processing gain = 127.	70

3.16	Mean Acquisition Time versus Number of Users for $\zeta(ZHI) = 12, CLIMIT = 6$, SNR's: 4dB and 8dB for Hard Decision Case and SNR's: 0dB and 4dB for Soft Decision Case. Chip rate is 1M chips/sec, processing gain = 127.	71
3.17	Probability of Acquisition versus Number of Users for $\zeta(ZHI) = 12, CLIMIT = 6$, SNR's 4dB and 8dB for Hard Decision case and SNR's: 0dB and 4dB for Soft Decision Case. Chip rate is 1M chips/sec, processing gain = 127.	72
3.18	Soft Decision Comparison of the Mean Acquisition Time versus Number of Users for $\zeta(ZHI) = 6, 8, 10, 12$ and $CLIMIT = 6$ for Signal to Noise Ratio (SNR)=4dB. Chip rate is 1M chips/sec, processing gain = 127.	73
3.19	Soft Decision comparison of the Probability of Acquisition versus Number of Users for $\zeta(ZHI) = 6, 8, 10, 12$ and $CLIMIT = 6$ for Signal to Noise Ratio (SNR)= 4dB. Chip rate is 1M chips/sec, processing gain = 127.	74
4.1	Block Diagram of the Simplified Acquisition Scheme for a Fading Channel	77
4.2	I-Q Matched Filter detector structure	78
4.3	Structure of the Matched Filter Correlator	78
4.4	Circular State Transition Diagram of the Simplified Acquisition Scheme for a Rayleigh Fading channel	80
4.5	Mean Acquisition Time versus SNR/Chip (in dB) in a Rayleigh Fading channel for subcode lengths (M, in chips) 7, 15, 31, 63, 127, 255, 511, Normalized Threshold (ZHI) $\zeta = 3, CLIMIT = 6$. The number of subcodes per user Basic code is 6, Chip rate=1Mchips/sec	92

4.6	Mean Acquisition Time versus SNR/Chip (in dB) in a Rayleigh Fading channel for subcode lengths (M , in chips) 127, 255, 511, Normalized Threshold (ZHI) $\zeta = 4$, $CLIMIT = 6$. The number of subcodes per user Basic code is 6, Chip rate=1Mchips/sec	93
4.7	Mean Acquisition Time versus SNR/Chip (in dB) in a Rayleigh Fading channel for subcode lengths (M , in chips) 127, 255, 511, Normalized Threshold (ZHI) $\zeta = 6$, $CLIMIT = 6$. The number of subcodes per user Basic code is 6, Chip rate=1Mchips/sec	94
4.8	Probability of Detection of Subcode versus SNR/Chip (in dB) for Subcode length(in chips) $M=7, 15, 31, 63, 127, 255, 511$. The Chip rate =1M chips/sec.	95
4.9	Mean Acquisition Time versus SNR/Chip (in dB) in a Rayleigh Fading channel for subcode lengths (M , in chips) 127, Normalized Threshold (ZHI) $\zeta = 3, 4, 6$, $CLIMIT = 6$. The number of subcodes per user Basic code is 6, Chip rate=1Mchips/sec	96
4.10	Overall Probability of Detection of user code versus SNR/Chip (in dB). The subcode length, $M = 127$ chips, Normalized Threshold $\zeta = 3, 4, 6$, $CLIMIT= 6$	97
4.11	Mean Acquisition Time \bar{T}_{ACQ} versus SNR/Chip (in dB) for Normalized Threshold (ZHI) $\zeta =3, 4, 6$. $CLIMIT = 6$, Subcode length $M=255$ chips	98
4.12	Overall Probability of Detection of user code versus SNR/Chip (in dB). The subcode length, $M = 255$ chips, Normalized Threshold $\zeta = 3, 4, 6$, $CLIMIT= 6$	99
4.13	Mean Acquisition Time \bar{T}_{ACQ} versus SNR/Chip (in dB) for Normalized Threshold (ZHI) $\zeta =3, 4, 6$. $CLIMIT = 6$, Subcode length $M=511$ chips	100

4.14	Overall Probability of Detection of user code versus SNR/Chip (in dB). The subcode length, $M = 511$ chips, Normalized Threshold $\zeta = 3, 4, 6$, $CLIMIT = 6$	101
4.15	σ_{Acq} Variance of the Acquisition Time versus SNR/Chip (in dB) for subcode lengths $M=127, 255, 511$ chips, $CLIMIT = 6$, Normalized Threshold (ZHI) $\zeta = 3$ Chip rate=1M chips/sec.	102
4.16	σ_{Acq} Variance of the Acquisition Time versus SNR/Chip (in dB) for subcode lengths $M=127, 255, 511$ chips, $CLIMIT = 6$, Normalized Threshold (ZHI) $\zeta = 4$ Chip rate=1M chips/sec.	103

LIST OF SYMBOLS

T_s	Symbol period
T_c	Chip period
PN	Pseudo Noise
Chip	Pulses of code sequence
RASE	Rapid Acquisition by Sequential Estimation
RARASE	Recursion-Aided RASE
SWI	Sync-worthiness indicator
τ_d	Dwell time
P_D	Probability of Detection
P_{FA}	Probability of False Alarm
$Q(x)$	Gaussian probability integral
T_u	Uncertainty time
q	Number of possible code alignments
T_{ACQ}	Acquisition time
σ_{ACQ}^2	Variance of acquisition time
\bar{T}_{ACQ}	Mean Acquisition time
$\theta_{bb'}(k)$	Discrete periodic cross-correlation function
$\theta_b(k)$	Discrete periodic auto-correlation function
$R_c(\tau)$	Auto-correlation function
$R_{cc'}(\tau)$	Cross-correlation function
$S_c(f)$	Power spectral density function
Subcode	Gold Code of 127 chips
Basic Code	User specific sequence of N subcodes
CLIMIT	Subcode count limit
PIVCT	Pivot count
\overline{AC}	Mean Accumulator Value

ζ	Normalized threshold value
C	Sequential subcode count
X	Accumulator weight
T_{search}	Time duration of a search scenario
A_k	Amplitude of the k^{th} user
AWGN	Additive White Gaussian Noise
$n(t)$	AWGN
ϕ_k	Phase of k^{th} user
SNR	Signal to Noise Ratio
Δ	Phase update size
σ_n^2	Variance of noise
Z_I	Output of in-phase branch of matched filter
Z_Q	Output of quadrature branch of matched filter
J	False alarm penalty
$P_{D-Overall}$	Overall probability of detection
$P_{FA-Overall}$	Overall probability of false alarm

Chapter 1

Introduction

In the following chapter, a brief introduction to the Spread Spectrum Systems—the Direct Sequence, Frequency Hopping, Time Hopping, Chirp will be presented. This will be followed by a brief summary of the layout of this thesis.

1.1 Spread Spectrum Communications

Spread Spectrum Communications is a modulation and demodulation technique in which the transmission bandwidth employed is much greater than the minimum bandwidth required to transmit the digital information. A number of modulation techniques use a transmission bandwidth much larger than the minimum required for data transmission, but are not spread spectrum modulations. To be classified as a spread spectrum system, the modem must have the following characteristics.

1. Bandwidth occupancy by the transmitted signal must be much larger than the information bit rate.
2. Demodulation must be accomplished in part by correlation of the received signal with a replica of the signal used in the transmitter to despread the information signal.

3. The codes used for spreading the signal must be maximal length sequences, which are a type of pseudo noise codes (PN sequences).

Some of the salient features of spread spectrum techniques are

- Interference rejection capability.
- Multiple access.
- Improved spectral efficiency.

Spread spectrum techniques may be broadly classified as

1. Direct Sequence (DS)
2. Frequency Hopping (FH)
3. Time Hopping (TH)
4. Chirp
5. Hybrid Systems (which combine two or more of the above techniques)

1.2 Direct Sequence Systems (DS)

Bandwidth spreading by direct modulation of a data modulated carrier by a wideband spreading signal or code is called Direct Sequence (DS) spread spectrum. The wideband spreading signal or code is a baseband pulse (of normalized amplitudes of +1 or -1), representing pseudorandom sequences generated by pseudorandom code generators (see chapt 3). Pseudorandom sequences are long binary sequences (of ones and zeros) at bit rates much higher than the bit rate of the information sequence. Figure 1.1 (page 6), shows a DS system with binary phase modulation. The processing gain of the DS system (processing gain is the performance improvement achieved through use of spread spectrum techniques over techniques without spread

spectrum) is equal to the number of chips (pulses of code sequence) in a symbol interval

$$G_p = \frac{T_s}{T_c}$$

where T_s and T_c are the data symbol period and chip period respectively.

1.3 Frequency Hopping Systems (FH)

In this technique the spectrum of the data modulated carrier is widened by changing the frequency of the carrier periodically. Typically, each carrier frequency is chosen from a set of frequencies which are spaced approximately the width of the data modulation bandwidth apart. The spreading code in this case does not directly modulate the data-modulated carrier but is instead used to control the sequence of carrier frequencies. In the receiver, the frequency hopping is removed by down converting (mixing) with a local oscillator signal which hops synchronously with the received signal, as illustrated in Figure 1.2 (page 7)

Frequency hopping may be classified as fast or slow depending upon whether the hop frequency band changes many times per symbol (FFH) or the hop frequency band changes more slowly than the symbols coming out of the data modulator. The processing gain in a frequency hopping spread spectrum system is equal to

$$G_p = \frac{W_s}{W_d}$$

where W_s is the total FH band and W_d is the data bandwidth.

1.4 Time Hopping Systems (TH)

In this technique, the code sequence is used to key the transmitter on and off. The transmitter on and off times are therefore pseudorandom. Time hopping Figure 1.3 (page 8) may be used to aid in reducing interference between systems in time-division multiple access where stringent timing requirements must be placed on the

overall system to ensure minimum overlap between transmitters. One of the primary advantages offered by this type of spread spectrum communications in interference rejection is the reduced duty cycle; i.e., an interfering transmitter to be really effective would be forced to transmit continuously. Thus the power required by a reduced duty cycle time hopper would be less than that of the interfering transmitter by a factor equal to the signal duty cycle. Time hopping systems are very useful for Ranging, multiple access because of the relative simplicity of generating the transmitted signal.

1.5 Chirp Systems

This technique is one of the only types of spread spectrum modulation that does not necessarily employ coding but does use a wider bandwidth than the minimum required, so that it can realize the processing gain. This form of spread spectrum has found its main application in radar and is also applied in communications. Chirp transmissions are characterized by pulsed RF signals whose frequency varies in some known way during each pulse period. The advantage of these transmissions for radar is that significant power reduction is possible. The receiver used for chirp signals is a matched filter, matched to the angular rate of change of the transmitted frequency-swept signal.

1.6 Code Division Multiple Access (CDMA)

The inherent interference rejection capability, high spectral efficiency and multiple access capability of spread spectrum systems eventually lead to the development of CDMA. Code Division Multiple Access (or Spread Spectrum Multiple Access) is a new and promising multiple access system for the Second Generation Wireless communication era. In a CDMA system, all users transmit data on the same bandwidth.

Each user is assigned a unique spreading sequence (signature sequence) $s_k(t)$.

Some major attributes of DS/CDMA are

1. Universal frequency reuse.
2. Fast and accurate power control.
3. Constructive combining of multipath propagated components by means of a RAKE receiver.
4. Soft handoff between contiguous-cell base stations using the same RAKE receiver.
5. Autonomous capacity increase for variable rate speech or data transmission.
6. Natural and seamless exploitation of sectorized antennas and adaptive beamforming.
7. Capacity increase with forward error-correcting (FEC) coding without overhead penalty.

Some of the important components of the DS/CDMA system are

- System Features:
 - Frequency assignment.
 - System Pilot Acquisition.
 - Mobile station assisted soft handoff.
 - Variable data rate Vocoder.
- Link waveform:
 - Forward Link Waveform.
 - Reverse Link Waveform.

- Network and Control:
 - CDMA Power Control.
 - The Sync Channel.
 - Framing and Signaling.
 - Service Options.
 - Authentication, Encryption and Privacy.

- System Functional Description:
 - MTSO Functions.
 - CDMA Equipment Design.
 - Dual Mode Mobile Station/Portable.

There are a number of references in literature about this new and promising technology. A few are listed in the bibliography [1] -[7].

1.7 Thesis Outline

The information and work presented in this thesis is organized as follows:

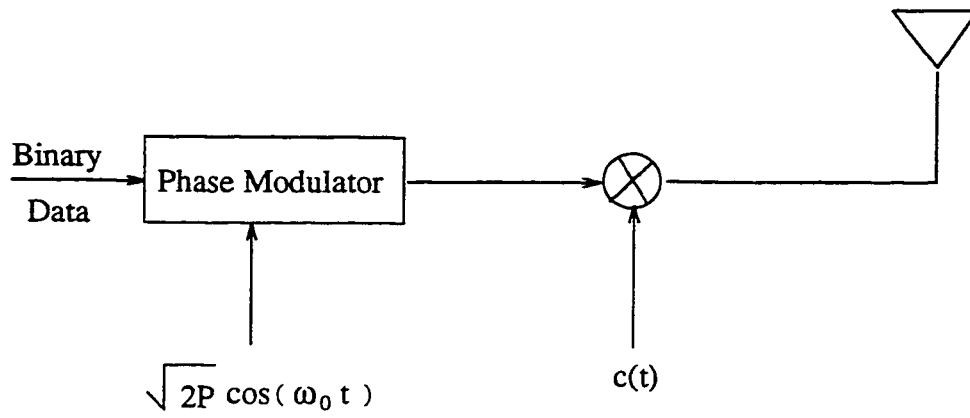
Chapter 2 recounts some of the acquisition schemes used for PN synchronization. A detailed discussion of the Single Dwell serial search scheme is presented and brief discussions of the Multiple Dwell; PN search procedures for Non Uniformly Distributed signal location; and the Sequential Detection technique are presented.

Chapter 3 begins with an introduction to Maximal Pseudonoise sequences and Gold Codes. This is followed by a detailed presentation of the New Hybrid Acquisition Scheme for CDMA systems. In the end Simulation results of the scheme are presented.

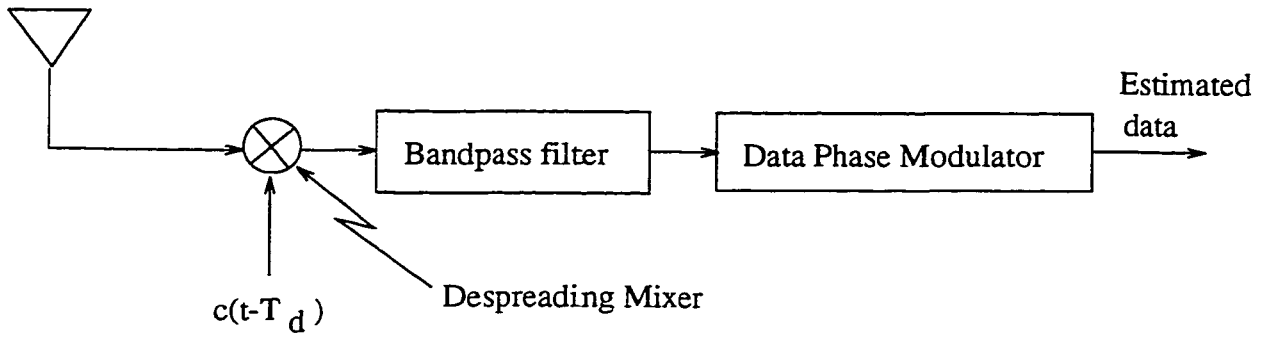
In Chapter 4 we present a Simplified Analytical Model of the proposed acquisition scheme. Expressions for Mean and Variance of the acquisition time for this

simplified model are derived. Finally this Simplified Model is studied in a Rayleigh Fading environment.

Chapter 5 summarizes the work done as part of this thesis and sums up with certain conclusions.

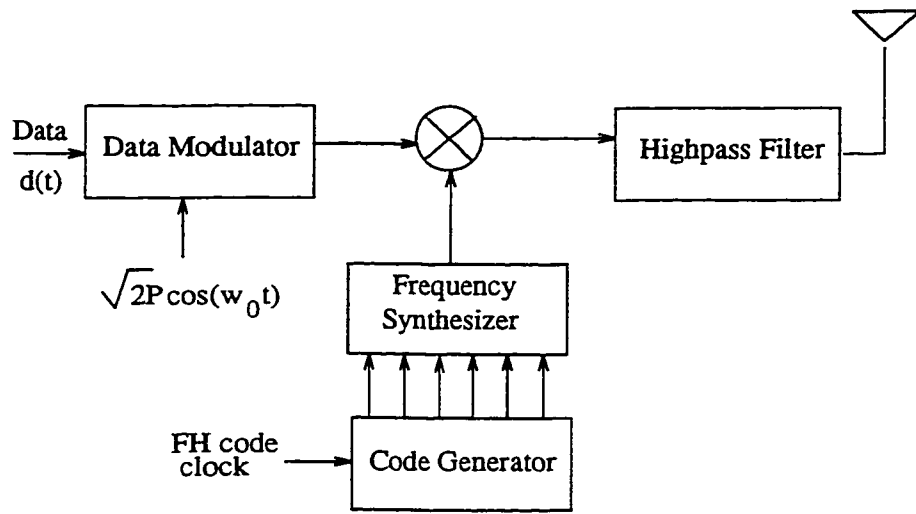


(a) Transmitter

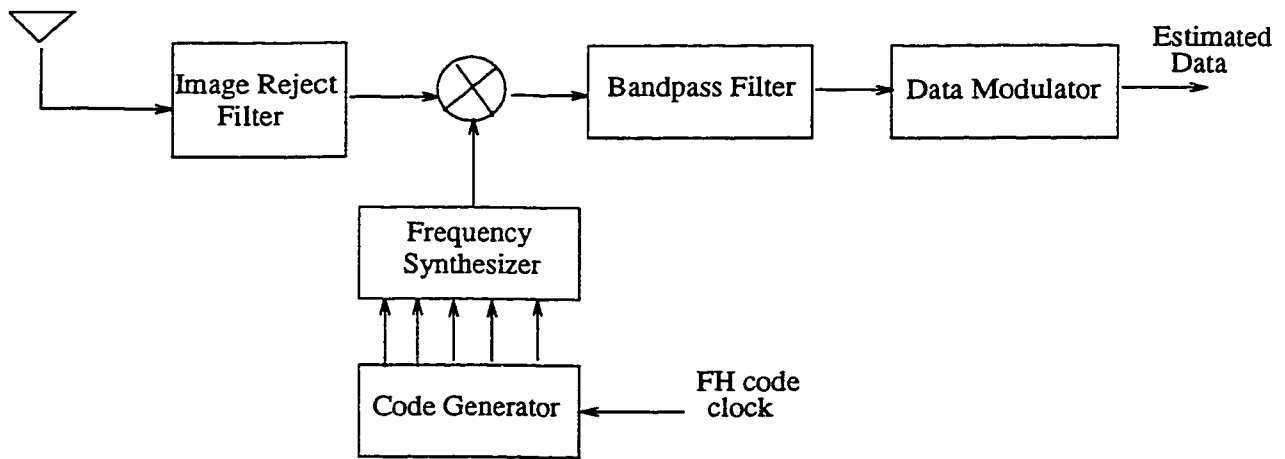


(b) Receiver

Figure 1.1: BPSK Direct Sequence Spread Spectrum transmitter/receiver

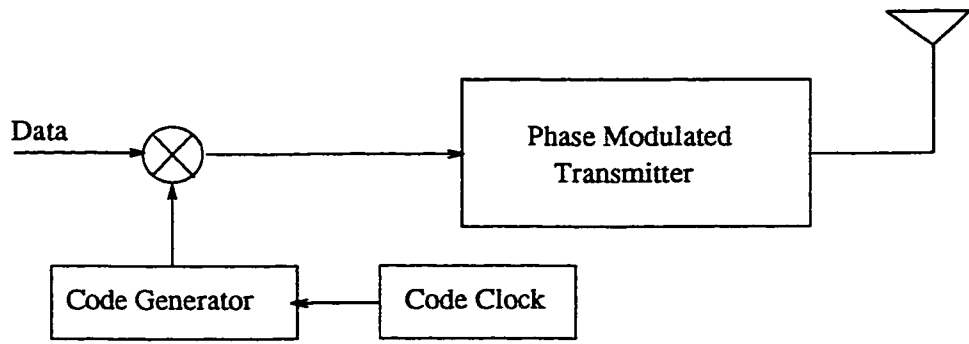


(a) Transmitter

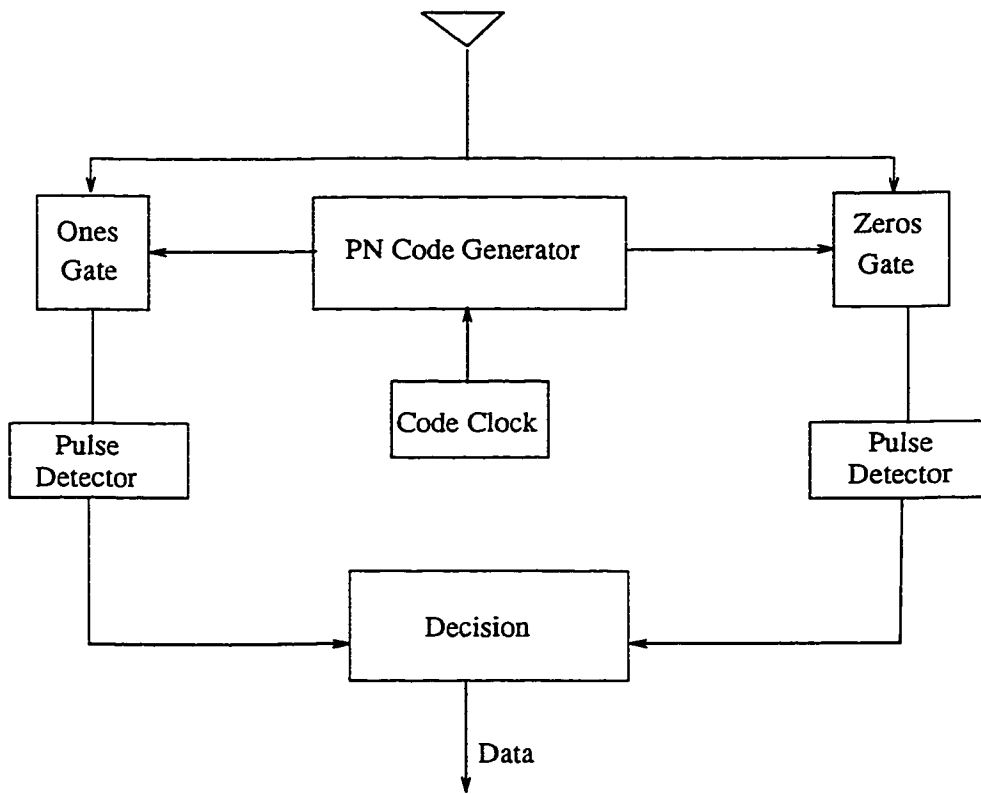


(b) Receiver

Figure 1.2: Coherent Frequency Hop Spread Spectrum modem



(a)



(b)

Figure 1.3: Time Hopping System (a)Transmitter, (b)Receiver

Chapter 2

Pseudorandom Code Acquisition in Direct Sequence Spread Spectrum Systems

This chapter begins with an introduction to the different types of Detectors for the purpose of acquisition and the various acquisition schemes present in the literature. A detailed description of the Single Dwell Serial Search will be developed using the Markov Chain Acquisition Model. The Acquisition Time Performance of the single dwell search scheme will be discussed. This is followed by a brief look at the various other search schemes, the Multiple Dwell Serial Search— as an extension of the single dwell search scheme, PN synchronization search procedures for a Non Uniformly Distributed signal location, and finally PN synchronization using Sequential Detection. A number of papers were consulted during the course of this work, a few relevant papers are [8] -[17].

2.1 Introduction

The primary function of a direct sequence (DS) spread spectrum receiver is to despread the received pseudonoise (PN) code. The process involves generating a local replica of the PN code in the receiver and then synchronizing this local PN signal to the received one. The process of synchronizing the local and received PN signals is accomplished in two stages. Initially, a coarse alignment of the two PN signals is produced to within a small residual relative timing offset. This process of bringing the two codes into coarse alignment is referred to as *PN Acquisition*. Once the incoming PN code has been acquired, a fine synchronization system takes over and continuously maintains the best possible waveform alignment by means of a closed loop operation. The process of maintaining the two codes in fine synchronism is referred to as *PN Tracking*.

2.2 Historical Perspective

2.2.1 Classification of Detectors for PN code Acquisition

The common denominator among almost all methods in the literature discussing PN acquisition techniques is that the received and local PN signals are first multiplied and integrated to produce a measure of correlation between the two. This correlation measure is then processed by a suitable detector/decision rule and search strategy to decide whether the two codes are in synchronism and what to do if they are not. The differences between the various schemes depends on

1. The type of detector (and the decision strategy) used.
2. The nature of the search algorithm that acts on the detector outputs to reach the final verdict.

The broadest categorization of detectors in any PN acquisition system is Coherent and Non-Coherent. By far the most common found in acquisition systems for DS/SS receivers is the non coherent detector. The reason why the Non-Coherent detector is most commonly found is because the despreading operation typically takes place ahead of the carrier synchronization function. Another convenient classification of detectors for PN acquisition schemes is depending upon whether they are the *fixed* or *variable* integration time type. Within the category of *fixed* integration time detectors, one can further subdivide them into single dwell types [18], [19] and multiple dwell types [20] depending, respectively, upon whether the detector's decision is made on the basis of a single (suitably processed) fixed time observation of received signal plus noise or many such observations (not necessarily independent of one another). Depending upon the duration of the observation, or equivalently, the time allotted to make a decision, relative to the PN code period, single dwell time detectors can be further differentiated according to whether they utilize partial or full period code correlation. The multiple dwell detectors differ from one another in the way in which the additional observations are used to verify the temporary decision made based on the first observation alone.

Since all of the detector structures of interest make decisions based on a threshold comparison test of one form or another, following a threshold exceedance of the first dwell (integration) output, the additional dwells in combination with threshold testing are used in accordance with a specified *verification algorithm*, to produce a final decision on whether the code phase position under test corresponds to true synchronization. This verification mode of operation of the detector structure typically falls into one of two categories. In the type of multiple dwell acquisition system discussed by [20], a code phase position is immediately rejected or dismissed as corresponding to an incorrect synchronization condition as soon as any dwell output fails to satisfy its threshold exceedance test. All other types of verification modes of operation, often referred to as search/lock strategies [21], employ algorithms which

require repeated threshold testing of given dwell output or use a majority logic type of decision on the total set of multiple dwell threshold tests.

Variable integration time detectors are the types where the dwell time (which is the time for a continuously integrated stochastic process to exceed a threshold) is a random variable. The various PN acquisition systems that contain a variable integration time detector typically employ the classical method of *sequential detection*.

The next classification of detector structures is in accordance with the rate at which decisions are made on each code phase position under test. High decision rate detectors, such as those used in “matched filter” PN acquisition systems, refer to those structures that make their decisions on the out-of-sync code phase offsets between incoming and local codes at the PN code chip rate or an integer multiple of it. Low decision rate detectors, which employ active correlation, make these same decisions at a rate significantly slower than the code chip rate.

For the purpose of completion of this discussion of detector types, one can categorize them according to the criterion used for deciding between in-sync and out of sync hypotheses, e.g., Bayes, Neyman-Person etc.

Figure 2.1 is a summary of the classification of the structure of the detectors used for PN acquisition purposes.

2.2.2 Classification of Acquisition Schemes

Acquisition schemes are classified according to the search strategy. The simplest of the search techniques is the “*maximum-likelihood*” algorithm. The algorithm basically requires that the input PN signal be correlated with all possible code positions (or even fractional code positions) of the local PN code replica. The correlations are assumed to be performed in parallel and the corresponding detector outputs all pertain to the identical observation of received signal plus noise. The correct PN alignment is chosen as that local code phase position which produces the

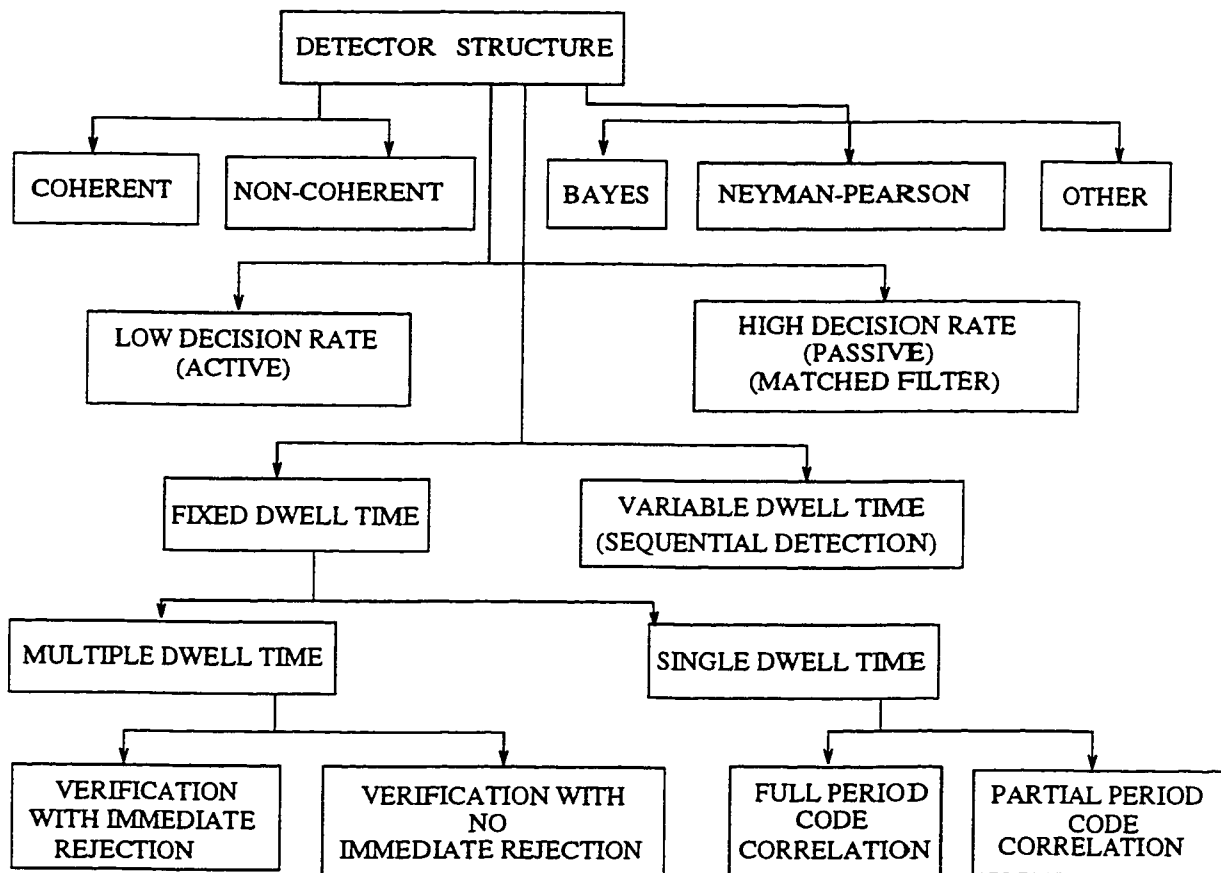


Figure 2.1: Block Diagram of Detectors for Acquisition Purposes.

maximum detector output. The maximum likelihood algorithm can be implemented in a serial fashion. Here the input PN signal is serially correlated with all possible code positions of the local PN code replica and the corresponding detector outputs are stored. At the end of the test, the correct PN alignment is chosen as that local code phase position which produces the maximum detector output. Such a brute force acquisition procedure, whether implemented in parallel or serial form, has the advantage that a definite decision will be made after only a single examination of all code phase positions, or a single search through the entire code period. Thus, multiple examination of each code phase position or multiple searches through the code are avoided by this procedure. The obvious disadvantage is that a decision cannot be reached unless every code phase position has been examined, i.e., the entire code period has been searched. For long codes, complexity of the parallel implementation or the time to search the entire code to reach a synchronization decision in the serial version is often prohibitive.

Another scheme introduced by Ward [22] is based on a sequential estimation of the shift register states of the PN generator. The RASE (Rapid Acquisition by Sequential Estimation) system makes its best estimate of the first n received PN code chips (n represents the number of stages of the code generator) and loads the receiver sequence generator with that estimate, thus defining a particular initial condition (starting state) from which the generator begins its operation. Since a PN sequence has the property that the next combination of register states depends only on the present combination of states, if indeed this present combination is correct, all the following states can be predicted based on the knowledge of only this initial condition. Such is the manner in which the RASE maintains synchronization once it has been determined that the n detected chips provide the correct starting position, i.e., from that point on it no longer needs estimates of the input code chips. Until such time, however, the local PN shift register must be periodically, at a rate determined by an examination period generator, loaded with new estimates where

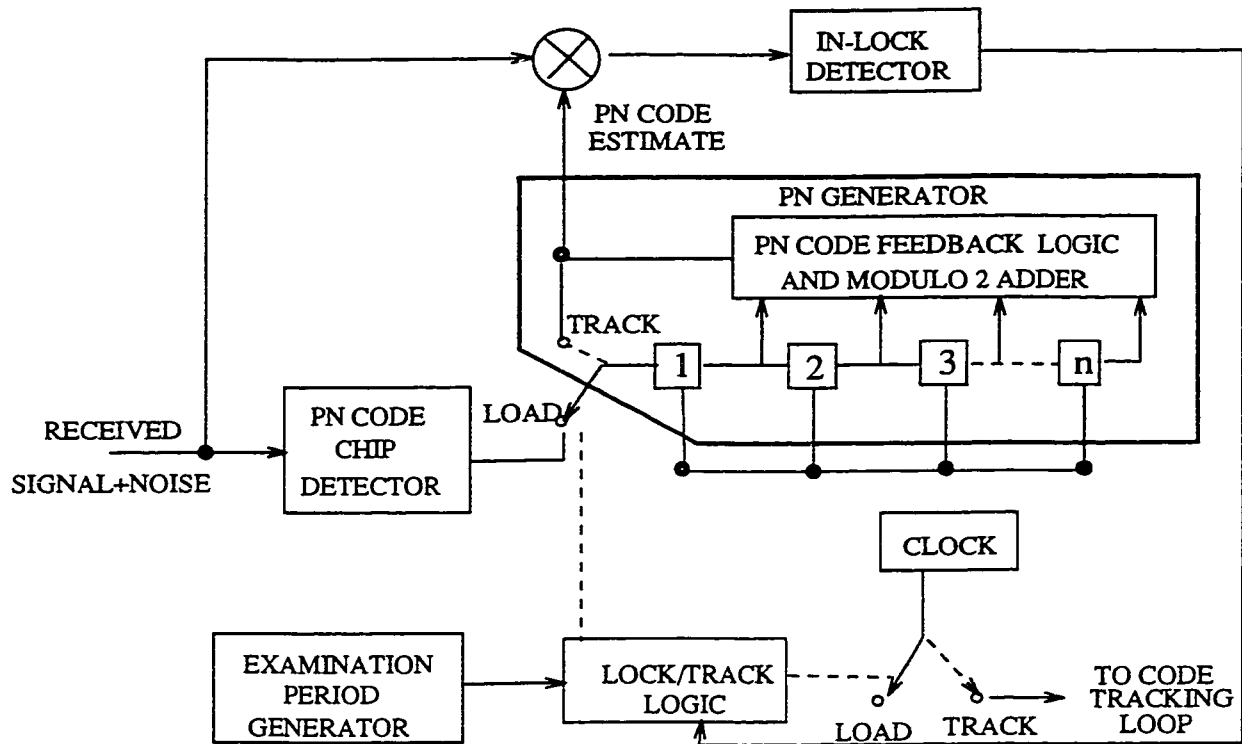


Figure 2.2: A rapid acquisition by sequential estimation (RASE) technique.

the decision when to stop the reload procedure is based upon a threshold crossing of an in-lock detector. The test-statistic upon which this in-lock detector makes its decision is the cross-correlation of the input code with that produced by the local PN generator whose shift register contents correspond to the present estimate of the input state. Once it is determined that a correct estimate was made, the lock detector threshold crossing inhibits further reloading of the local shift register. This register is then closed within the tracking loop which is responsible for maintaining code phase from that time on. Figure 2.2 illustrates the schematic of the RASE technique.

A modification of the RASE system is the RARASE (Recursion-Aided Rapid Acquisition Sequential Estimation). Here additional estimated code chips are summed to form a sync-worthiness indicator(SWI) which is used along with the inlock indicator to determine when the n-stage shift register should shift from a reload to a

tracking condition. When compared with the basic RASE system, which uses only a simple in-lock detector, the RARASE system was shown to achieve an acquisition time reduction by a factor of 7.5 for a PN code length of $2^{15} - 1$.

One of the earliest references of serial synchronization of pseudonoise signals was reported by Sage [23]. In this version, a serial search was performed by linearly varying the time difference between the PN modulation on the incoming carrier and the PN waveform generated at the receiver with a continuous decision process determining when synchronization was achieved. Such a system is also referred to in the literature as a “*sliding correlator*” PN acquisition circuit. Since the test for synchronization was based on the crossing of a threshold by the output of the detector, when compared with the serial realization of the maximum-likelihood technique discussed earlier, this scheme trades off shorter acquisition time against reduced accuracy in the detection of synchronization.

In recent years, the trend has been to accomplish the variation of the time difference between the incoming and local PN waveforms by a discrete stepping process wherein the phase of the local PN code is, at uniform increment in time, advanced (or retarded) by fixed amount which is typically a fraction of a chip. This time discrete sweep of the uncertainty region can be accomplished by a uniform search from one end of the region to the other, as in the case of no *a-priori* information about the received PN code phase, or by a non-uniform search typically starting in the region of highest code phase certainty and expanding as a function of time to regions of lesser certainty.

We can continue on the classification of search strategies by distinguishing two different philosophies with regard to the time elapsed before reaching the final acquisition state. In the first case the search is allowed to proceed as long as it is necessary to achieve acquisition with a given fidelity criterion. Such serial search techniques are classified as having “non limited” permitted acquisition time and are typically employed in applications where information modulation is always

present in the received waveform. Serial search strategies with “limited” permitted acquisition time are characteristic of DS/SS systems where information modulation commences to be transmitted only after PN code acquisition has been ensured. In such applications, a fixed time is usually allotted to achieve code acquisition, and furthermore this achievement must be accomplished with high probability.

The final classification of serial search strategies is in accordance with the way in which the false alarm event is handled. False alarm in serial search PN code acquisition occurs when the detector erroneously decides that an in-sync condition has occurred and proceeds to direct the appropriate logic circuitry to initiate PN code tracking. Under normal circumstances, an erroneous entry into the tracking mode of operation will be detected by the code loop lock detector, and after a given amount of time (referred to as the *false alarm penalty time*), the system will return to the acquisition mode and continue searching where it last left off. Such a recoverable false alarm state is referred to as a “returning state”. Sometimes, an entry into the false alarm state is catastrophic in that the system cannot recover from this event. In this instance code acquisition is completely lost and thus this type of false alarm state is referred to as “absorbing”. Figure 3.6 is a brief summary of the different acquisition techniques.

2.3 Serial PN Acquisition System: Single-Dwell

A simple model of a single dwell serial PN acquisition system is illustrated in Figure 2.4. The model employs a standard type, Non-Coherent (square-law) detector. Briefly, the received signal plus noise is actively correlated with a local replica of the PN code and then passed through a bandpass filter. The output of the filter is then square-law envelope detected with the detector output being integrated for a fixed time duration, τ_d (the dwell time), and then compared to a preset threshold.

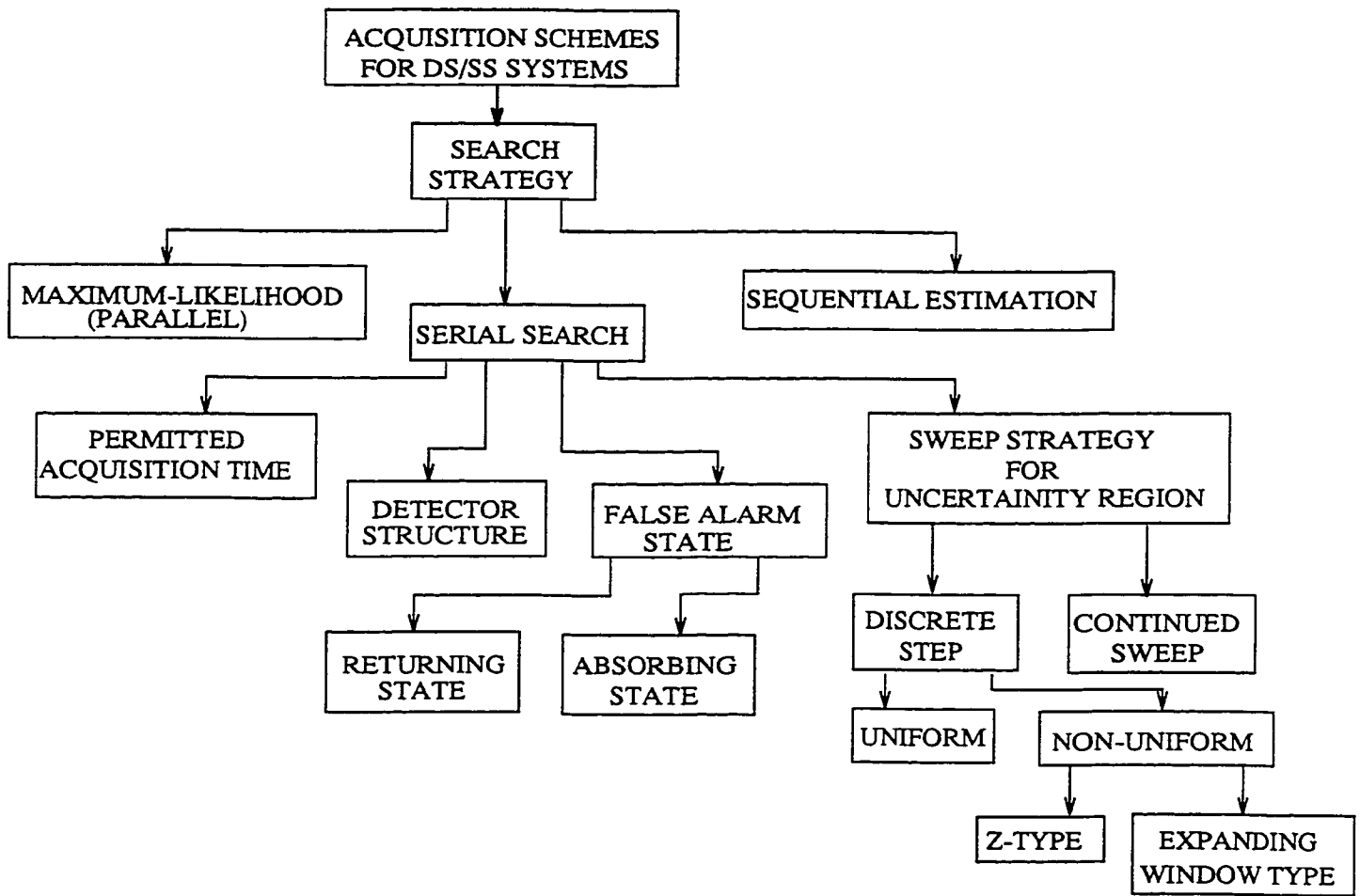


Figure 2.3: Block diagram of Acquisition Schemes.

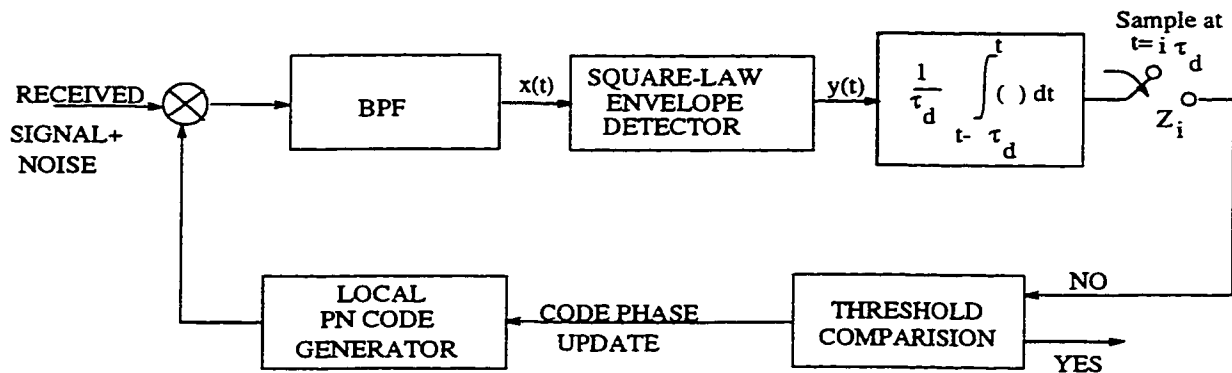


Figure 2.4: Block Diagram a of a single dwell PN acquisition system with Non-Coherent detection.

2.3.1 Markov Chain Acquisition Model

The markovian nature of the acquisition process results from how the detector output is processed. If the detector output is above the preset threshold, then a *hit* is declared. If this hit actually represents a true hit (i.e., the correct code phase has been determined), then the system has officially acquired and the search comes to an end. If the hit is a false alarm, then the verification process cannot be consummated and the search must continue. In general the verification is characterized by an extended dwell time (e.g., $K\tau_d$, $K \gg 1$) assumed to be fixed and an entering into the code tracking loop mode. Since a true hit corresponds to a single code phase position, which can occur only once per search through the code, the time interval $K\tau_d$ sec can be regarded as the *Penalty time* associated when a false alarm is declared. If the detector output falls below the preset threshold, then the local PN code generator steps to its next position and the search proceeds. Thus, at each test position, one of the two events can occur, namely, a false alarm i.e., an indication that acquisition has occurred when the PN codes are actually misaligned or no false alarm. The former event can occur with a probability of P_{FA} whereas the latter can occur with a probability of $(1-P_{FA})$ —hence the Markov chain model. Furthermore, at the true code phase position, either a correct detection can happen, i.e., an indication that acquisition has occurred when the PN codes are indeed

aligned, with probability P_D , or no detection occurs, with probability $(1-P_D)$. In the absence of any a-priori information regarding the true code phase position, the uncertainty in misalignment between the received PN code and the local replica of it could be as much as a full code period. For long PN codes, the corresponding time uncertainty to be resolved could typically be quite large. In order to represent a reasonable compromise between the time required to search through this code phase uncertainty region and the accuracy within which the final alignment position is determined, the amount by which the local PN code generator is stepped in position as the search proceeds must be judiciously chosen. It is typical in practise to require that the received and the local PN code signals be aligned to within one-half a code chip period $(T_c)/2$ before relinquishing control to the fine synchronization system (tracking loop). In accordance with this requirement, the time delay of the local PN code signal would be retarded (or advanced) in discrete steps of one half a chip period and a check for acquisition made after each step. If T_u represents the uncertainty time to be resolved and $T_u = N_u T_c$, then $q = 2N_u$ would be the number of possible code alignments (these are referred to as *cells*) to be examined during each search through the uncertainty region.

The time to declare a true hit, T_{ACQ} (which is generally referred to as the *Acquisition Time*), is a random variable and generally depends upon the initial code phase position of the local PN generator relative to that of the received code. The probability density function gives a complete statistical description of this random variable. The determination of the PDF would ultimately allow computation of the probability of successful synchronization for the single dwell serial synchronization system, but one is often content with measuring performance in terms of the first two moments of the PDF of T_{ACQ} namely the *mean* acquisition time \bar{T}_{ACQ} , and the acquisition time *variance* σ_{ACQ}^2 .

2.3.2 Single Dwell Acquisition Time Performace

In the following presentation of the acquisition time performance of a single dwell system, it will be assumed, for the sake of simplicity, that no code doppler is present in the received signal and that the probability P_D is constant (i.e., time invariant) which is equivalent to assuming that only one cell corresponds to a “correct” code alignment. In the absence of *a-priori* knowledge concerning the relative code phase position of the received and locally generated codes, the local PN generator is assumed to start the search at any code phase position with equal probability. Stated mathematically, the probability P_1 of having the signal present (true hit) in the first cell searched is $1/q$ and the probability of not being present there is $1 - 1/q$. For example, if the number of code chips to be searched is denoted by N_u and the search proceeds in half chip increments, then the number of cells to be searched is $q = 2N_u$ and $P_1 = \frac{1}{2N_u}$. Figure 2.5 illustrates the generating function flow graph for the q -state Markov chain which characterizes the acquisition process of the single dwell system. As is customary in such flow graphs, each branch is labelled with the product of the transition probability associated with going from the branch to the node at its terminating end, and an integer power of a parameter denoted by z . The parameter z is used to mark time as one proceeds through the graph and its power represents the number of time units (dwell times) spent in traversing that branch. Furthermore, the sum of the branch probabilities (letting $z = 1$) emanating from each node equals unity.

One can show, using standard signal flow graph reduction techniques [24], [25] that the generating function is given by

$$U(z) = \frac{(1 - \beta)z}{1 - \beta z H^{q-1}(z)} \left(\frac{1}{q} \sum_{i=0}^{q-1} H^i(z) \right) \quad (2.1)$$

where $\beta = 1 - P_D$ and $H(z) = P_{FA}z^{k+1} + (1 - P_{FA})z$.

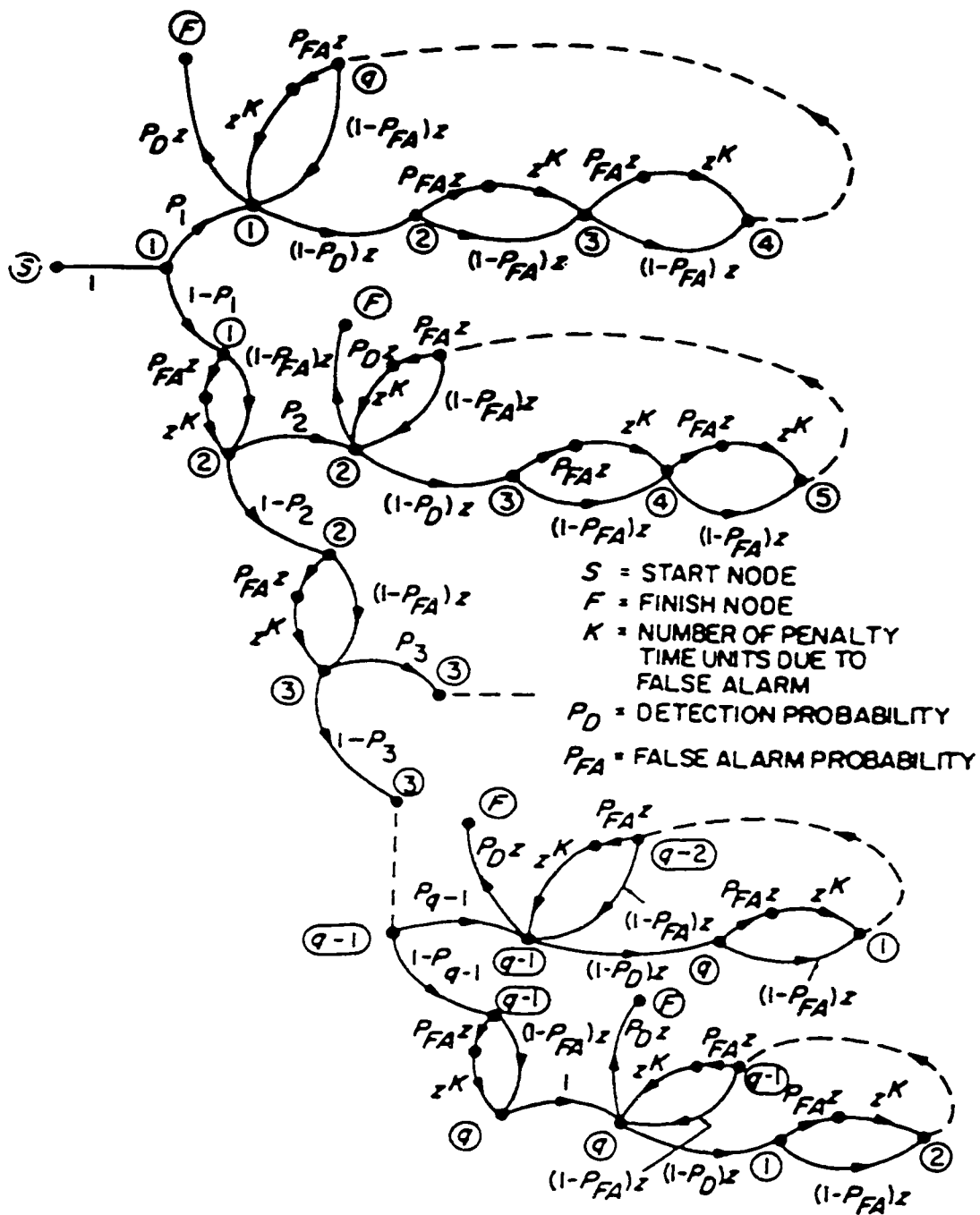


Figure 2.5: Markov chain model for Single Dwell System

The mean acquisition time \bar{T}_{ACQ} is obtained by differentiating $U(z)$ with respect to z and evaluating the result at $z = 1$.

$$\bar{T}_{ACQ} = \left[\frac{\delta}{\delta z} U(z) \right] \Big|_{z=1} \quad (2.2)$$

considerable algebraic simplification is experienced when $U(1) = 1$, and the R.H.S of equation (2.2) can be expressed as

$$\frac{\delta}{\delta z} U(z) \Big|_{z=1} = \frac{\delta}{\delta z} \ln U(z) \Big|_{z=1} \quad (2.3)$$

since

$$\frac{\delta}{\delta z} \ln U(z) \Big|_{z=1} = \frac{1}{U(z)} \frac{\delta}{\delta z} U(z) \Big|_{z=1} = \frac{1}{U(z)} \Big|_{z=1} \frac{\delta}{\delta z} U(z) \Big|_{z=1} \quad (2.4)$$

therefore equation (2.2) can be written as

$$\bar{T}_{ACQ} = \frac{\delta}{\delta z} \ln U(z) \Big|_{z=1} \quad (2.5)$$

Since eqn (2.1) satisfies the condition that $U(1) = 1$, applying eqn (2.5), one arrives at the following result after some algebra,

$$\bar{T}_{ACQ} = \frac{2 + (2 - P_D)(q - 1)(1 + KP_{FA})}{2P_D} \tau_d \quad (2.6)$$

which for $q \gg 1$ (the number of cell to be searched is large, which is of practical interest) simplifies to

$$\bar{T}_{ACQ} = \frac{(2 - P_D)(1 + KP_{FA})}{2P_D} (q\tau_d) \quad (2.7)$$

The variance of the acquisition time is determined from the first two derivatives of $U(z)$ as

$$\sigma_{ACQ}^2 = \left[\frac{\delta^2 U(z^{\tau_d})}{\delta z^2} + \frac{\delta U(z^{\tau_d})}{\delta z} - \left(\frac{\delta U(z^{\tau_d})}{\delta z} \right)^2 \right] \Big|_{z=1} \quad (2.8)$$

but since $U(1)=1$, one can use the equivalent relation

$$\sigma_{ACQ}^2 = \left[\frac{\delta^2 \ln U(z^{\tau_d})}{\delta z^2} + \frac{\delta \ln U(z^{\tau_d})}{\delta z} \right] \Big|_{z=1} \quad (2.9)$$

It can be shown that for ($q \gg 1$ and $K \ll q$) then

$$\sigma_{ACQ}^2 = \tau_d^2 (1 + K P_{FA})^2 q^2 \left(\frac{1}{12} + \frac{1}{P_D^2} - \frac{1}{P_D} \right) \quad (2.10)$$

It should be noted that although the simple dwell system discussed is for a Non-Coherent bandpass detector, the above results apply equally to a single dwell system with a coherent detector, the only difference being the interrelation of the parameters τ_d , P_{FA} and P_D for the detector. The above analytical results for the mean and variance of the acquisition time can also be obtained by a simple heuristic approach, a detailed description of which can be found in [26].

2.3.3 Evaluation of P_D (Detection probability) and P_{FA} (False alarm probability) in terms of system parameters

The mean and variance of the acquisition time are all functions of the probability of detection P_D , probability of false alarm P_{FA} and dwell time τ_d . It is also important to note that for a given probability of false alarm and pre-detection signal to noise ratio, the probability of detection P_D is implicitly a function of τ_d . In the following, P_D and P_{FA} are evaluated in terms of PN acquisition system parameters for the simple case of no code doppler or doppler derivatives.

When the signal is present (i.e., the cell being searched corresponds to a sample value on the PN correlation curve), then the input to the square-law envelope detector can be expressed in the form

$$x(t) = s(t) + n(t) \quad (2.11)$$

$$\begin{aligned} &= \sqrt{2}A \cos(\omega_0 t + \psi) + \sqrt{2}n_c(t) \cos(\omega_0 t + \psi) \\ &\quad - \sqrt{2}R(t) \cos(\omega_0 t + \psi + \theta(t)) \end{aligned} \quad (2.12)$$

$$= \sqrt{2}R(t) \cos(\omega_0 t + \psi + \theta(t)) \quad (2.13)$$

where $R(t) = \sqrt{(A + n_c(t))^2 + n_s^2(t)}$, $\theta(t) = \arctan\left(\frac{n_s(t)}{A + n_c(t)}\right)$, A represents the rms signal amplitude, ω_0 , the radian carrier frequency and $n_c(t)$ and $n_s(t)$ band-limited, independent, lowpass zero mean gaussian noise process with variance $\sigma^2 = N_0B/2$, N_0 is the single sided noise spectral density and B is the noise bandwidth of the pre-detection filter. The output of the square-law envelope detector in response to an input $x(t)$ is $y(t) = x(t)^2 = R(t)^2 = (A + n_c(t))^2 + n_s^2(t)$ (ignoring the second harmonics of the carrier) and has a non-central chi-squared probability distribution function, which is given by

$$p(y) = \begin{cases} \frac{1}{2\sigma^2} \exp\left[-\left(\frac{y}{2\sigma^2} + \gamma\right)\right] I_0\left(2\sqrt{\frac{\gamma y}{2\sigma^2}}\right) & \text{if } y \geq 0 \\ 0 & \text{otherwise} \end{cases} \quad (2.14)$$

where $\gamma = \frac{A}{N_0B}$, is the predetection signal to noise ratio, $I_0()$ is the Bessel function of first kind and zero order. In the absence of signal, $A = 0$ and equation (2.11) reduces to the central chi-squared probability density function given by

$$p(y) = \begin{cases} \frac{1}{2\sigma^2} \exp\left(-\frac{y}{2\sigma^2}\right) & \text{if } y \geq 0 \\ 0 & \text{otherwise} \end{cases} \quad (2.15)$$

and this probability density function characterizes the square law output in all search cells that contain noise only.

The integrate and dump output can be approximated by a summation over the sampled values ($y(t)$ is sampled at intervals of $T=1/B$) i.e.,

$$Y = \frac{1}{\tau_d} \int_0^{\tau_d} y(t) dt \simeq \frac{1}{N} \sum_{k=0}^{N-1} y(kT) \quad (2.16)$$

where $N = \frac{\tau_d}{T} = B\tau_d$. Substituting the above approximation in the first order probability density function, the pdf of Y (namely $p(Y)$), for the signal present is given by

$$p(Y)_{\text{present}} = \begin{cases} \frac{N}{2\sigma^2} \left(\frac{Y}{2\gamma\sigma^2}\right)^{(N-1)/2} \exp\left[-N\left(\frac{Y}{2\sigma^2} + \gamma\right)\right] I_{N-1}\left[2\sqrt{\frac{N^2\gamma Y}{2\sigma^2}}\right] & \text{if } Y \geq 0 \\ 0 & \text{otherwise} \end{cases} \quad (2.17)$$

and for the signal absent,

$$p(Y)_{\text{absent}} = \begin{cases} \frac{N}{2\sigma^2} \frac{\left(\frac{YN}{2\sigma^2}\right)^{(N-1)}}{(N-1)!} \exp\left(-\frac{YN}{2\sigma^2}\right) & \text{if } Y \geq 0 \\ 0 & \text{otherwise} \end{cases} \quad (2.18)$$

Letting $Y_{\text{norm}} = \frac{YN}{2\sigma^2}$ (random variable Y normalized by $\frac{2\sigma^2}{N}$), one can express the pdf of Y in a more simplified form as

$$p(Y_{\text{norm}})_{\text{present}} = \begin{cases} \left(\frac{Y_{\text{norm}}}{N\gamma}\right)^{(N-1)/2} \exp(-Y_{\text{norm}} - N\gamma) I_{N-1}\left[2\sqrt{NY_{\text{norm}}\gamma}\right] & Y_{\text{norm}} \geq 0 \\ 0 & \text{otherwise} \end{cases} \quad (2.19)$$

and

$$p(Y_{\text{norm}})_{\text{absent}} = \begin{cases} \frac{Y_{\text{norm}}^{N-1}}{(N-1)!} \exp(-Y_{\text{norm}}) & Y_{\text{norm}} \geq 0 \\ 0 & \text{otherwise} \end{cases} \quad (2.20)$$

The false alarm probability P_{FA} , is the probability that Y exceeds the threshold η when the signal is absent. Stated in terms of the normalized random variable Y_{norm} and normalized threshold $\eta_{\text{norm}} = \frac{\eta N}{2\sigma^2}$ we have

$$P_{FA} = \int_{\eta_{\text{norm}}}^{\infty} p(Y_{\text{norm}}) dY_{\text{norm}} \quad (2.21)$$

$$= 1 - \int_0^{\eta_{\text{norm}}} \frac{(Y_{\text{norm}})^{N-1}}{(N-1)!} \exp(-Y_{\text{norm}}) dY_{\text{norm}} \quad (2.22)$$

$$= \exp(-\eta_{\text{norm}}) \sum_{k=0}^{N-1} \frac{(\eta_{\text{norm}})^k}{k!} \quad (2.23)$$

The detection probability P_D is the probability that Y exceeds the threshold η when the signal is present and is given by

$$P_D = 1 - \int_0^{\eta_{\text{norm}}} \left(\frac{Y_{\text{norm}}}{N\gamma}\right)^{(N-1)/2} \exp(-Y_{\text{norm}} - N\gamma) I_{N-1}\left[2\sqrt{N\gamma Y_{\text{norm}}}\right] dY_{\text{norm}} \quad (2.24)$$

and can also be expressed if desired in terms of the generalized Marcum's Q-function. For the case of the most practical interest, N can be assumed large and the expression becomes much simpler. Defining $y_k^* = y(kT)/2\sigma^2$ then eqns (2.14) and (2.15) can be expressed as

$$p(y_k^*)_{\text{present}} = \begin{cases} \exp(-(y_k^* + \gamma)I_0(2\sqrt{\gamma y_k^*})) & y_k^* \geq 0 \\ 0 & \text{otherwise} \end{cases} \quad (2.25)$$

$$p(y_k^*)_{\text{absent}} = \begin{cases} \exp(-y_k^*) & y_k^* \geq 0 \\ 0 & \text{otherwise} \end{cases} \quad (2.26)$$

Now, $Y_{\text{norm}} = \sum_{k=0}^{N-1} y_k^*$ and since the y_k^* 's are independent random variables, then for large N, Y_{norm} is approximately Gaussian distributed with mean $\bar{Y}_{\text{norm}} = N\bar{y}^*$ and $\sigma_{Y_{\text{norm}}}^2 = N\sigma_{y^*}^2$. The mean and variance of the pdf's in eqns (2.22) and (2.23) are well known to be for the signal present and absent respectively as

$$\begin{aligned} \bar{y}^* &= 1 + \gamma \\ \sigma_{y^*}^2 &= 1 + 2\gamma \end{aligned} \quad (2.27)$$

$$\begin{aligned} \bar{y}^* &= 1 \\ \sigma_{y^*}^2 &= 1 \end{aligned} \quad (2.28)$$

Thus, for the signal present we have,

$$\bar{Y}_{\text{norm}} = N(1 + \gamma) \quad (2.29)$$

$$\sigma_{Y_{\text{norm}}}^2 = N(1 + 2\gamma) \quad (2.30)$$

and for the signal absent

$$\bar{Y}_{\text{norm}} = N \quad (2.31)$$

$$\sigma_{Y_{\text{norm}}}^2 = N \quad (2.32)$$

Using the Gaussian assumption, the false alarm probability is

$$P_{FA} = \int_{\eta_{\text{norm}}}^{\infty} \frac{1}{\sqrt{2\pi N}} \exp\left[-\frac{(Y_{\text{norm}} - N)^2}{2N}\right] dY_{\text{norm}} \quad (2.33)$$

$$\begin{aligned}
&= Q\left(\frac{\eta_{norm} - N}{\sqrt{N}}\right) \\
&= Q(\beta)
\end{aligned} \tag{2.34}$$

where $Q(x)$ is the gaussian probability integral. Now if P_{FA} is specified, then β can be evaluated. The probability of detection is given by

$$P_D = \int_{\eta_{norm}}^{\infty} \frac{1}{\sqrt{2\pi N(1+2\gamma)}} \exp\left[-\frac{Y_{norm} - N(1+\gamma)^2}{2N(1+2\gamma)}\right] dY_{norm} \tag{2.35}$$

$$P_D = Q\left(\frac{\beta - \sqrt{N}\gamma}{\sqrt{1+2\gamma}}\right) \tag{2.36}$$

Equations (2.9)–(2.34) presented here are referred from [26]

2.4 Serial PN Acquisition System: Multi– Dwell

Multi–dwell techniques are a generalization of the single dwell serial PN acquisition with additional threshold testing that does not constrain the examination interval per cell to a constant interval of time. Nevertheless, this scheme falls into the class of fixed dwell time PN acquisition systems because of the fact that the variation in integration time is achieved here by allowing the examination interval to consist of a series of fixed short dwell periods (each generally longer than its predecessor) with a decision being made after each. Allowing the integration time in a given cell examination interval to increase towards its maximum value in *discrete steps*, permits dismissal of an incorrect alignment earlier than would be possible in a single dwell system which is constrained to always integrate over the full examination interval. Since most of the cells searched correspond to incorrect alignments, the ability to quickly eliminate them produces a considerable reduction in acquisition time (particularly in the case of long codes).

Figure 2.6 and Figure 2.7 illustrates the N-dwell serial synchronization system with half chip search and Non–Coherent detection respectively. The received signal plus noise is firstly multiplied by the local replica of the PN code and this is applied to

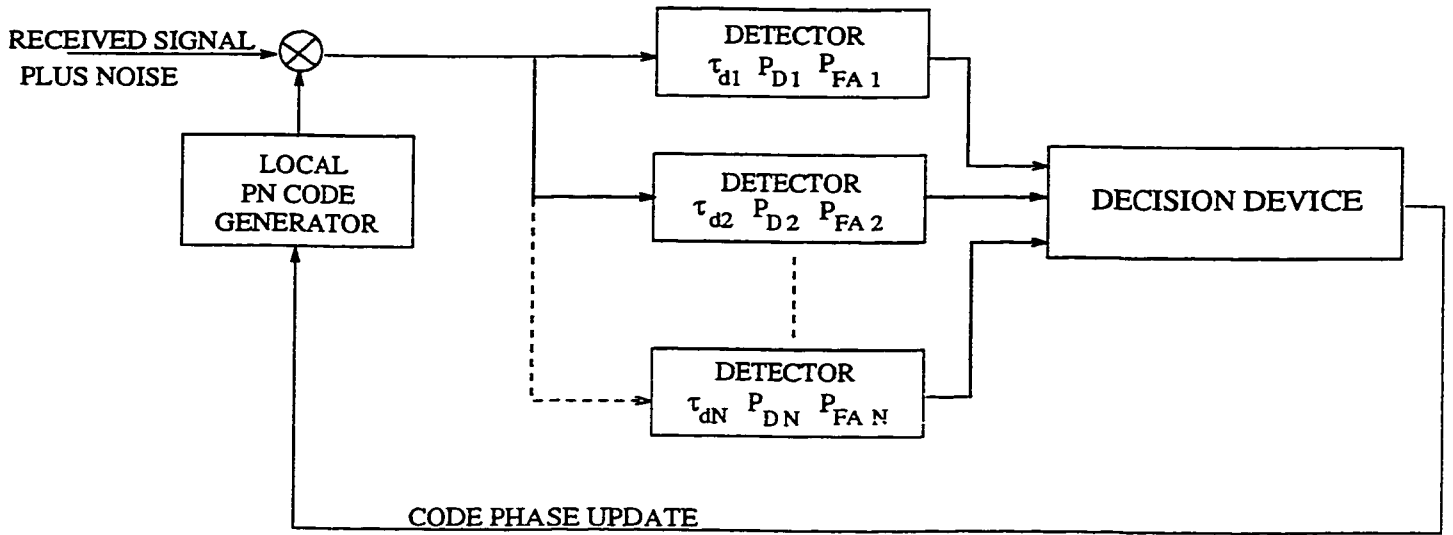


Figure 2.6: The N-dwell serial synchronization system with half chip search.

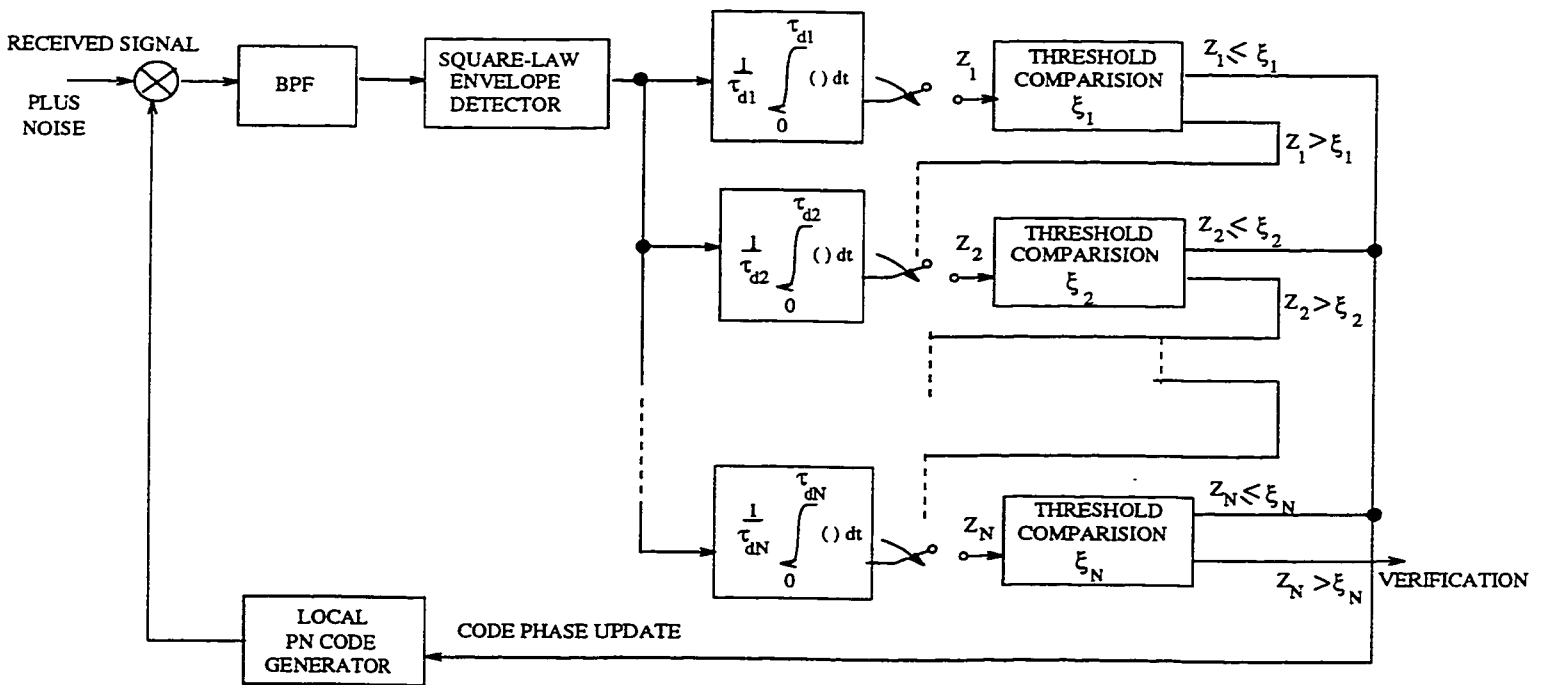


Figure 2.7: Block diagram of an N-dwell time PN acquisition system with Non-Coherent detection.

each of N non-coherent detectors. The i th detector, $i=1,2,\dots,N$ is characterized by a detection probability P_{D_i} , a false alarm probability $P_{FA,i}$ and a dwell time τ_{d_i} . If it is assumed that the detector dwell times are ordered such that $\tau_{d1} \leq \tau_{d2} \leq \dots \tau_{dN}$ then the decision to continue or stop the search at the present cell is made by sequentially examining the N -detector outputs (starting with the first) and applying the following algorithm:

1. If all the N detectors (tested in succession) indicate that the present cell is correct, i.e., each produces a threshold crossing, then the decision is made to stop the search.
2. If any one detector fails to produce a threshold crossing (i.e., fails to indicate that the present cell is correct), then the decision is made to continue the search, the delay τ of the local PN generator is retarded by the chosen phase update increment, and the next cell is examined. Thus, as soon as one detector indicates that the codes are misaligned, the search may move on without waiting for the decisions of the remaining detectors.

The power of the N -dwell system over the single dwell system lies in the fact that the maximum time to search a given cell is τ_{dN} , the minimum time is τ_{d1} , thus most of the cells can be dismissed after a dwell time τ_{dk} , $k \leq N$, whereas the single dwell system requires that each and every cell be examined for a time equivalent of τ_{dN} . Figure 2.7 illustrates a block diagram of an N -dwell time PN acquisition system using Non-Coherent detection. All the N integrate-and-dump circuits initiate their integration at the same instant in time, each one dumping, however, at a later and later time instant (because of the assumption that $\tau_{d1} \leq \tau_{d2} \leq \dots \tau_{dN}$). The probability that the Z_i crosses its threshold depends on the probability that Z_k , $k=1,2,3\dots i-1$ crossed their respective thresholds. Thus in accordance with the search update algorithm, the output of the i th integrate-and-dump is sampled and compared to a threshold only if all of the $(i-1)$ integrate-and-dump outputs have previously exceeded their

respective thresholds. Otherwise, the first integrate-and-dump output that fails to exceed a threshold causes the local code to update its phase and search the next cell thereby resetting all of the integrate-and-dump circuits. A false alarm occurs when all N detector outputs exceed their respective thresholds for a cell that does not correspond to the correct code alignment.

2.5 PN Synchronization procedures for Non Uniformly Distributed Signal Location

In the previous discussion of the signal dwell and multi-dwell system, it was implicitly assumed that the “a-priori” pdf of the signal location across the uncertainty region was uniform, i.e., the correct cell was equally likely to occur in any of the q -cells searched in one complete pass. When the “a-priori” pdf of the signal location is in some sense peaked rather than uniform, then it is more likely to find the correct code phase in the “region” surrounding the peak, and therefore one’s sweep strategy should be adjusted accordingly. Suppose now that the received phase distribution is defined by $p(n)$, the probability that the received phase is within the n^{th} phase cell. When $p(n)$ is known, the sweep strategy should be modified to search the most likely phase cells first and then the less likely cells. For example, if the received phase distribution were Gaussian, a reasonable search strategy would be to search the cells within one standard deviation of the most likely cell first and then expand the search to cells within two standard deviations and so on [27]. It is important to note that $p(n)$ is a discrete distribution and therefore cannot be Gaussian, whereas the received phase is continuous, the function $p(n)$ can be easily derived from the continuous density and cell boundaries. Figure 2.8 illustrates the Gaussian distribution and the search strategy proposed by [27].

The average synchronization time for the system is calculated using

$$\bar{T}_s = \sum_{n,j,k} Pr(n, j, k) \quad (2.37)$$

where n, k, j respectively, are the particular location for the correct phase, the particular number of FA's and the number of missed detections of the correct phase. The proper limits for all summations for the three variables n, j and k must be determined. If ΔT represents the time uncertainty region, Δt the phase step size, then $\frac{\Delta T}{\Delta t}$ is an integer and represents the number of cells to be searched. The limits for the first summation are then $-C/2 \leq n \leq C/2$ where cell number zero is at the center of the uncertainty region. The discrete probability of the n^{th} phase cell being correct is

$$p(n) = A \exp\left(-\frac{n^2}{2T^2}\right) \quad -C/2 \leq n \leq +C/2 \quad (2.38)$$

where A is a constant calculated from $\sum_{n=-C/2}^{+C/2} p(n) = 1.0$, $T = c/6$. Let each pass through the uncertainty region be numbered using the variable 'b'. Furthermore let N_b , and $N_{(b+1)}$ denote the starting and ending cell number for the bth pass. For the strategy of Figure 2.8, $N_1 = -C/6$, $N_2 = C/6$, $N_3 = C/3$, $N_4 = +C/3$, and so on, where all fractions are rounded to the nearest integers. Let $f(n)$ denote the number of the pass that evaluated cell 'n' for the first time. For example if $C/6 < n < C/3$, the cell will not be evaluated until the third sweep. The limits of the sum over 'j' are $0 \leq j \leq \infty$, the variable 'k' is the total number of false alarms in all incorrect phase cells is denoted by $K(n, j)$, and is given by

$$K(n, j) = \sum_{b=1}^{f(n)+j-1} |N_{b+1} - N_b| + |n - N_{f(n)+j}| - j \quad (2.39)$$

The false alarm can occur in any order within the $K(n, j)$ incorrect phase cells and the number of false alarms is binomially distributed. Combining all of the above information yields

$$P[n, j, k] = A \exp\left(-\frac{n^2}{2T^2}\right) P_d (1 - P_d)^j \binom{K(n, j)}{k} P_{fa}^k (1 - P_{fa})^{K(n, j) - k} \quad (2.40)$$

and

$$\bar{T}_s = \sum_{n=-C/2}^{n=C/2} \sum_{j=0}^{\infty} \sum_{k=0}^{K(n,j)} [K(n,j) + j]T_i + kT_{fa}A \exp\left(-\frac{n^2}{2T^2}\right) P_d(1 - P_d)^j \binom{K(n,j)}{k} P_{fa}(1 - P_{fa})^{K(n,j)-k} \quad (2.41)$$

The above equation has been evaluated in [27]. Modified sweep strategies have been used for many years in radar. Their use results in reduced average synchronization time when the distribution of the received phase is non-uniform.

2.6 PN Synchronization Using Sequential Detection

The single dwell time PN acquisition system is insufficient from an acquisition time standpoint, since its detector spends as much time rejecting a false sync position as it does in accepting the correct one. If one is to minimize the acquisition time, what is needed is a detector that quickly dismisses a false sync position, but is allowed to integrate over a much longer time interval during the single cell which corresponds to the correct code alignment. The multiple dwell time system also discussed previously was an attempt at accomplishing the above mentioned objective wherein the detector integration time was increased in discrete steps until the test failed (with one output falling below the threshold). Another alternative is to allow the integration time to be “*continuous*”, and thus replace the multiple threshold tests by a continuous test of a single dismissal threshold. Such a variable integration time detector is referred to as a “*Sequential Detector*” and the corresponding acquisition system is designed so that the mean time to dismiss the false sync position is much smaller than the integration time of a single dwell system.

To illustrate the above technique, consider the serial sequential detection PN acquisition system illustrated in Figure 2.9. Until the output of the square-law envelope detector, the system operates identically to the single dwell acquisition system as discussed in the previous sections. Figures 2.10, 2.11 and 2.12 represent the outputs of the continuous time integrator. Figure 2.10 represents the case when the bias voltage 'b' is absent, for both cases of the signal plus noise and the noise alone. In particular, the integrator output would follow along the integrated mean of the square-law detector output, given by $N_0 B t$ or $N_0 B (1 + \gamma) t$, thus for both hypotheses, the integrator output tend to increase linearly with time but at different slopes. Now suppose one subtracts a fixed bias voltage 'b' from the signal before integration and if this bias is assigned a value between the means of the square-law detector outputs, i.e., $N_0 B < b < N_0 B (1 + \gamma)$, then the integrator output will tend to decrease linearly when the signal plus noise is present as illustrated in Figure 2.11. If one now chooses a threshold ζ (of negative value) which causes a dismissal whenever the integrator output falls below it, then the smaller the magnitude of this threshold, the faster the output for the noise only condition will dip below it. This quick dismissal for the noise only condition is what forms the heart of the sequential detection system and provides the acquisition time advantage. But because of the small magnitude of the threshold, the possibility of the signal plus noise case to also dip below the threshold is relatively high. Therefore a compromise threshold value is generally assigned, leading to a relatively quick dismissal of false sync position and also allowing the integrator output for the true sync position to remain above the threshold. A test truncation time τ_0 is often allocated and if the threshold is exceeded before this time, then the test is terminated and the signal is declared present in the cell being searched.

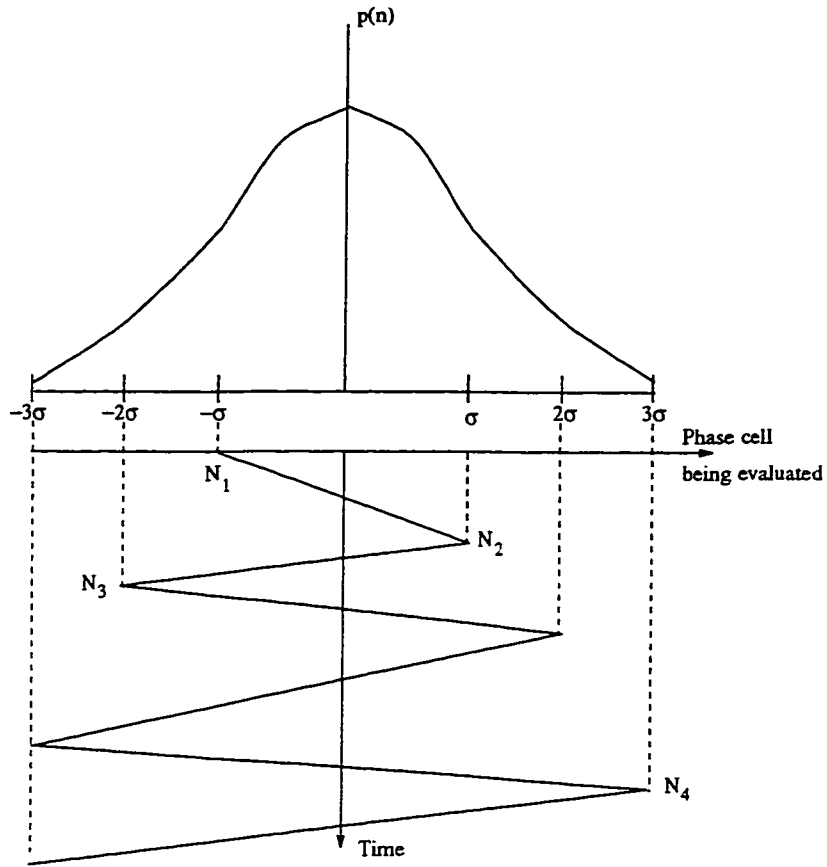


Figure 2.8: Non Uniformly distributed signal location and possible sweep strategy.

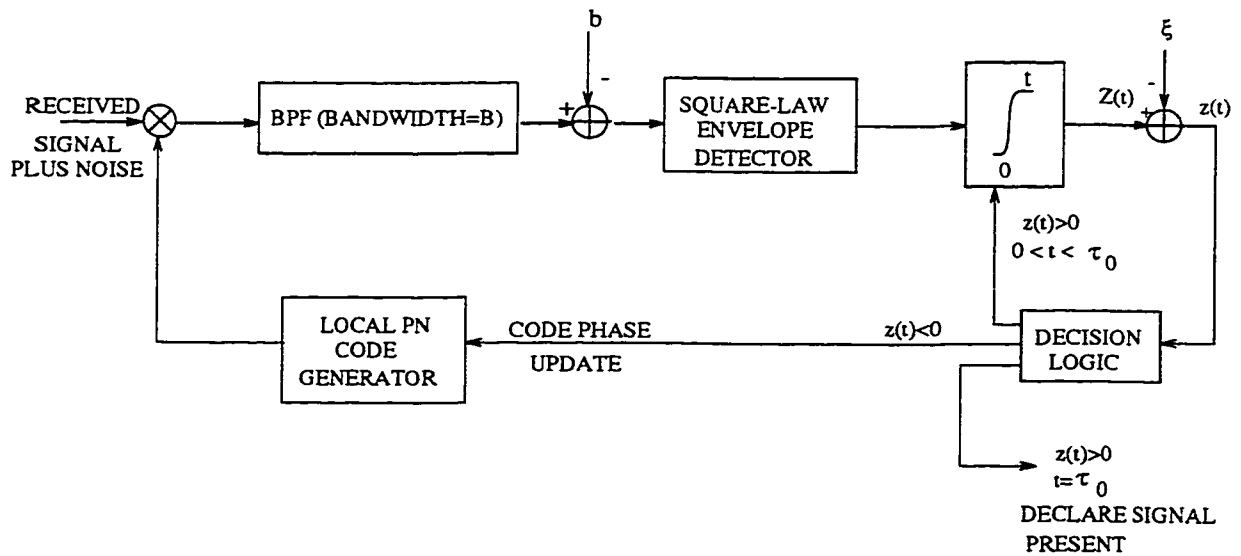


Figure 2.9: Serial Sequential Detection PN acquisition system with timeout feature

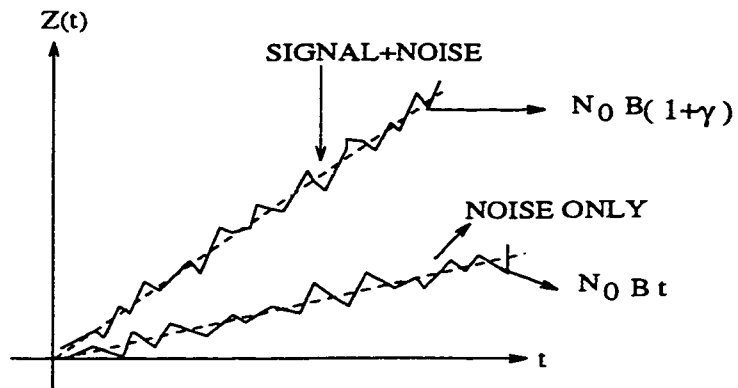


Figure 2.10: (a): Integrator output with bias voltage absent

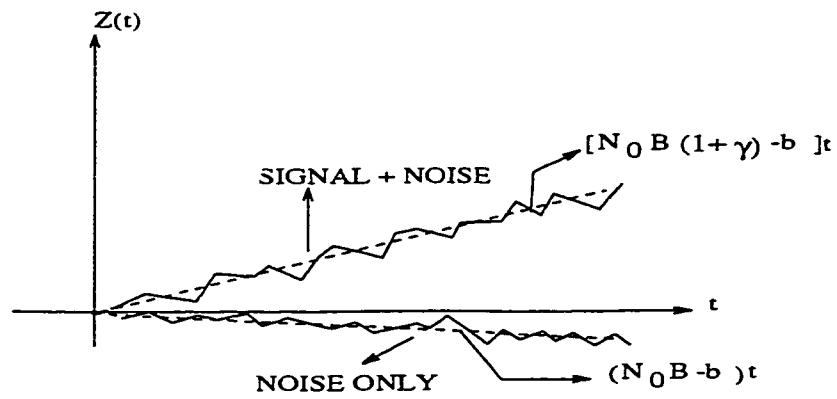


Figure 2.11: (b): Integrator output with bias voltage present.

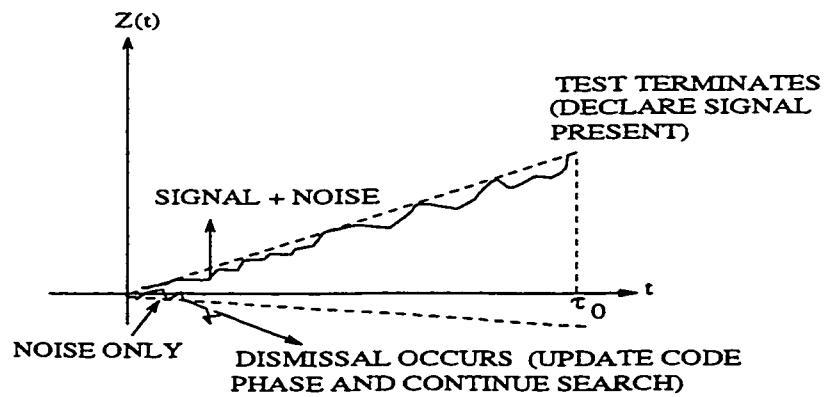


Figure 2.12: (c): Integrator outputs with threshold dismissal and test truncation

Chapter 3

A New Hybrid Acquisition Scheme for CDMA Systems employing Short Concatenated Codes

This chapter begins with an introduction to the codes used by spread spectrum systems: the Maximal Length Sequences, and Gold Codes. This is followed by a detailed description of a New Hybrid Acquisition Scheme for CDMA systems. An outline of the procedure used for simulating the scheme is discussed followed by the performance analysis of the Acquisition scheme in a multiple access environment.

3.1 Introduction

In the previous chapter, an overview of the various acquisition schemes for the purpose of PN synchronization was presented. Before presenting the proposed hybrid acquisition scheme, a brief introduction to the maximal length sequences and Gold Codes will be presented for the sake of completeness.

3.1.1 Coding for Spread Spectrum Systems

Spread Spectrum systems employ special types of codes for the purpose of communications. In fact the type of code used, its length, its chip rate, set serious bounds on the capability of the system. Some of the salient features of codes used for spread spectrum systems are

- Protection against Interference.
- Provision for Privacy.
- Noise-Effect reduction.

Figure 3.1 illustrates the block diagram of generation of linear and nonlinear codes. It is important to point out that a spread spectrum system is not a secure system unless the codes used are cryptographically secure, and that linear codes used in spread spectrum systems do not provide any security.

3.1.2 Maximal-Length Sequences

Given a shift register of a specific length, the longest codes that can be generated are by definition, *Maximal-Length* sequences. For an 'n' stage shift register, the maximal length sequence is $2^n - 1$ chips long. A shift register sequence generator consists of a shift register working in conjunction with an appropriate logic, which feeds back a logical combination of the state of two or more of its stages to its input. The output of a sequence generator and the contents of its 'n' stages at any sample time, is a function of the stages fed back at the preceding sample time. Feedback connections from 3 to 100 stages have been tabulated for maximal code generators. If $\theta_{bb'}(k)$ represents the *discrete periodic cross-correlation function* and $\theta_b(k)$, the *discrete periodic auto-correlation function*, then by definition,

$$\theta_{bb'}(k) = \frac{1}{N} \sum_{n=0}^{N-1} a_n a'_{n+k} \quad (3.1)$$

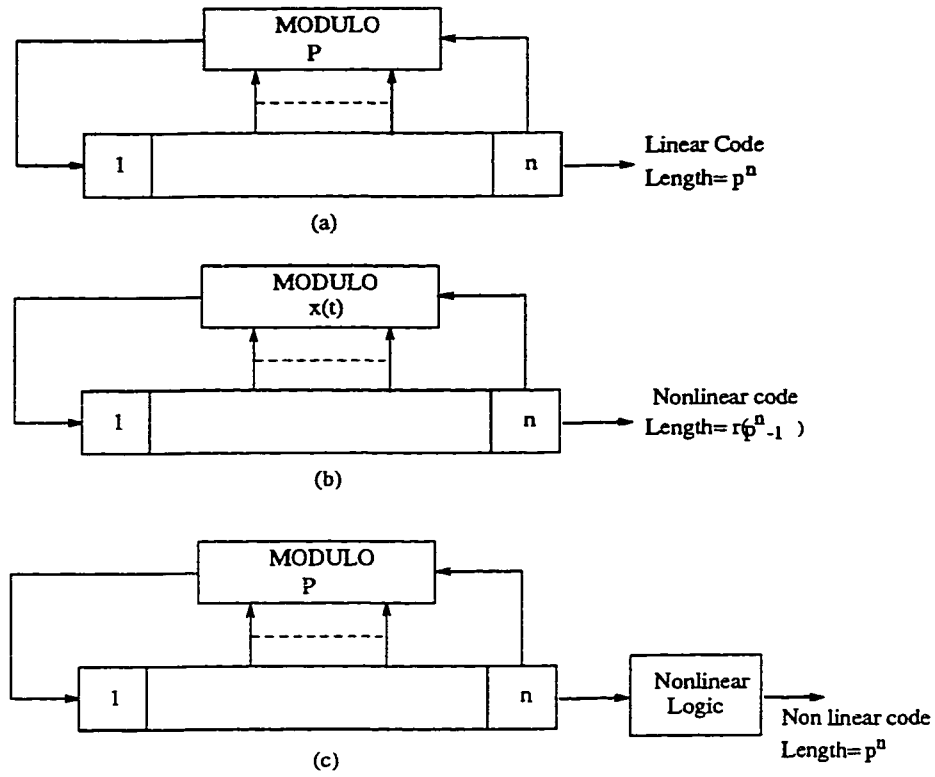


Figure 3.1: Linear and Nonlinear code generator configurations

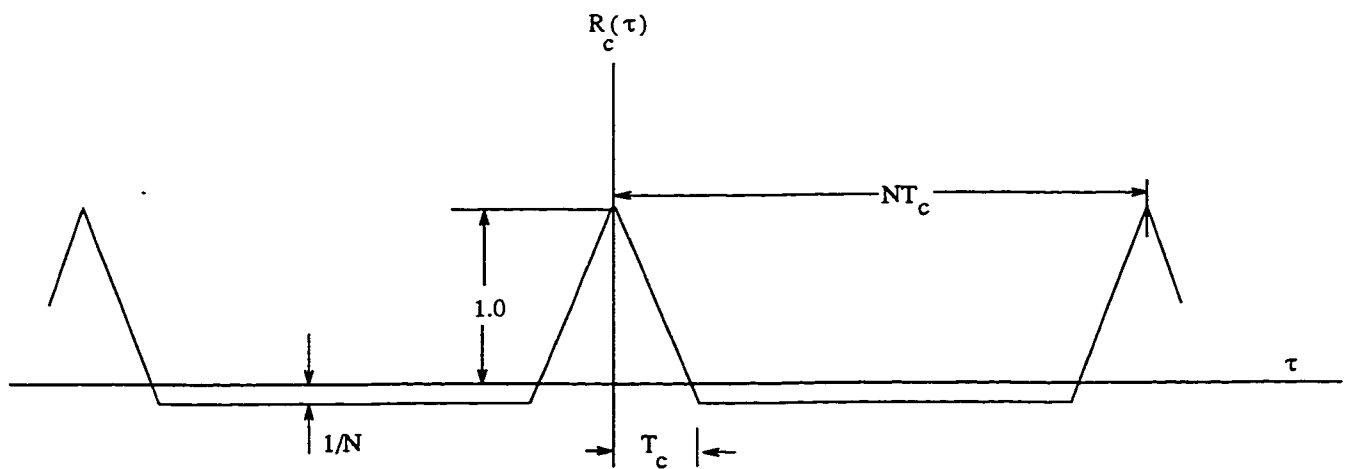


Figure 3.2: Autocorrelation function of Maximal length sequences

$$\theta_b(k) = \frac{1}{N} \sum_{n=0}^{N-1} a_n a_{n+k} \quad (3.2)$$

where $a_n = (-1)^{b_n}$, $b_n \in \{0,1\}$, N being the period of the code. It is well known that the periodic autocorrelation function $\theta_b(k)$ for maximal length sequences is two-valued and is given by

$$\theta_b(k) = \begin{cases} 1.0 & k = lN \\ -\frac{1}{N} & k \neq lN \end{cases} \quad (3.3)$$

where l is any integer. If $R_c(\tau)$ and $R_{cc'}(\tau)$ represent the autocorrelation function and crosscorrelation functions respectively, and are defined as,

$$R_c(\tau) = \frac{1}{T} \int_0^T c(t)c(t+\tau)dt \quad (3.4)$$

and

$$R_{cc'}(\tau) = \frac{1}{T} \int_0^T c(t)c'(t+\tau)dt \quad (3.5)$$

where $c(t) = \sum_{n=-\infty}^{+\infty} a_n p(t - nT_c)$, $p(t)$ is a unit pulse beginning at zero and ending at T_c , then it can be shown that the discrete auto/cross correlation function and the continuous auto/cross correlation functions are related as

$$R_{cc'}(\tau) = R_{cc'}(k, \tau_c) = \left(1 - \frac{\tau_c}{T_c}\right) \theta_{bb'}(k) + \frac{\tau_c}{T_c} \theta_{bb'}(k+1) \quad (3.6)$$

For the specific case of maximal length sequences, the auto correlation function can be expressed (in terms of the discrete autocorrelation function) as

$$R_c(\tau) = \begin{cases} 1 - \frac{\tau}{T_c} \left(1 + \frac{1}{N}\right) & 0 \leq \tau \leq T_c, k = 0, \tau_c = \tau \\ -\frac{1}{N} & T_c < \tau < (N-1)T_c, k \neq lN \quad (k+1) \neq lN \text{ for any integer} \\ \frac{\tau}{T_c} \left(1 + \frac{1}{N}\right) - \frac{1}{N} & (N-1)T_c \leq \tau < NT_c, \quad k = (N-1), \quad (k+1) = N, \\ & \tau_c = \tau - (N-1)T_c \end{cases} \quad (3.7)$$

Figure 3.2 illustrates the autocorrelation function for a maximal length sequence with chip duration T_c and period NT_c . The power spectral density of maximal length sequences is given by

$$S_c(f) = \sum_{-\infty}^{+\infty} P_m \delta(f - mf_0) \quad (3.8)$$

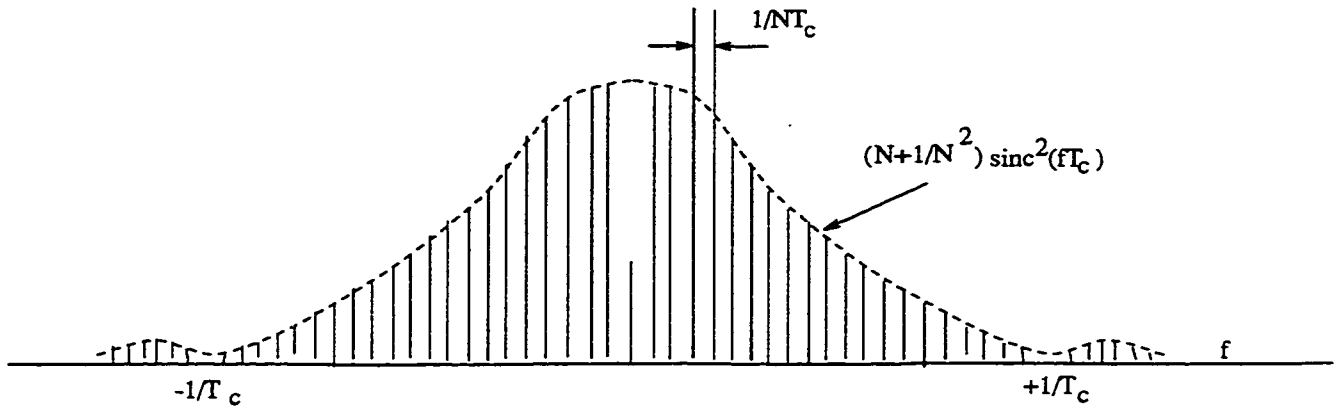


Figure 3.3: Power Spectral Density of Maximal length sequences

where $P_0 = \frac{1}{N^2}$, $P_m = \left[\frac{(N+1)}{N^2} \right] \text{sinc}^2(m/N)$ and $f_0 = \frac{1}{NT_c}$. Figure 3.3 illustrates the PSD of a maximal length sequence with chip duration T_c and period NT_c .

3.1.3 Gold Codes

Spread Spectrum multiple access techniques permit all users to transmit simultaneously using the same band of frequencies. Each user is assigned a unique spreading code (signature sequence) enabling the receiver to separate each user during the de-spreading operation. Therefore the goal of a spread spectrum system designer for a multiple access system is to find a set of spreading waveforms such that a maximum number of users can be accommodated in the same band of frequencies with as little mutual interference as possible. A detailed treatment on Pseudo random sequences can be obtained in [28].

Gold Codes were invented in 1967 at the Magnavox Corporation specifically for multiple access applications of spread spectrum. A large set of Gold Codes exist, which have well controlled cross-correlation properties. They are constructed by a modulo 2 addition of specific relative phases of a preferred pair of m-sequences. Equation [3.1] represents the discrete cross-correlation function between two spreading codes. The cross-correlation spectrum is a list of all possible values of $\theta_{bb'}(k)$ and the number of values of 'k' which yield that particular cross-correlation. The

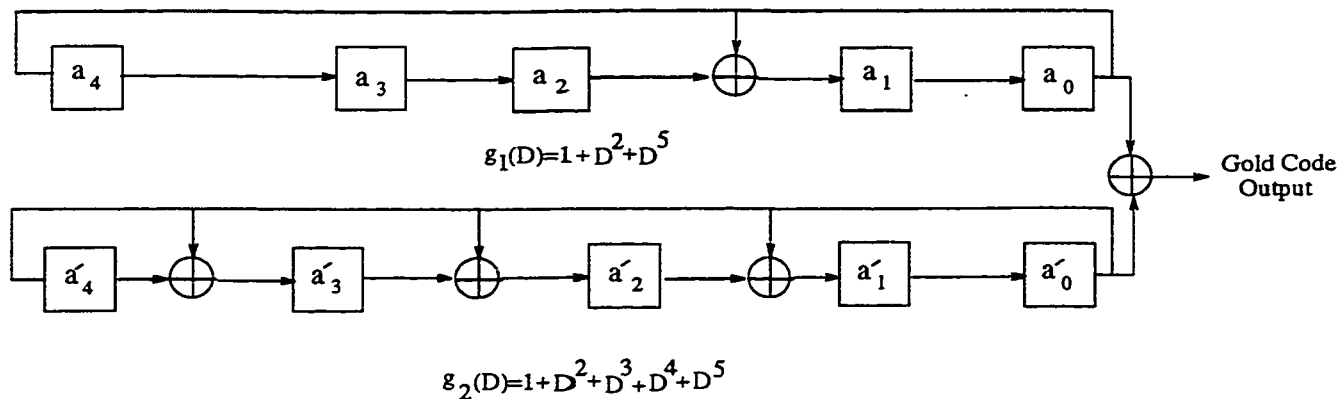


Figure 3.4: Gold Code Generator

Gold Code sets have a cross correlation spectrum which is three valued given by,

$$\begin{aligned}
 &-\frac{1}{N}t(n) \\
 &\quad -\frac{1}{N} \\
 &\frac{1}{N}[t(n) - 2]
 \end{aligned} \tag{3.9}$$

where

$$t(n) = \begin{cases} 1 + 2^{0.5(n+1)} & n \text{ odd} \\ 1 + 2^{0.5(n+2)} & n \text{ even} \end{cases} \tag{3.10}$$

and $N = 2^n - 1$. If $b(D)$ and $b'(D)$ represent a preferred pair of m-sequences having a period $N = 2^n - 1$, then the family of codes defined by $b(D), b'(D), b(D) + Db'(D), \dots, D^{N-1}b'(D)$ is called the set of Gold Codes. For m sequences of period 'N', the total number of Gold Codes is $(N+2)$. Figure 3.4 illustrates a typical Gold Code generator configuration.

3.2 A New Hybrid Acquisition Scheme for CDMA Systems

In this section, we present a new hybrid acquisition scheme for CDMA systems. Before discussing the details of the acquisition scheme, a new coding scheme is proposed [29], [30].

3.2.1 Proposed Concatenated Signature Coding Scheme

The signature coding scheme proposed is slightly different from that used in conventional spread spectrum systems. Conventional CDMA systems use long PN codes for each user as signature sequences. The proposed coding scheme also uses long codes as signature sequences for each user. The difference between the two lies in the structure of the long codes. Unlike the former, the latter is made up of shorter codes. Figure 3.5 illustrates the proposed structure of the Long code. The Long signature code is composed of repetition of a shorter code (which we call the user “Basic” code) M times (M being an integer suitable chosen for a specific scenario). Each of these repetitive Basic codes are further composed of unique sequences of shorter concatenated codes. It is important to clarify that the term “Concatenated” here differs from the previous reference in [31], where it is defined as a combination of two sequences such that each bit of one sequence is further encoded by another sequence. Here the term is used to signify the serial stacking of short codes comprising the user Basic code.

Each of the user Basic code is composed of a unique sequence of N short concatenated codes. These N short codes are called “Subcodes”. Each of these subcodes is a Gold code of 127 chips length, and every user is assigned a unique sequence of these subcodes. Here there are two possibilities.

1. The set of N subcodes comprising a user Basic code is completely different from the set of subcodes comprising any other user. (This was followed for the

simulation of the proposed scheme).

2. The set of N subcodes comprising a user Basic code is not completely different from the set comprising a different user.

Thus the sequence of N subcodes is user specific and hence different from user to user. This signature coding scheme proposed is specifically designed towards the acquisition scheme.

One of the main ideas behind the coding scheme is to replace the search of the phase (single) of a long code by the search of independent phases of many shorter, logically connected sequential subcodes comprising the user Basic code. A few perceivable benefits of such a coding scheme are that, firstly, the event of missed detection shifts from its possibility of occurrence over entire length of the code to the possibility of its occurrence over each of the subcodes. This could lead to a decrease in the mean acquisition time since missing the phase of a long code would mean searching the entire uncertainty region again. Secondly, acquisition of the user code could be declared without searching the entire length of the code (although this point would be appreciated only after discussion of the acquisition scheme in conjunction with the above mentioned coding scheme). Before closing the discussion of the coding scheme, a brief summary of the coding terms used is given below. These terms would be frequently used during the discussion of the acquisition scheme.

- Subcode : Short Gold Codes of 127 chips length.
- Basic Code : A user specific sequence of N subcodes.
- Long Code : The code composed of the repetition of the user Basic code M times. Thus the length of the user Long code is $MN \times 127$ chips.

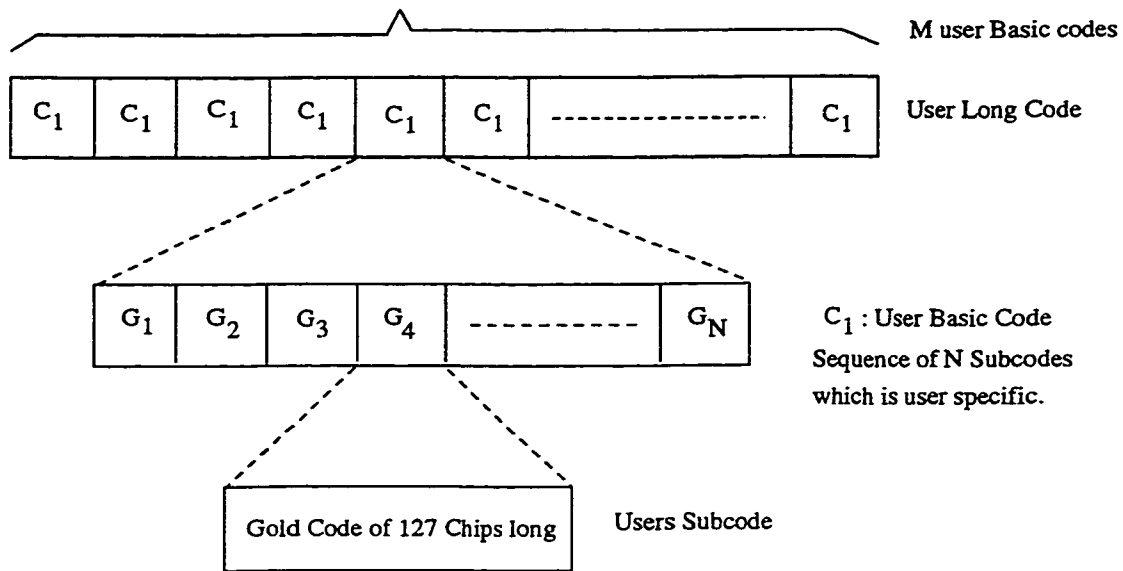


Figure 3.5: Coding Scheme Structure

3.2.2 Hybrid Acquisition Scheme for CDMA Systems

The schematic of the receiver structure of the proposed scheme is shown in Figure 3.6. The received signal plus noise is first fed into a bank of N matched filters. This bank of filters at the receiver is user specific, with each filter matched to one of the N subcodes of only the particular user code that is to be acquired. Thus it is assumed that the receiver possesses knowledge of the particular user being acquired, in terms of the user specific sequence of subcodes. Such information is available from the call signaling channel, the details of which will not be discussed here. Before elaborating the various steps involved in the acquisition process, a summary of the important parameters of the scheme are presented in the following for the sake of clarity.

1. **LP1:** Parameter indicating the identity of the filter that gives a maximum value out of the bank of matched filters. This information translates directly into the identity of the most probable subcode comprising the specific user Basic code.

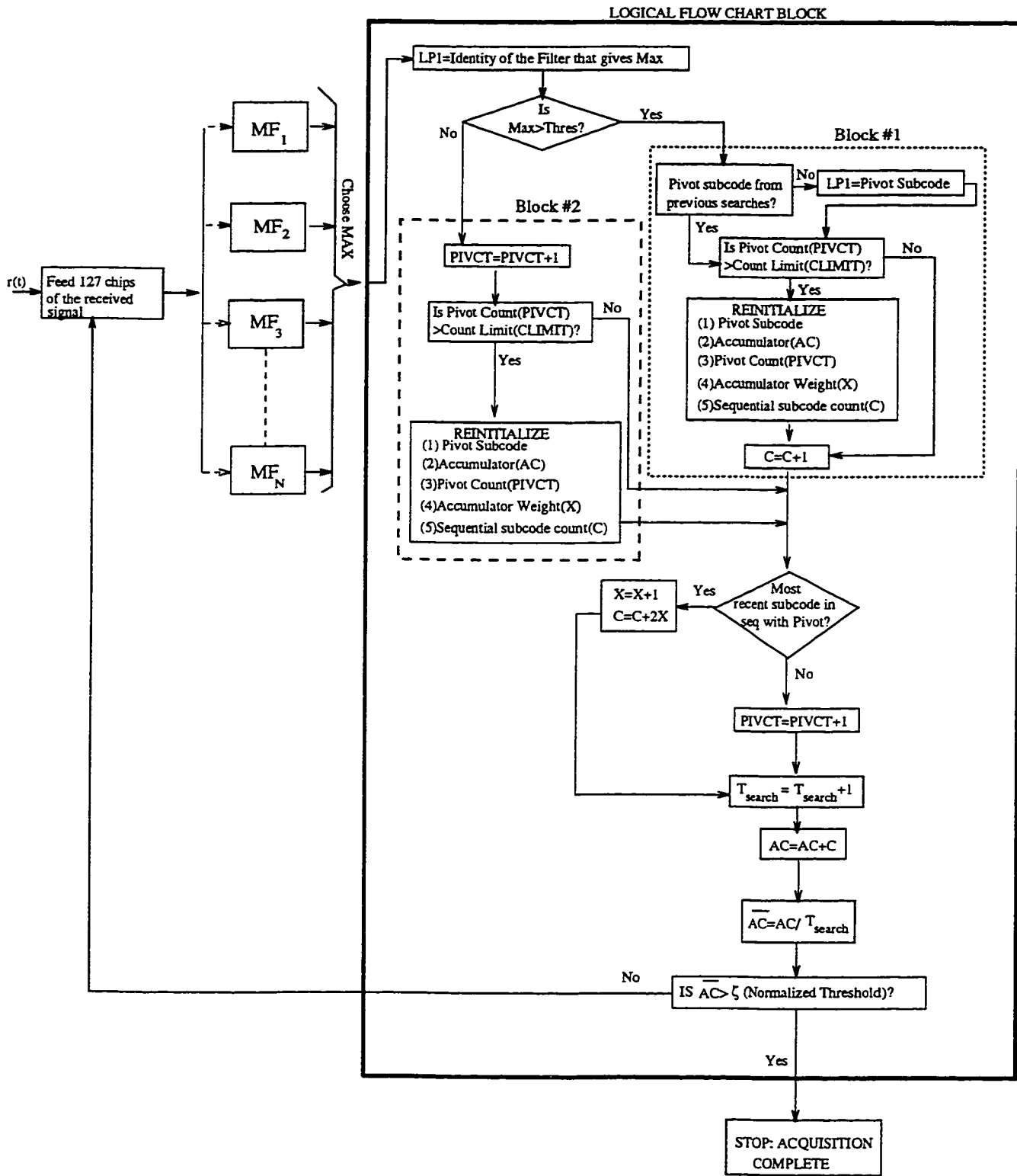


Figure 3.6: Block Diagram of the Proposed Acquisition Scheme

2. **Pivot Subcode:** The pivot subcode plays a very important role in the search scheme. At the beginning of the search, the first detected subcode is assigned the role of the pivot subcode. The pivot subcode could be visualized as a sort of “*anchor*” or “*reference*” in a search scenario. All subcodes detected after the pivot subcode during a search scenario are checked against it for sequential integrity. Any subcode in sequence contributes towards the final declaration of Acquisition. The particular subcode playing the role of the pivot is different from one search scenario to another. One of the features of the acquisition scheme is a running search scenario. Depending on the value of certain parameters of the acquisition scheme, the search is restarted with all parameters of the scheme being re-initialized.
3. **PIVCT (Pivot Count):** This is a counter that is incremented every time either a subcode during a search scenario is not in sequence with the pivot subcode or the filter that peaks (out of the back of matched filters) does not cross the threshold value. A high value of PIVCT during a search scenario indicates the accumulation of wrong subcodes (subcodes out of sequence with respect to the pivot).
4. **CLIMIT (Subcode Count Limit):** This parameter indicates the tolerance of the search scenario. It is the maximum value of the PIVCT allowable during a search scenario. If the PIVCT exceeds CLIMIT, then all parameters of the search scenario are re-initialized, the pivot subcode dropped and a new subcode is assigned the role of the pivot. CLIMIT can also be viewed as a “*window*” length of the search scenario. Thus as mentioned before, depending on whether the value of the PIVCT exceeds (or not) the value of the CLIMIT within the window length as defined by the value of CLIMIT, the search scenario could (or not) lead to a successful declaration of acquisition.

5. \overline{AC} (**Accumulator Value**): This parameter is the running average of the search scenario. Every subcode in sequence with the pivot subcode increments the accumulator value in varying degrees depending upon the value of the accumulator weight “X”. This means subcodes detected in the later periods of the search scenario would contribute more to the accumulator as compared to the earlier ones.
6. ζ (**ZHI: Normalized threshold**): “ ζ ” represents the normalized threshold value for a search scenario. The mean accumulator value is checked against ζ to decide whether acquisition is successful or not. If the mean accumulator value (\overline{AC}) exceeds ζ , then acquisition is complete and the tracking loop is enabled. The value of ζ fixed in a certain search scenario must be chosen judiciously to avoid high false alarms.
7. **C (Sequential Subcode Count)**: The counter indicates the number of filter outputs during a particular search scenario that cross the threshold value and also the subcodes that fall in sequence with the pivot Subcode.

Let us assume the receiver is matched to a particular user, say $User_1$. This means the bank of matched filters at the receiver are each matched to one of the ‘N’ subcodes of $User_1$. The first step at the receiver is to feed the received signal into the bank of matched filters simultaneously. As mentioned previously, there exists a one-to-one correspondence between the filter identity and subcode identity (which means that if filter ‘i’ peaks then it means that the identity of the subcode is “most probably” G_i where we use the word “most probably” to emphasize the probabilistic aspect of the identity of the detected subcode). The filter that gives a maximum (as compared to the rest) is then compared to a suitably chosen threshold. Here there are two possibilities. Firstly the maximum value exceeds the threshold. In this case the subcode is processed along Block # 1 (see Figure 3.6). The other possibility is that the maximum does not exceed the threshold, in which case the subcode is

processed for the next few steps along Block # 2.

Block # 1

1. Step # 1 : The first step is to enquire about the existence of a pivot subcode for the present search scenario. In the event that there is no pivot subcode (which is possible because, either LP1 (the present subcode) could be the first detected subcode implying the beginning of acquisition with respect to some arbitrary time reference $t = 0$ i.e., 1st search scenario, or LP1 (present subcode) is the first in a newly initiated search scenario, implying the existence of previous search scenarios each with assigned pivots), LP1 (the present subcode) is assigned the role of the pivot. If a pivot subcode exists then it indicates that LP1 (present subcode) enters the search scenario after a previously assigned pivot, and in such a case other questions are addressed.
2. Step # 2: The second step along Block # 1 is checking the value of PIVCT against CLIMIT. If $PIVCT > CLIMIT$, then as illustrated in the block diagram Figure 3.6, we enter the “*Re-Initialize*” block, where the parameters AC (accumulator value), PIVCT (pivot Count), X (Accumulator weight), C (Sequential subcode count) are reset, the pivot subcode for the search scenario dropped, and LP1 (present subcode) assigned the role of the pivot. Therefore a completely new search scenario is started. It is important to indicate that the time spent in the previous search scenarios is not discarded but is accounted for in the final evaluation of mean acquisition time. If $PIVCT < CLIMIT$, then the present search scenario continues.
3. Step # 3: The final step is incrementing the parameter “C”. As mentioned previously, C represents a count of the number of filter outputs in a particular search scenario that cross the threshold value and cases where the subcodes are in sequence with the pivot. Since Block # 1 is for the cases where the filter output exceeds the threshold, therefore parameter C is incremented.

Block # 2

1. Step # 1: When the filter that gives a maximum output value from the bank of matched filters does not cross the threshold value, then instead of discarding this case altogether (which is done in many conventional acquisition schemes), the parameter PIVCT is incremented.
2. Step # 2: The next and final step along Block # 2 is to check whether PIVCT is $>$ (or $<$) CLIMIT. As mentioned in Step #2 of Block # 1, depending upon the outcome, the parameters are either re-initialized or not.

After the steps in Block # 1 and # 2, the next step of the acquisition scheme is to check for sequential integrity of LP1 (present subcode) with respect to the pivot. In the event of the existence of a previous pivot subcode for the search scenario, LP1 (present subcode) is checked against it to verify whether it falls in sequence with it. Since the receiver has the knowledge of the exact sequence of subcodes comprising $User_1$'s Basic (and Long) code, the receiver uses that information to check for sequential integrity. If LP1 (present subcode) falls in sequence, then as illustrated in the block diagram, the accumulator weight "X" and parameter "C" are incremented. The value of C is finally added to the accumulator "AC". It is important to note how the accumulator value builds up. It is clear that since "C" is not incremented in equal steps ($C = C + 2X$), the subcodes detected further along the search scenario contribute to the accumulator more than those detected in the earlier stages of the search scenario.

If LP1 (present subcode) is the pivot subcode for the search scenario then even in this case the same set of steps are carried out as in the previous case as mentioned above.

If LP1 (present subcode) is not in sequence with the pivot subcode, then as usual the parameter PIVCT is incremented. The final step of the scheme is the evaluation of the mean accumulator value ($\overline{AC} = \frac{AC}{T_{search}}$). T_{search} represents

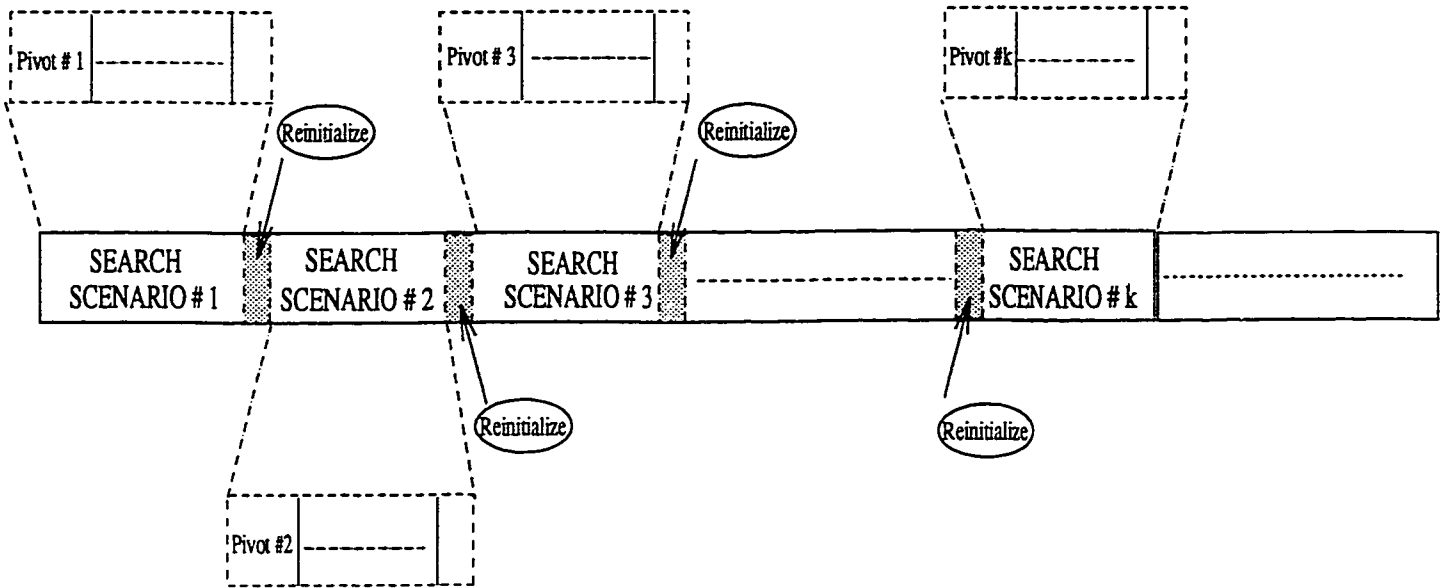


Figure 3.7: Structure of the Acquisition scheme comprising many Search Scenarios

the duration of a search scenario (and hence is indirectly related to the value of $CLIMIT$). The final step of the proposed scheme is to check the value of the mean accumulator value against the normalized threshold ζ . If the mean accumulator value $\overline{AC} < \zeta$ then the next 127 chips of the received signal are fed into the bank of filters and the entire operation as discussed till now is carried out again. If $\overline{AC} > \zeta$ then this means that acquisition is successful (with a certain probability of detection) and the tracking loop is enabled.

Figure 3.7 illustrates the main structure of the acquisition scheme as comprised of many search scenarios. At the end of every unsuccessful search scenario, the value of $PIVCT > CLIMIT$ and therefore the scheme encounters a re-initialize block (as mentioned earlier). Each scenario has a pivot subcode guiding the search and each search scenario is completely independent from preceding or succeeding ones. The process continues until $\overline{AC} > \zeta$ for a search scenario.

Let us illustrate the acquisition process via an example. Assume that $User_1$ has to be acquired in a multiple access environment. Without any loss of generality we can make the assumption of synchronous transmission for $User_1$. Let $User_1$'s

sequence of subcodes be $G_3G_1G_5G_{11}G_{13}G_2G_6$. Thus $N=7$ and this sequence repeats. Thus $User_1$'s Long code would be $G_3G_1G_5G_{11}G_{13}G_2G_6G_3G_1G_5G_{11}G_{13}G_2G_6\dots$. Because of the interference encountered in the channel, assume that the received sequence is different from the transmitted one and is $G_3G_1G_1G_2G_{13}G_1G_3G_1G_6G_{11}G_{11}G_{13}G_6G_2G_3G_1G_5G_{11}G_2G_2G_6G_3G_5G_5G_{11}G_{13}\dots$. Figure 3.8 illustrates the transmitted sequence and the received sequence. The first detected subcode is G_3 and hence it is assigned the role of the pivot (pivot # 1 for search scenario # 1). The next received subcode is G_1 and is in sequence with G_3 , thus the parameters C , X , AC are incremented. The next two subcodes are G_1 and G_2 which are not in sequence with G_3 , therefore $PIVCT$ is incremented ($PIVCT=2$). Assume that $CLIMIT = 5$ for the acquisition scheme. The next detected subcode is G_{13} and is in sequence with G_3 (Pivot # 1). This is followed by detection of the G_1 , G_3 , G_1 , G_6 . As is clear, these subcodes are not in sequence with G_3 , $PIVCT$ is incremented for each of three subcodes and hence the value of $PIVCT = 6$ at this stage of the search scenario. At this point of $PIVCT > CLIMIT$ and all parameters are re-initialized, the pivot subcode G_3 dropped and a new search scenario initiated as is illustrated in Figure 3.8. The next search scenario illustrates the consequences of assigning a wrong subcode the role of the pivot. The pivot subcode for search scenario # 2 is G_{11} . But the correct subcode should have been G_5 (assuming synchronous transmission of $User_1$ code sequence at some arbitrary time reference $t=0$) Thus inspite of the fact that the next two subcodes G_{11} and G_{13} are correct (with respect to the the time reference $t=0$), they obviously do not fall in sequence with the assigned pivot and hence would be counted as wrong subcodes. Search scenario # 2 illustrates the importance of the pivot. The fourth detected subcode in search scenario # 2 is G_6 and happens to be in sequence with G_{11} (the pivot # 2) and hence AC is incremented. The next four subcodes detected (again although are correct with respect to the time reference $t = 0$) do not fall in sequence with the pivot and thus $PIVCT$ is incremented. At this stage $PIVCT > CLIMIT$ and thus the reinitialization

procedure is invoked. Assume for the sake of illustration that at the end of the third search scenario, $\overline{AC} > \zeta$. In such a case, the acquisition procedure is stopped and the tracking loop invoked. The third search scenario illustrates a subtle point of the scheme that a search scenario leading to a successful declaration of acquisition could have a couple of subcodes that are not in sequence with the pivot. This aspect of the scheme reflects its inherent robustness.

Given below are some important features of the acquisition scheme.

1. The process of acquisition in the proposed scheme is the process of accumulation of sufficient sequential subcodes within a certain search scenario.
2. The number of sequential subcodes required for \overline{AC} to exceed ζ depends upon the value of ζ chosen. Therefore ζ should be cautiously fixed taking into account the level of interference encountered in the channel so as to minimize the probability of error.
3. The length of a search scenario is not fixed and depends indirectly upon the value of CLIMIT.
4. The number of subcodes to be searched and detected to declare acquisition of a user code is not fixed. Also it is not necessary to search the entire length of the user code to declare acquisition.
5. It is possible that a search scenario leading to acquisition contains a few subcodes not in sequence with the pivot.

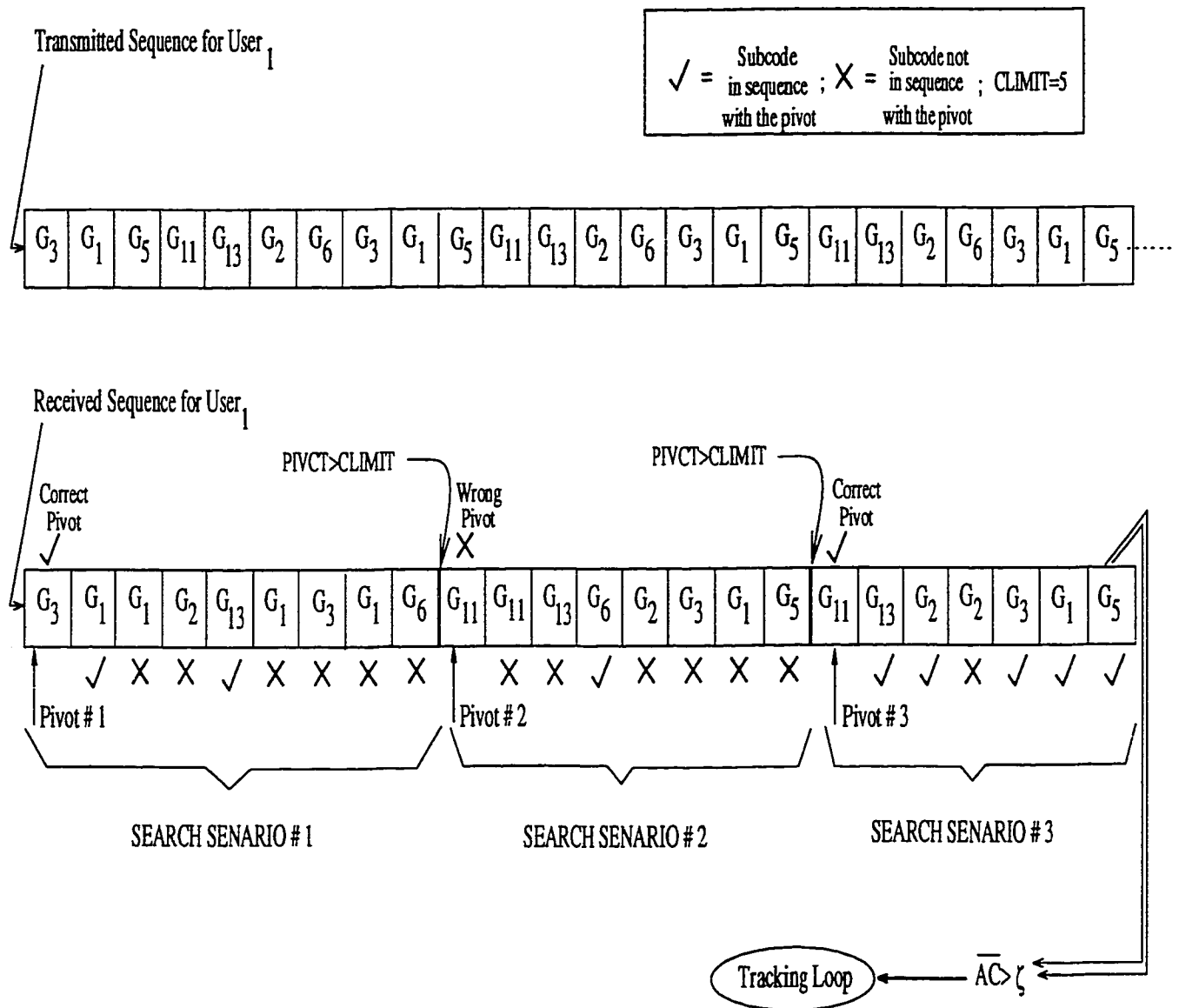


Figure 3.8: Processing of the received signal for CLIMIT= 5

3.2.3 Simulation Procedure and Performance in a Multiple Access Environment

Simulation studies of the Hybrid Acquisition scheme were performed in an additive white gaussian channel in the presence of multiple access interference. The general steps involved in the process of simulation are given below.

1. The first step was generating Gold Codes of length 127 chips. The code generators were developed in matlab (appendix contains the source code for the functions used in simulation). After generating Gold Codes of length 127 chips, each user was assigned a specific sequence of these short codes. The user basic code length 'N' of 6 and the value of repetition 'M' used for the user long code was 20 in the simulation studies.
2. Generation of random phases of the Gold Codes. The random phases were assigned to the codes using the random generator of Matlab which follow a Normal distribution with mean zero and variance one.
3. Each user was then created by assigning a specific sequence of the above mentioned short Gold Codes (along with the random phases that were assigned to each of these short codes).
4. After the creation of all users, the transmitted signal was represented by a sum of all the user signals. AWGN was then introduced in the signal by adding additive white gaussian noise (AWGN) which was again the random generator of Matlab, with mean zero and variance as defined by the SNR in the simulation graphs. This final signal constitutes the *transmitted signal*.
5. At the receiver end the signal was fed into a bank of user specific matched filters. Details of the source code of the matched filters are listed in the appendix.

6. After feeding the received signal into a user specific bank of matched filters, the maximum value of the filter out of the bank of matched filters represented the most probable phase of the transmitted signal, and this information was processed along the steps of the block diagram of the proposed acquisition scheme as described in the previous sections.

The received signal at the bank of matched filters can be expressed as,

$$r_k(t) = \sum_{k=1}^K A_k s_k(t - \tau_k) \cos(\omega_c t + \phi_k) + n(t) \quad (3.11)$$

where it was assumed that data modulation of the users is absent.

K = Number of simultaneous users in the channel.

A_k = Amplitude of the k^{th} user.

$s_k(t)$ = Signature code of the k^{th} user at a specific rate R_c chips/sec.

$n(t)$ = Additive White Gaussian Noise with a specific variance.

τ_k = Time delay of the k^{th} user.

ϕ_k = Phase of the k^{th} user.

It was also assumed that the receiver had knowledge of the phase ϕ_k of the user and therefore accurate carrier recovery was assumed. Under such an assumption the received signal can be expressed as

$$r_k(t) = \sum_{k=1}^K A_k s_k(t - \tau_k) + n(t) \quad (3.12)$$

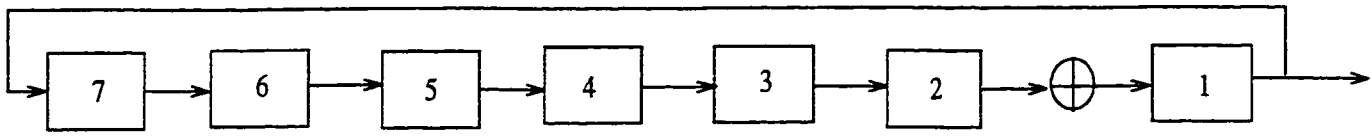
The detection of the user subcode at the receiver involves correlation of the receiver replica of the signature sequence and hence, the output of the bank of matched filters can be mathematically expressed as

$$\hat{s}_k(t) = \max \left(\int_0^{NT_c} r(t) s_i(t + \hat{\tau}_k) dt \right) \quad (3.13)$$

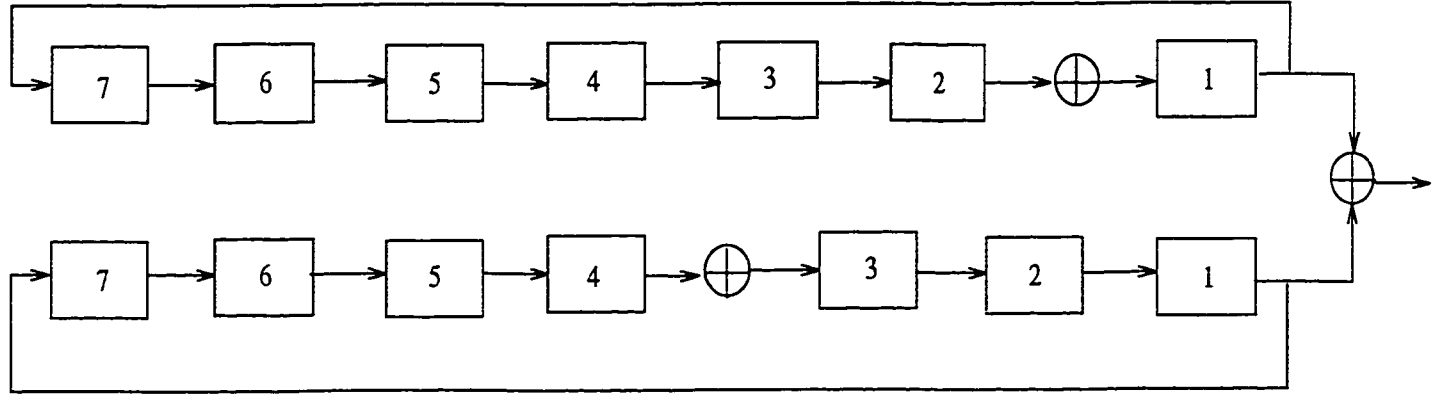
where $i \in \{1, 2, 3, \dots, N\}_k$, (i belongs to the set of the N subcodes assigned to the user 'k', assuming that 'k' represents the intended user), $\hat{s}_k(t)$ represents the receiver estimate of the most probable subcode, $\hat{\tau}_k$, the receiver estimate of the delay of the

subcode. This maximum value is processed along the steps mentioned previously to evaluate the mean acquisition time and probability of acquisition.

The characteristic polynomial of the shift registers used for generating the Gold Codes are $g_1(x) = 1 + x^3 + x^7$ and $g_2(x) = 1 + x + x^7$. The family of Gold Codes of length 127 chips (a total of 129) were generated as shown in Figure 3.9. The Simulation was performed in Matlab. The details of the simulation programs are given in the Appendix for interested readers.



(a)



(b)

Figure 3.9: (a) The Shift Register used to generate the Maximal Length Sequences.
 (b) The Gold Code generator of length 127 ($n = 7$)

3.2.4 Simulation Results

As mentioned in the previous section, the simulations were performed in a non-fading channel and in the presence of multiple access interference. Two sets of performance parameters were evaluated for the scheme, the first one being the Mean Acquisition Time (T_{ACQ}), the second being the Overall Probability of Detection, or (equivalently the probability of acquisition) P_{ACQ} (P_{FA} being related to the P_{ACQ} as $P_{ACQ} + P_{FA} = 1$). The performance parameters were studied for different values of the parameters of the scheme. The two main parameters of the scheme are the sub-code count limit ($CLIMIT$), and the normalized threshold value (ζ). All simulations were performed for $CLIMIT = 6$, and ζ ranging from 6 to 12. Two separate detection processes were studied, the Hard decision detection and Soft decision detection cases. Also each of these cases were studied for SNR's (Signal to noise ratios) ranging from 0dB to 8dB. Hard decision refers to the firm decision made on the received signal quantizing each received chip to $\{0,1\}$ (and subsequently into $\{-1, +1\}$). This is implemented in the simulation by simply employing a limiter at the receiver. Soft decision detection involves processing the received signal (without making any hard decision) as it is.

Before going into the details of the simulation results, a small note on another performance parameter, the variance of the acquisition time σ_{ACQ}^2 . Although we have not evaluated this parameter in our simulation studies, useful information can be obtained from this parameter. The process of evaluation would involve finding the mean square $\overline{T^2}$, and the square of the mean acquisition time \overline{T}^2 , and the usual formula of the variance.

- Figure 3.10 (page 65) is the simulation plot of the mean time to acquire a specific user code (T_{ACQ}) as a function of the number of simultaneous users (multiple access interference). A total of six graphs are shown in the figure. A set of three are for the hard decision detection for SNR's of 0dB, 4dB, 8dB,

the other set of three plots are for the soft decision detection for SNR's of 0dB, 4dB, 8dB. The value of ζ (normalized threshold) is 6, and $CLIMIT=6$. As is clearly visible, soft decision detection results in lower acquisition time as compared to hard decision detection. This reflects the fact that in the case of soft decision, the mean accumulator value (\overline{AC}) crosses ζ faster as compared to the hard decision case, which means that within a certain search scenario, more detected subcodes fall out of sequence with the pivot (as the identity of the detected subcodes are in error!) as compared to the soft decision case. It can also be observed from the plots that the time to acquire a user code for $SNR = 8dB$, hard decision detection, is almost the same as the case of soft decision detection for $SNR=0dB$. It is also important to interpret the results of Figure 3.10 in conjunction with Figure 3.11.

- Figure 3.11 (page 66) is a plot of the probability of acquisition (P_{ACQ}) as a function of the multiple access interference. Again two sets of plots, one for hard decision (SNR's= 0dB, 4dB, 8dB) and the other for soft decision (SNR's 0dB, 4dB, 8dB) are illustrated. The value of $\zeta = 6$ and $CLIMIT = 6$. It can be observed that in low levels of multiple access interference, the probability of acquiring the user code is high, but decreases with increasing load. In conjunction with Figure 3.10, we see that for both cases of hard and soft decision detection, as multiple access interference increases, the probability of acquisition decreases with a corresponding increase in the mean acquisition time.
- Figure 3.12 (page 67) is the plot of mean acquisition versus the number of users for SNR's 0dB and 4dB (hard decision) and SNR's 0dB, 4dB, 8dB (soft decision) for $\zeta = 8$, $CLIMIT = 6$. As it is visible, because of the higher value of the normalized threshold ($\zeta = 8$), the mean acquisition time is higher as compared to Figure 3.10 ($\zeta = 6$).

- Because of a higher threshold value, the probability of detection Figure 3.13 (page 68) (or acquisition) is visibly higher (for the same level of load) as compared to Figure 3.11. Hence we encounter a trade-off! Higher threshold(ζ) values for a certain fixed value of $CLIMIT$, although they have a better performance in terms of the probability of detection (and thus have a lower value probability of false alarm), require more time to acquire the codes. Therefore depending upon the requirements of a particular application at hand, the value of the system parameters must be fixed to meet the required performance criterion.
- Figure 3.14 (page 69) is the simulation plot of the mean acquisition again as a function of users in the channel for $\zeta = 10$, $CLIMIT = 6$ for SNR's 0dB, 4dB and 8dB (hard decision case) and SNR's 0dB, 4dB for soft decision detection. Again, a visible increase in the acquisition time is observed as compared to Figure 3.10.
- Figure 3.15 (page 70) represents the probability of acquisition as a function of multiple access interference for $\zeta = 10$, $CLIMIT = 6$, SNR's of 4dB and 8dB (soft decision case).
- Figure 3.16 (page 71) are simulation results for the mean acquisition for $\zeta = 12$, $CLIMIT = 6$, SNR's 4dB and 8dB for hard decision case and SNR's of 0dB, 4dB for soft decision case.
- Figure 3.17 (page 72) is the plot of the corresponding probability of detection for $\zeta = 12$, $CLIMIT = 6$, SNR's 4dB, 8dB for hard decision and SNR's 0dB, 4dB and 8dB for soft decision detection.
- Figure 3.18 (page 73) and Figure 3.19 (page 74) clearly illustrate the trade-off aspect between the mean acquisition time and probability of detection for $CLIMIT = 6$, $\zeta = 6, 8, 10, 12$, SNR=4dB and detection process being soft

decision. Higher values of ζ would require more time to acquire the codes but would have a better performance in terms of the probability of detection (i.e., low false alarms).

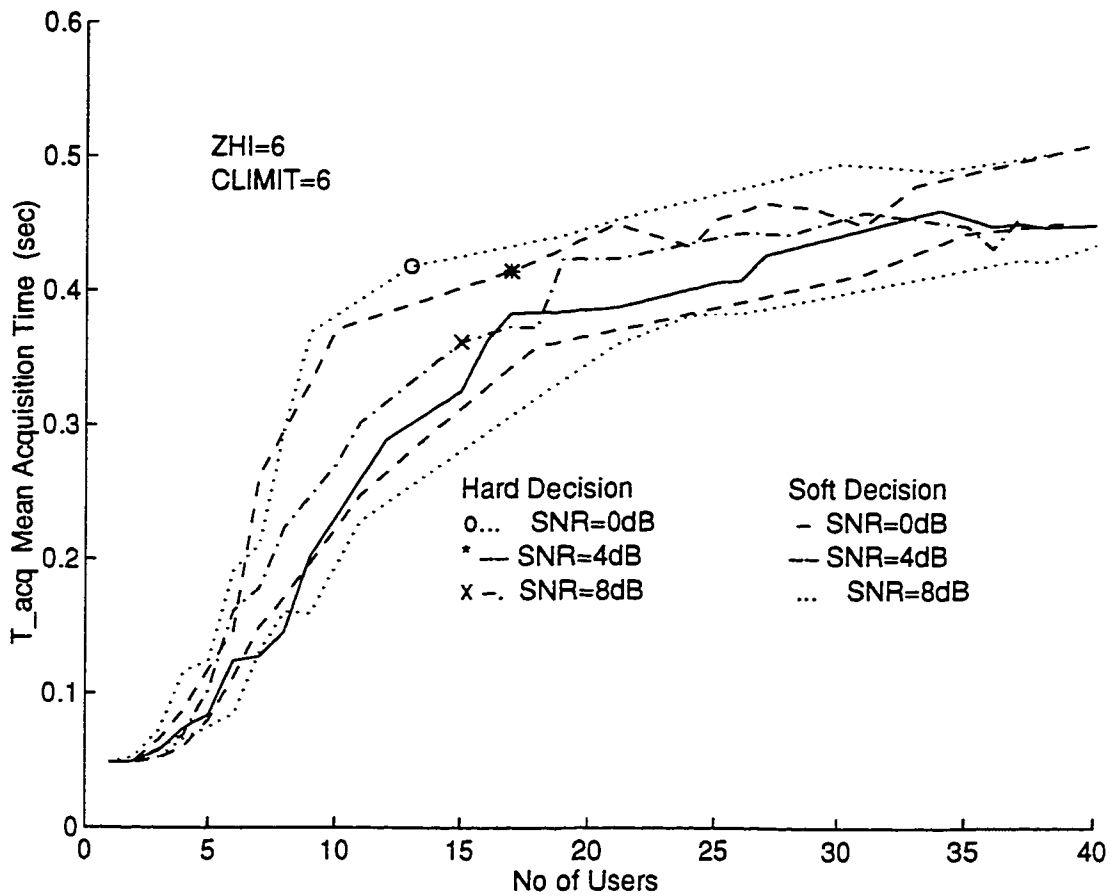


Figure 3.10: Mean Acquisition Time versus Number of Users for $\zeta(ZHI) = 6$, $CLIMIT = 6$ for Hard Decision and Soft Decision Cases and Signal to Noise Ratio's of 0dB, 4dB and 8dB. Chip rate is 1M chips/sec, processing gain = 127.

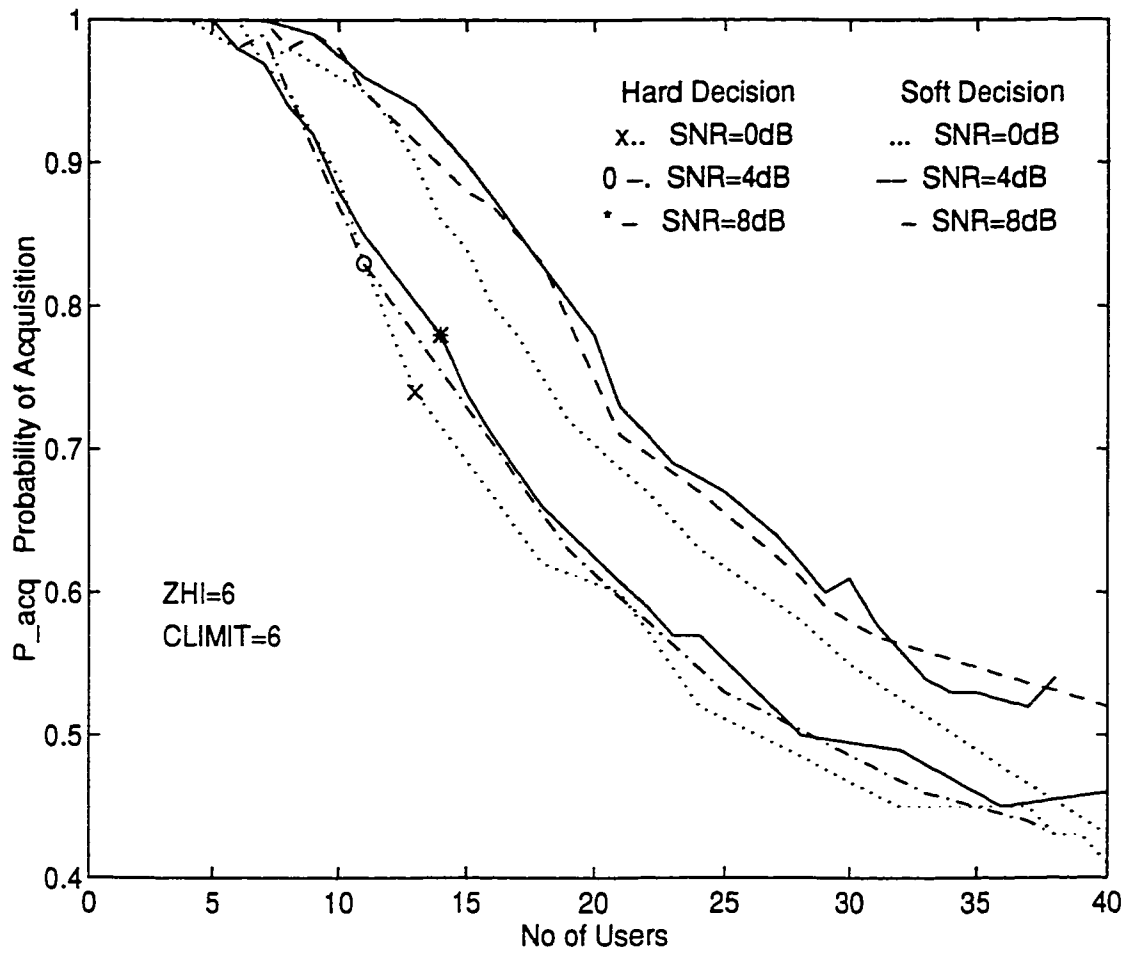


Figure 3.11: Probability of Acquisition versus Number of Users for $\zeta(ZHI) = 6$, $CLIMIT = 6$, SNR's: 0dB and 4dB for Hard Decision Case and SNR's 0dB, 4dB and 8dB for Soft Decision Case. Chip rate is 1M chips/sec, processing gain = 127.

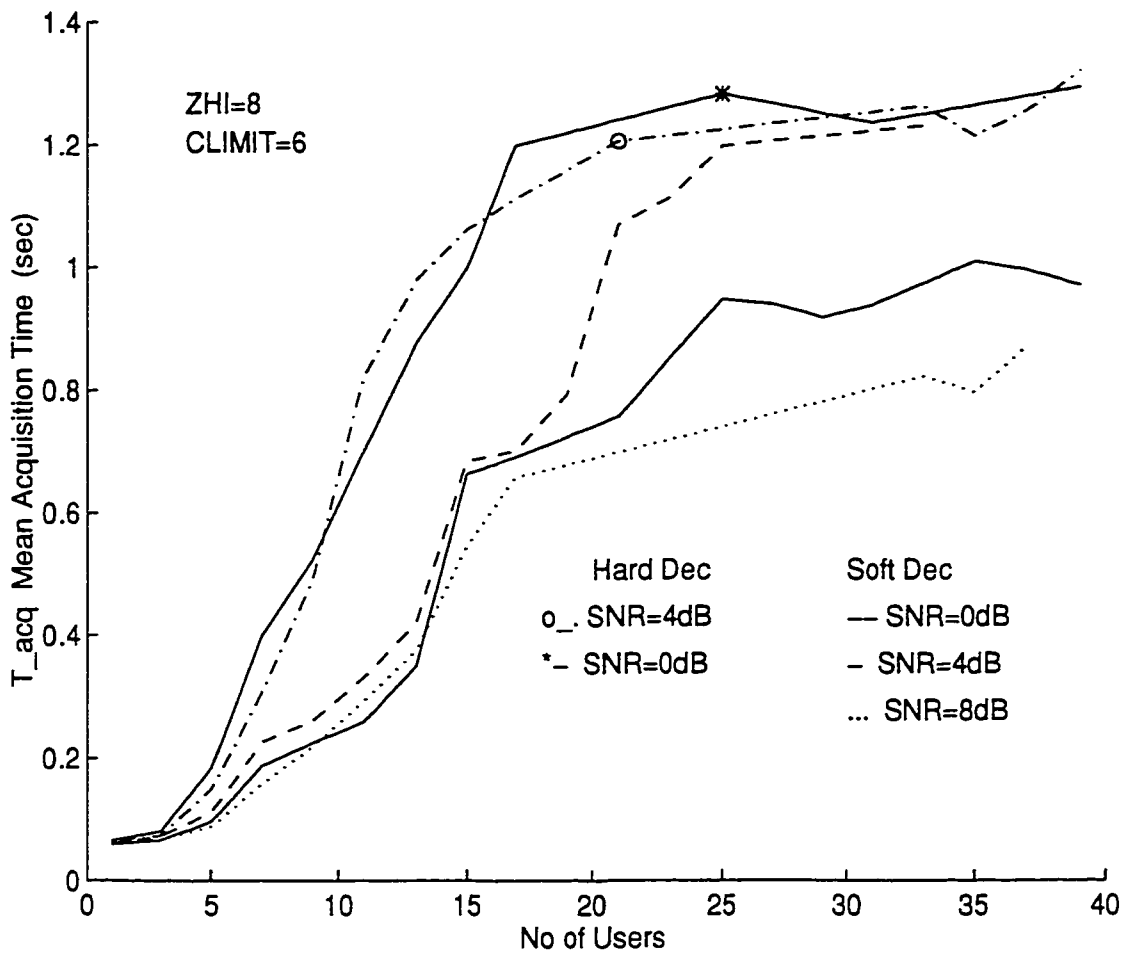


Figure 3.12: Mean Acquisition Time versus Number of Users for $\zeta(ZHI) = 8, CLIMIT = 6$ for SNR's: 0dB and 4dB for Hard Decision Case, SNR's 0dB, 4dB and 8dB for Soft Decision Case. Chip rate is 1M chips/sec, processing gain = 127.

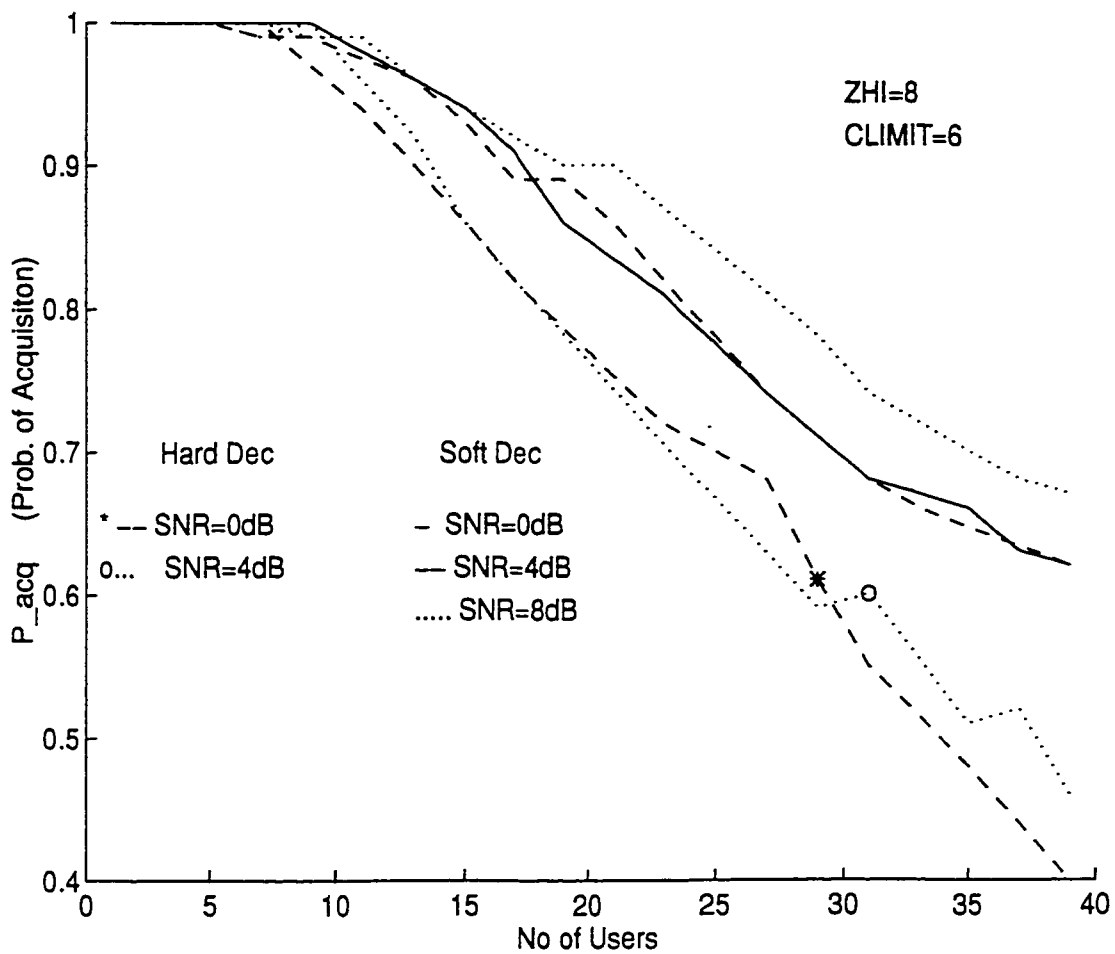


Figure 3.13: Probability of Acquisition versus Number of Users for $\zeta(ZHI) = 8$, $CLIMIT = 6$, SNR's: 4dB and 8dB for Hard Decision and SNR's: 0dB, 4dB and 8dB for Soft Decision Case. Chip rate is 1M chips/sec, processing gain = 127.

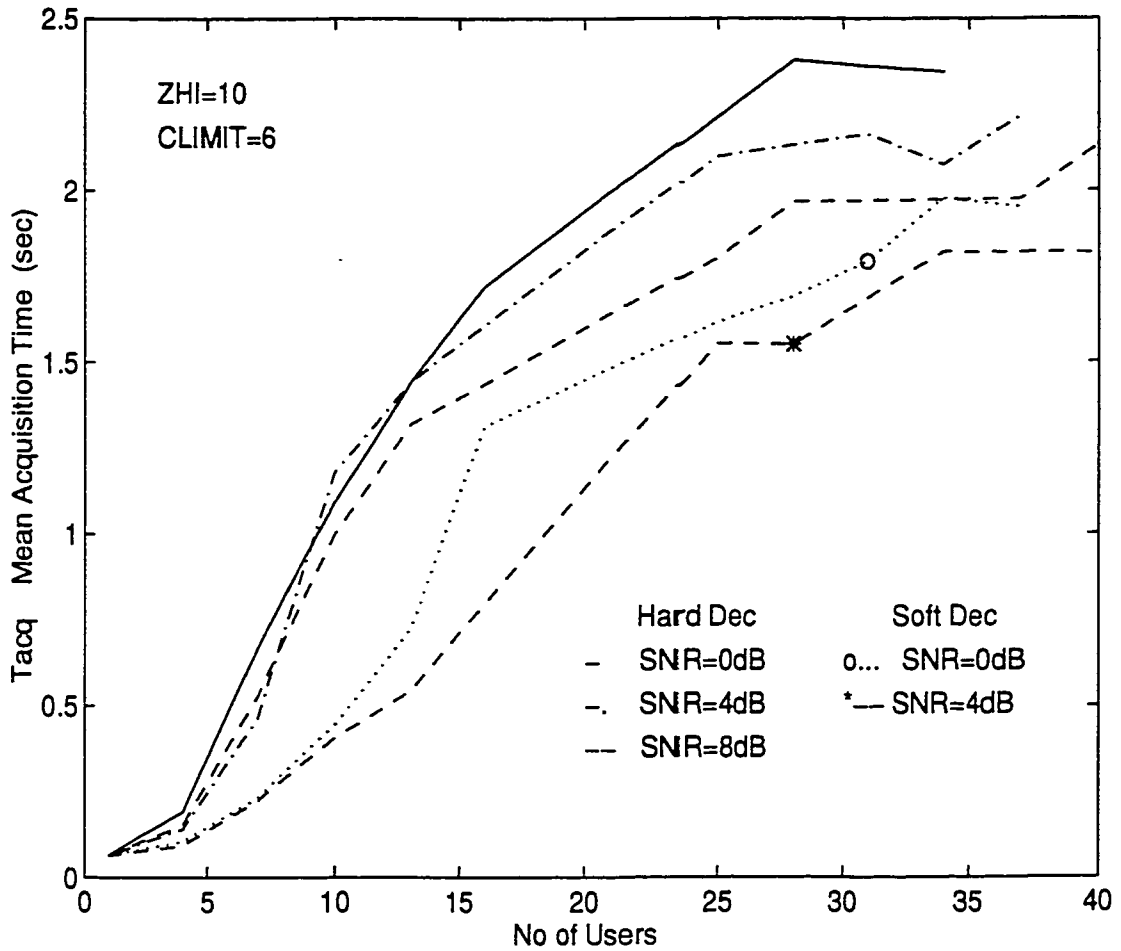


Figure 3.14: Mean Acquisition versus Number of Users for $ZHI = 10$, $CLIMIT = 6$, SNR's: 0dB, 4dB and 8dB for Hard Decision Case and SNR's: 0dB and 4dB for the Soft Decision Case. Chip rate is 1M chips/sec, processing gain = 127.

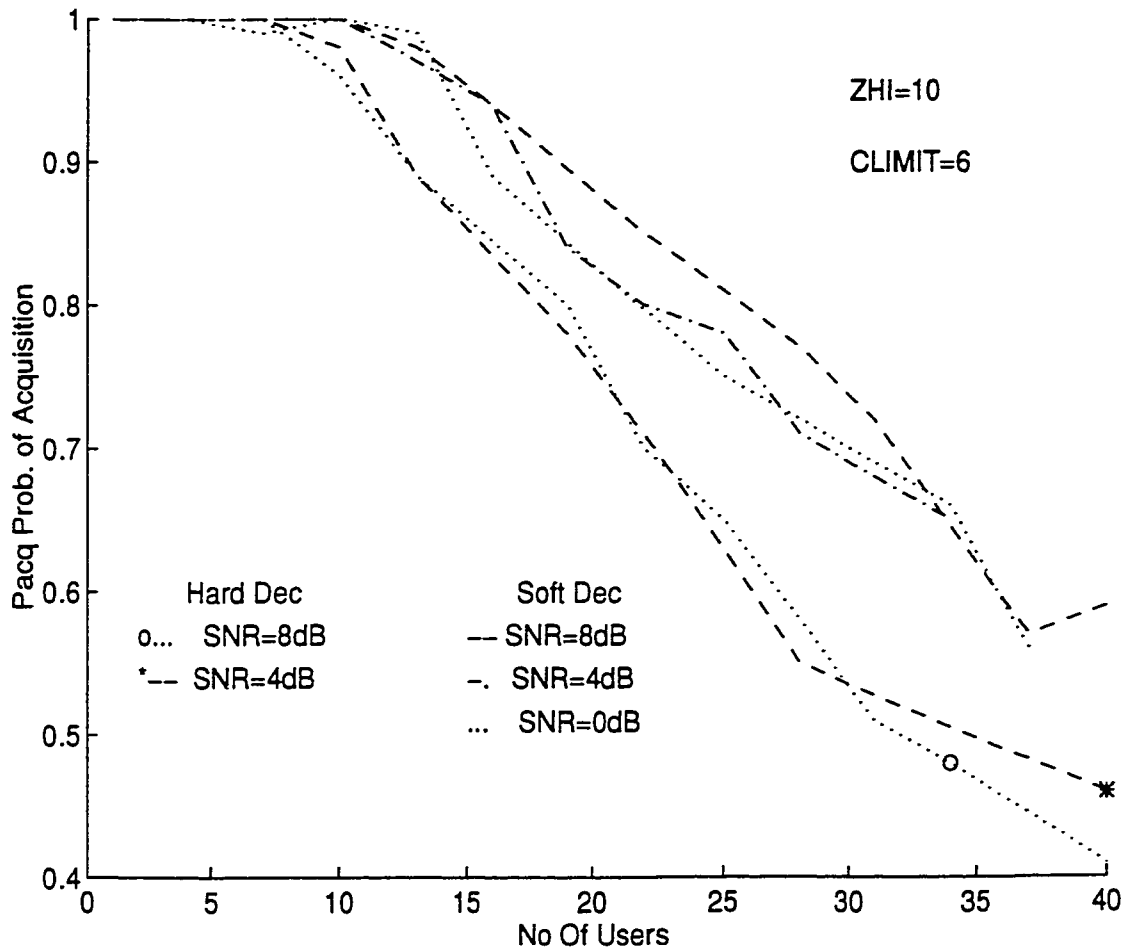


Figure 3.15: Probability of Acquisition versus Number of Users for $\zeta(ZHI) = 10$, $CLIMIT = 6$, SNR's: 4dB and 8dB for Hard Decision Case and SNR's 0dB, 4dB and 8dB for the Soft Decision Case. Chip rate is 1M chips/sec, processing gain = 127.

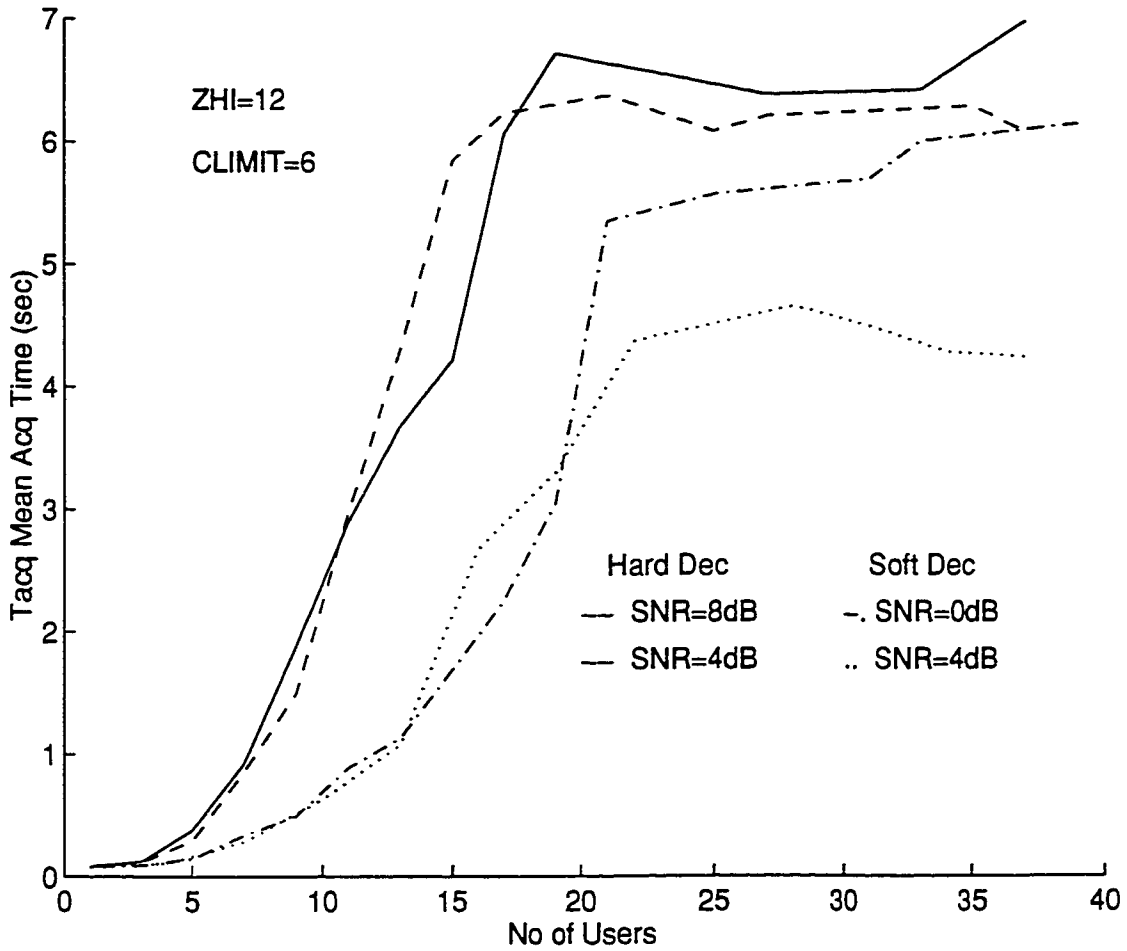


Figure 3.16: Mean Acquisition Time versus Number of Users for $\zeta(ZHI) = 12$, $CLIMIT = 6$, SNR's: 4dB and 8dB for Hard Decision Case and SNR's: 0dB and 4dB for Soft Decision Case. Chip rate is 1M chips/sec, processing gain = 127.

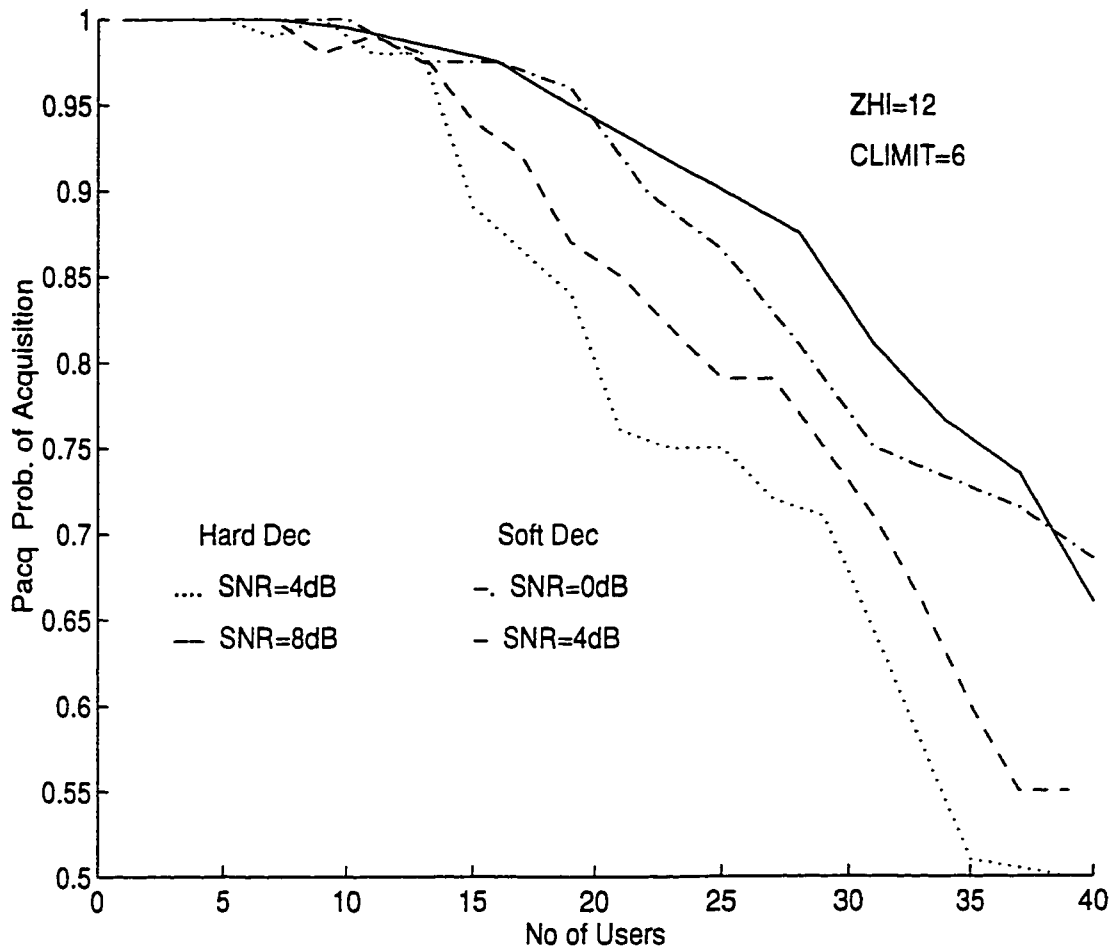


Figure 3.17: Probability of Acquisition versus Number of Users for $\zeta(ZHI) = 12, CLIMIT = 6$, SNR's 4dB and 8dB for Hard Decision case and SNR's: 0dB and 4dB for Soft Decision Case. Chip rate is 1M chips/sec, processing gain = 127.

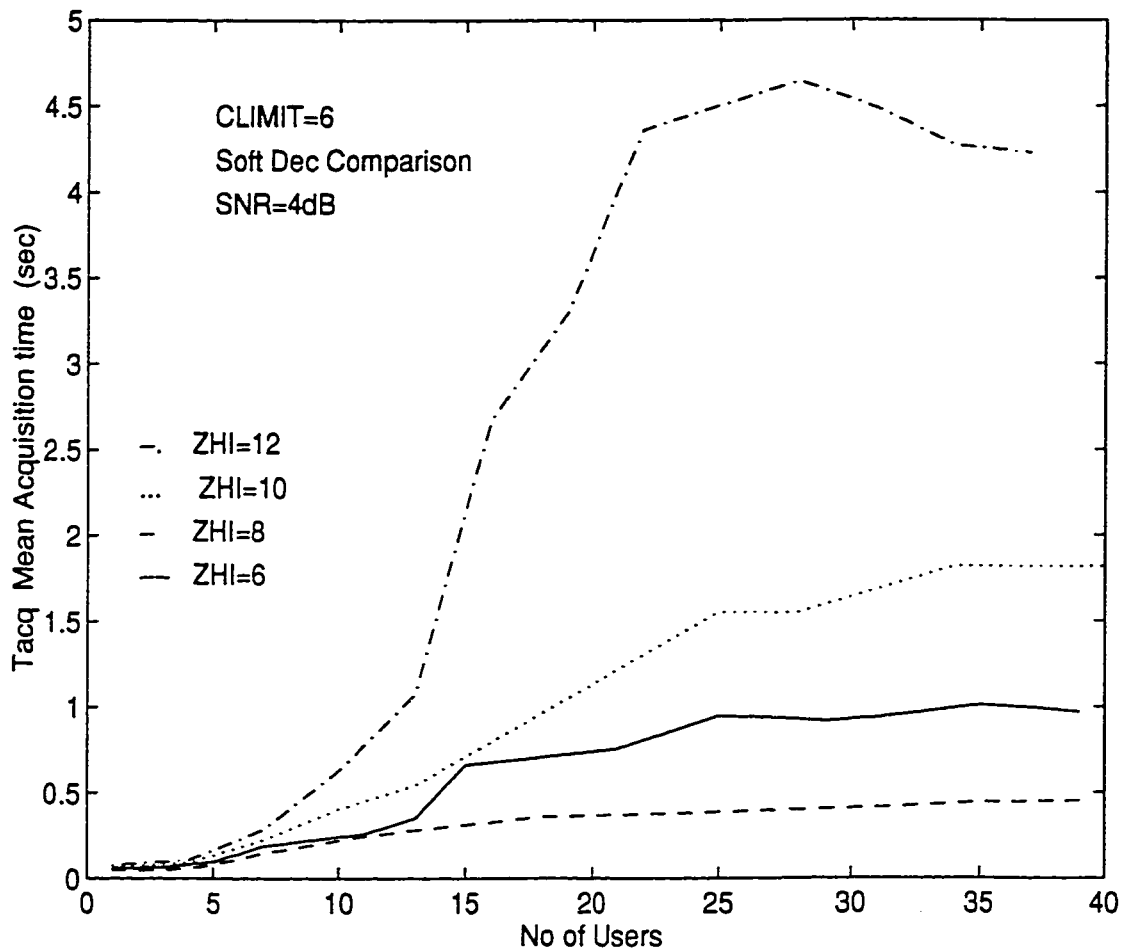


Figure 3.18: Soft Decision Comparison of the Mean Acquisition Time versus Number of Users for $\zeta(ZHI) = 6, 8, 10, 12$ and $CLIMIT = 6$ for Signal to Noise Ratio (SNR)=4dB. Chip rate is 1M chips/sec, processing gain = 127.

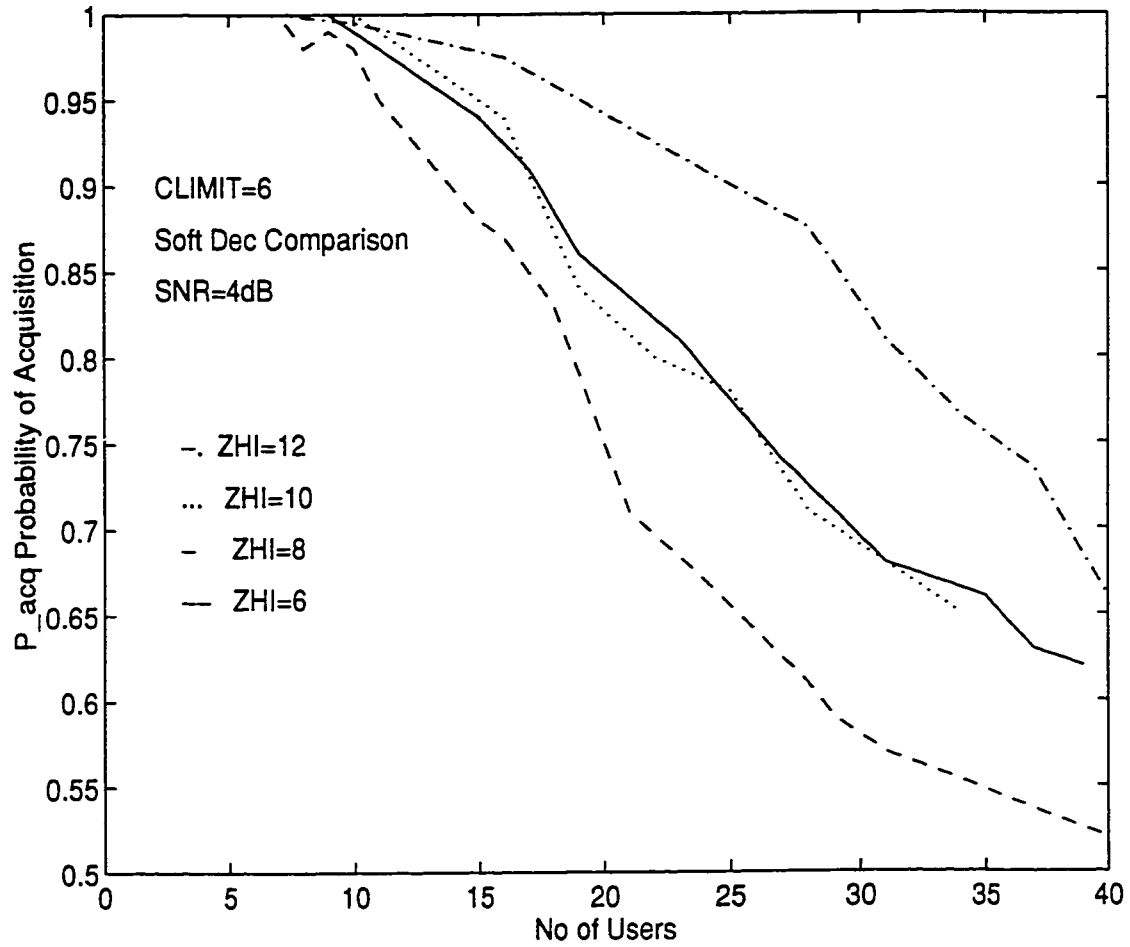


Figure 3.19: Soft Decision comparison of the Probability of Acquisition versus Number of Users for $\zeta(ZHI) = 6, 8, 10, 12$ and $CLIMIT = 6$ for Signal to Noise Ratio (SNR) = 4dB. Chip rate is 1M chips/sec, processing gain = 127.

Chapter 4

Simplified Analytical Model and Performance in a Non Selective Rayleigh Fading Channel

In this chapter we introduce a simplified analytical model of the proposed hybrid acquisition scheme. Certain assumptions are made in the analysis of the scheme to simplify the complexity involved in developing the expressions for the mean and variance of the acquisition time. The performance of this simplified acquisition scheme is studied in a Rayleigh fading environment. Expressions for the mean and variance of the acquisition time are developed using signal flow graph techniques. Finally numerical results of this model are presented.

4.1 Simplified Analytical Model

In the previous chapter a detailed description of the proposed Hybrid Acquisition scheme was presented. An analytical model of this acquisition scheme is developed here under certain set of assumptions. Although the assumptions do lead to a more restricted scheme, considerable simplification in analysis is realized. Also we adopt

the method followed by [32] and [33]

The two assumptions adopted in the Simplified model are

1. The length of the search scenarios is fixed and same from one search scenario to another.
2. Every subcode detected in a search scenario contributes equally to the accumulator value (which means that the accumulator weight X is set to zero).

Figure 4.1 illustrates the Block Diagram of the Simplified acquisition scheme for a fading channel. Figure 4.2 illustrates the structure of passive Non-Coherent I-Q matched filter, Figure 4.3 of the matched filter correlator. The phase update size of the search scheme is set to half a chip ($\Delta = 1/2$). In T seconds M/Δ samples from each of the MF's are collected and stored. As before, the filter with the maximum value is chosen as the most likely subcode and this information is processed further along the lines as described in chapter 3.

The markovian nature of the acquisition process allows the state transition diagram approach to be used in deriving the probability generating function for the acquisition time. Figure 4.4 illustrates the circular state transition diagram of the acquisition system. In MT_c seconds (M = length of the subcode), (MN/Δ) samples are stored from the bank of N matched filters. The maximum value among all samples represents the most likely transmitted subcode with a certain probability of detection P_D . This assumption could also be wrong with a certain probability, designated as the probability of false alarm P_{FA} . Since the maximum filter value is chosen from the bank of filter, and is not compared to any threshold value, this is equivalent to the case of having the threshold value as zero. Because of this, the probability of missed detection $P_M = 0$, and $P_D + P_{FA} = 1$. This information about the identity of the subcode is then processed along the lines of the block diagram as shown in Figure 4.1 (the detailed steps are described in chapter 3, pages 48-52). In the event that sufficient number of subcodes are not in sequence with the

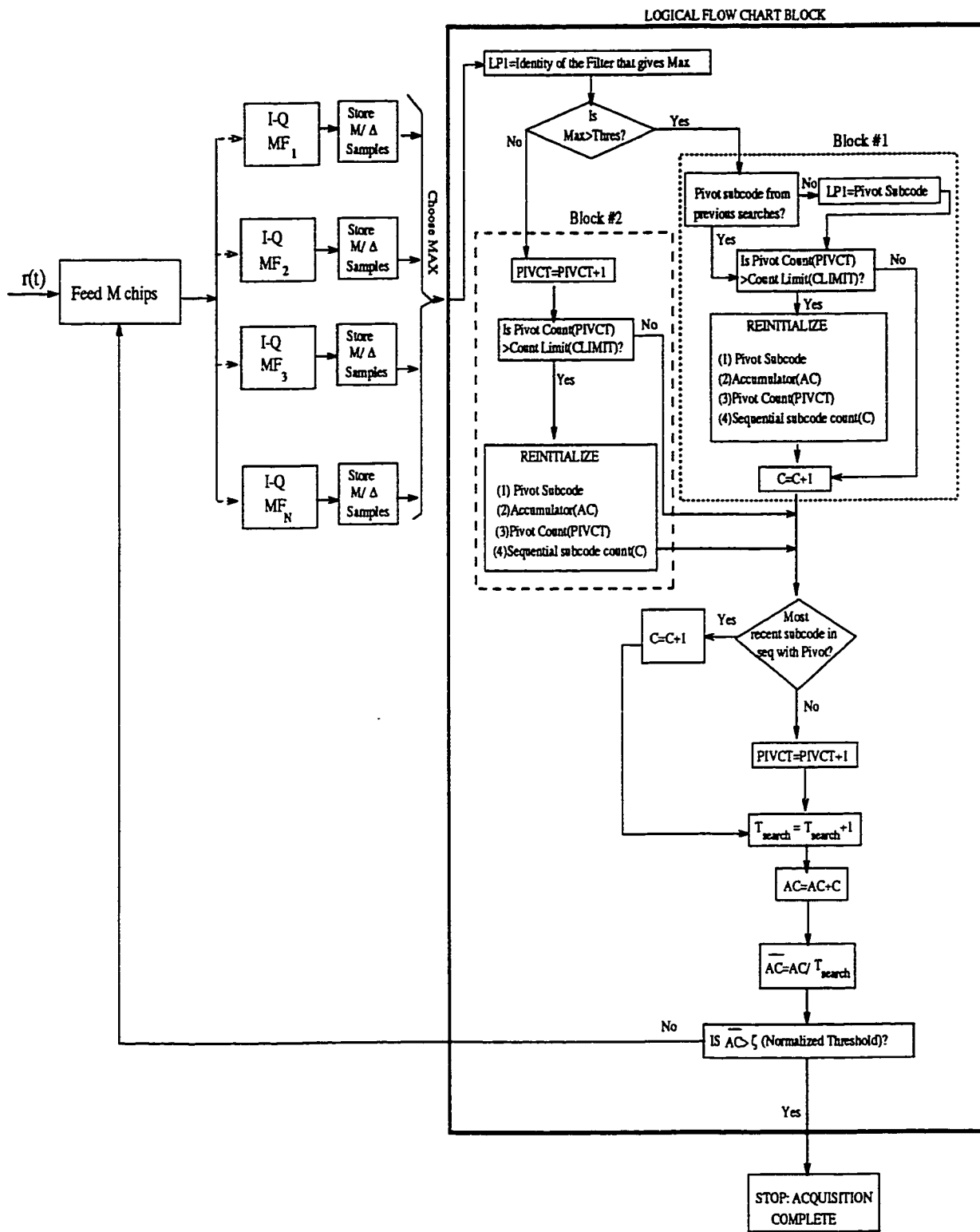
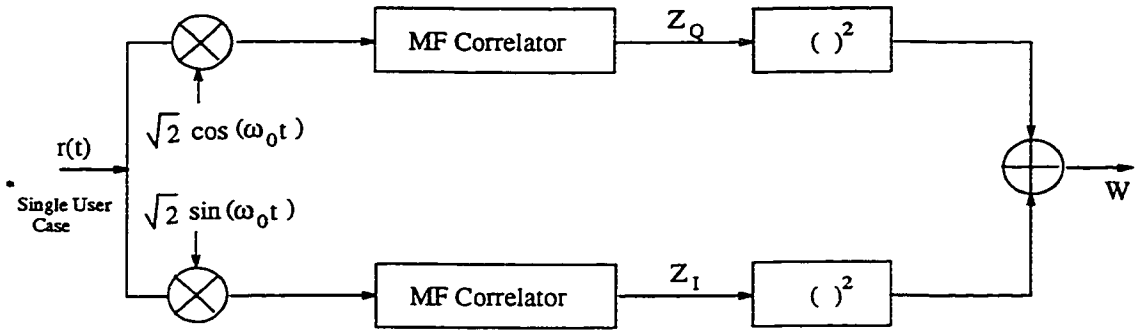


Figure 4.1: Block Diagram of the Simplified Acquisition Scheme for a Fading Channel



* The received signal is for a single user case (i.e., No multiple access interference treated).

Figure 4.2: I-Q Matched Filter detector structure

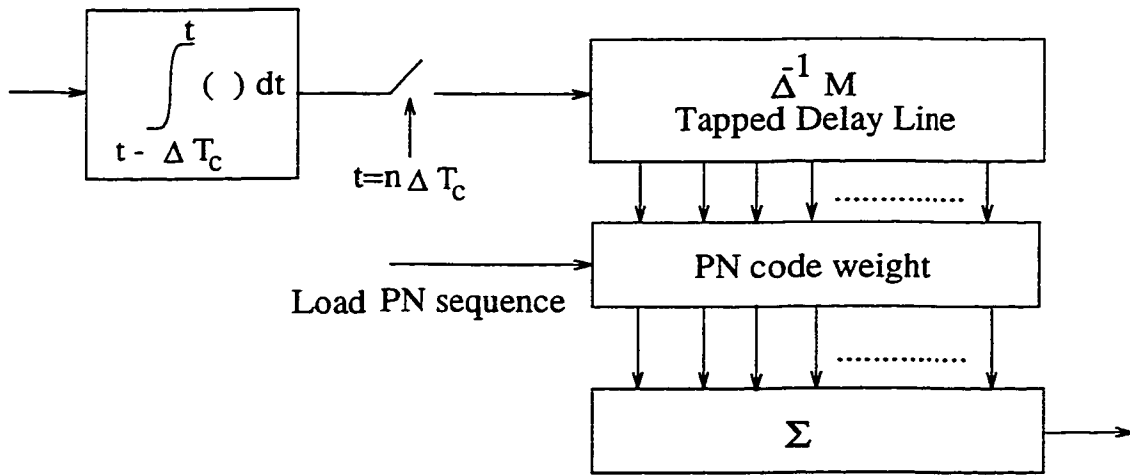


Figure 4.3: Structure of the Matched Filter Correlator

designated pivot subcode of the search scenario, the next set of M chips is loaded into the bank of I-Q matched filters and another set of M/Δ samples is chosen again. The process continues until either the value of PIVCT exceeds CLIMIT, which leads to reinitialization of all parameters of the acquisition process and the initiation of a new search scenario, or a declaration of acquisition (with a certain probability of detection designated as $P_{D-Overall}$). There is also a possibility that the above mentioned acquisition is incorrect, with a probability designated as $P_{FA-Overall}$. It is important to note that there are two types of probabilities discussed here, one being on the individual subcode level, (P_D, P_{FA}) , and the other on the level of the search scenario, $(P_{D-Overall}, P_{FA-Overall})$. In the event that acquisition is declared, and the corresponding phase is correct (with a probability $P_{D-Overall}$); the acquisition is complete, and tracking enabled. If the phase is incorrect (with a probability $P_{FA-Overall}$), the system goes back to acquisition after a certain penalty time of JT seconds.

The generating functions associated with the events of Detection $H_1(z)$, False Alarm $H_2(z)$, Missed Detection $H_3(z)$ (which is on the level of the search scenario and refers to the fact that sufficient number of subcodes are not in sequence with the designated pivot of the search scenario, and is not referred to on the individual subcode level), and penalty $H_4(z)$ are ($C=CLIMIT$) given in the following,

$$H_1(z) = \begin{cases} P_D \left[P_D^{\zeta-1} z^{\zeta T} + \binom{\zeta-1}{\zeta-2} P_D^{\zeta-1} (1-P_D) z^{(\zeta+1)T} + \binom{\zeta}{\zeta-2} P_D^{\zeta-1} \right. \\ \left. (1-P_D)^2 z^{(\zeta+2)T} + \binom{\zeta+k-2}{\zeta-2} P_D^{\zeta-1} (1-P_D)^k z^{(\zeta+k)T} + \dots \right. \\ \left. \dots + \binom{C-2}{\zeta-2} P_D^{\zeta-1} (1-P_D)^{(C-\zeta)} z^{CT} \right] & \zeta > 2 \\ P_D \left[P_D z^{2T} + P_D (1-P_D) z^{3T} + \dots + P_D (1-P_D)^{(C-2)} z^{(CT)} \right] & \zeta = 2 \end{cases} \quad (4.1)$$

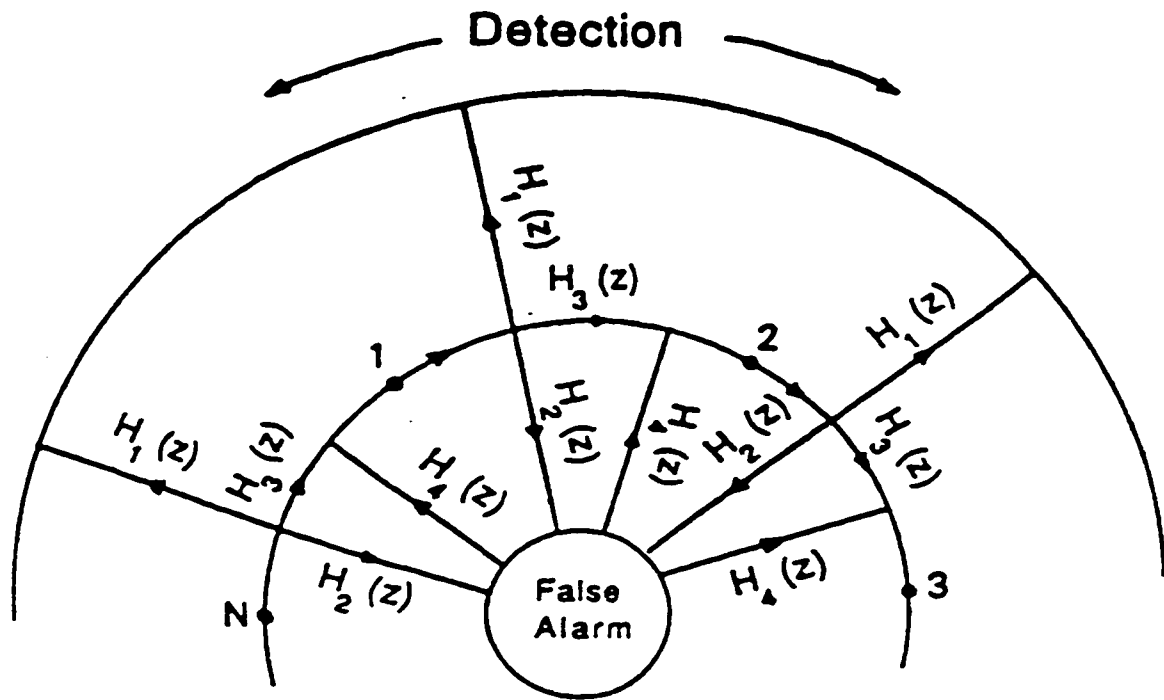


Figure 4.4: Circular State Transition Diagram of the Simplified Acquisition Scheme for a Rayleigh Fading channel

Equation (4.1) is an enumeration of all possible events leading to the declaration of detection. The first term represents the case of detecting $(\zeta - 1)$ consecutive subcodes, all in sequence with the pivot of the search scenario (the P_D term outside the square bracket represents the term corresponding to the pivot subcode). The second term in the expression represents the case of having again $\zeta - 1$ subcodes in sequence with the pivot, but this term includes one subcode not in sequence with the pivot (and therefore a total of $\zeta + 1$ subcodes are tested inclusive of the pivot). The final term in the series represents the case of detecting $(\zeta - 1)$ in sequence with the pivot along with $(C - \zeta)$ incorrectly positioned subcodes. The combinatorial term represents the possible distinct cases that lead to such a declaration.

$$H_2(z) = \begin{cases} P_F \left[P_F^{\zeta-1} z^{\zeta T} + \binom{\zeta-1}{\zeta-2} P_F^{\zeta-1} (1 - P_F) z^{(\zeta+1)T} + \binom{\zeta}{\zeta-2} P_F^{\zeta-1} \right. \\ \left. (1 - P_F)^2 z^{(\zeta+2)T} + \binom{\zeta+k-2}{\zeta-2} P_F^{\zeta-1} (1 - P_F)^k z^{(\zeta+k)T} + \dots \right. \\ \left. \dots + \binom{C-2}{\zeta-2} P_F^{\zeta-1} (1 - P_F)^{(C-\zeta)} z^{CT} \right] & \zeta > 2 \\ P_F \left[P_F z^{2T} + P_F (1 - P_F) z^{3T} + \dots + P_F (1 - P_F)^{(C-2)} z^{(CT)} \right] & \zeta = 2 \end{cases} \quad (4.2)$$

Equation (4.2) represents the generating function for the declaration of a false alarm in a particular search scenario. The series is identical to the previous expression for detection except for the difference that the term P_D in equation (4.1) should be replaced by P_{FA} . The first term represents the case of falsely identifying the pivot, followed by false declaration of $(\zeta - 1)$ subcodes (apparently in sequence with a wrong pivot subcode). It is important to note that a false alarm means that the maximum value out of the bank of filters, representing the most probable transmitted subcode is different from that transmitted.

$$H_3(z) = \begin{cases} P_D \left[(1 - P_D)^{C-1} + \binom{C-1}{1} P_D (1 - P_D)^{C-2} + \dots \right. \\ \left. \dots + \binom{C-1}{\zeta-2} P_D^{(\zeta-2)} (1 - P_D)^{(C-\zeta+1)} \right] z^{(CT)} \\ + P_F \left[(1 - P_F)^{C-1} + \binom{C-1}{1} P_F (1 - P_F)^{C-2} + \dots \right. \\ \left. + \binom{C-1}{\zeta-2} P_F^{(\zeta-2)} (1 - P_F)^{(C-\zeta+1)} \right] z^{(CT)} & \zeta > 2 \\ P_D \left[(1 - P_D)^{(C-1)} \right] z^{(CT)} + P_F \left[(1 - P_F)^{(C-1)} \right] z^{(CT)} & \zeta = 2 \end{cases} \quad (4.3)$$

Equation (4.3) is an expression for a missed detection on the search senario level. This would mean that the number of subcodes detected in sequence with the pivot within the search senario length is less than $\zeta - 1$ (excluding the pivot for the search senario). Upon reflection, it becomes clear that there would be two separate series representing such a situation, firstly, a correctly detected pivot subcode and insufficient number of subcodes in sequence with this pivot within a search senario, secondly, a wrongly declared pivot (a false alarm in detecting the pivot) and again insufficient number of subcode is sequence with this pivot within a search senario, leading to a probable false alarm. Finally equation. (4.4) represents the generating function for the penalty time after the declaration of a false alarm.

$$H_4(z) = z^{(JT)} \quad (4.4)$$

which in a shorter form can be expressed as

$$H_1(z) = \begin{cases} P_D^\zeta \left[\sum_{i=0}^{C-\zeta} \binom{\zeta-2+i}{\zeta-2} P_F^i z^{(\zeta+i)T} \right] & \zeta > 2 \\ P_D^2 \left[\sum_{i=0}^{C-2} P_F^i z^{(i+2)T} \right] & \zeta = 2 \end{cases} \quad (4.5)$$

$$H_2(z) = \begin{cases} P_F^\zeta \left[\sum_{i=0}^{C-\zeta} \binom{\zeta-2+i}{\zeta-2} P_F^i z^{(\zeta+i)T} \right] & \zeta > 2 \\ P_F^2 \left[\sum_{i=0}^{C-2} P_F^i z^{(i+2)T} \right] & \zeta = 2 \end{cases} \quad (4.6)$$

$$H_3(z) = \begin{cases} \left[\sum_{i=0}^{\zeta-2} \binom{C-1}{i} \{ P_D^{(i+1)} P_F^{(C-i-1)} + P_F(i+1) P_D^{(C-i-1)} \} \right] z^{(CT)} & \zeta > 2 \\ \left[P_D P_F^{(C-1)} + P_F P_D^{(C-1)} \right] z^{(CT)} & \zeta = 2 \end{cases} \quad (4.7)$$

and

$$H_4(z) = z^{(JT)} \quad (4.8)$$

Using standard signal flow graph reduction methods and the fact that the I-Q matched filters are similar, the overall generating function can be simplified to

$$H(z) = \frac{H_1(z)}{1 - H_3(z) - H_2(z)H_4(z)} \quad (4.9)$$

It is important to note that $P_D + P_{FA} = 1$ and also it can be verified that $H(1) = 1$.

4.1.1 Mean and Variance of the Acquisition Time

It can be verified that $H(z)|_{z=1} = 1$, and therefore following along the lines of equation. (2.2) and (2.7), chapter 2, the mean and variance of the acquisition time can be expressed as

$$\bar{T}_{ACQ} = \frac{\delta}{\delta z} \ln H(z) \Big|_{z=1} \quad (4.10)$$

$$\sigma_{ACQ}^2 = \frac{\delta^2}{\delta z^2} \ln H(z) + \frac{\delta}{\delta z} \ln H(z) \Big|_{z=1} \quad (4.11)$$

Using straight forward differentiation and some algebra an expression for the mean acquisition time \bar{T}_{ACQ} is give by

$$\bar{T}_{ACQ} = \frac{I_{T_{ACQ}} + II_{T_{ACQ}} + III_{T_{ACQ}} + IV_{T_{ACQ}}}{V_{T_{ACQ}}} \quad (4.12)$$

where,

$$I_{T_{ACQ}} = \left[P_D^\zeta \sum_{i=0}^{C-\zeta} (\zeta + i) \binom{\zeta - 2 + i}{\zeta - 2} P_F^i \right] T \quad (4.13)$$

$$II_{T_{ACQ}} = \left[P_F^\zeta \left[\sum_{i=0}^{C-\zeta} (\zeta + J + i) \binom{\zeta - 2 + i}{\zeta - 2} P_D^i \right] T \right] \quad (4.14)$$

$$III_{T_{ACQ}} = \left[\sum_{i=0}^{\zeta-2} \binom{C-1}{i} P_D^{i+1} P_F^{(C-i-1)} \right] (CT) \quad (4.15)$$

$$IV_{T_{ACQ}} = \left[\sum_{i=0}^{\zeta-2} \binom{C-1}{i} P_F^{i+1} P_D^{(C-i-1)} \right] (CT) \quad (4.16)$$

$$V_{T_{ACQ}} = \left[P_D^\zeta \sum_{i=0}^{C-\zeta} \binom{\zeta - 2 + i}{\zeta - 2} P_F^i \right] \quad (4.17)$$

Similarly the expression for the variance σ_{ACQ}^2 after considerable algebraic simplification can be expressed as

$$\sigma_{ACQ}^2 = I_{\sigma_{ACQ}^2} + II_{\sigma_{ACQ}^2} - III_{\sigma_{ACQ}^2} - IV_{\sigma_{ACQ}^2} + V_{\sigma_{ACQ}^2} \quad (4.18)$$

where the terms $I_{\sigma_{ACQ}^2} - IV_{\sigma_{ACQ}^2}$ do not represent any specific event in particular, but are an outcome of the simplification involved in the process of evaluating an expression for the variance, although the last term $V_{\sigma_{ACQ}^2}$ is the expression for the

mean acquisition time.

$$I_{\sigma_{\lambda C Q}^2} = \left[\frac{\sum_{i=0}^{C-\zeta} (\zeta+i)(\zeta+i-1) \binom{\zeta-2+i}{\zeta-2} P_F^i}{\sum_{i=0}^{C-\zeta} \binom{\zeta-2+i}{\zeta-2} P_F^i} \right] T^2$$

$$II_{\sigma_{\lambda C Q}^2} = \frac{II_A}{II_B} \quad (4.19)$$

$$II_A = (CT) \left[\sum_{i=0}^{\zeta-2} \binom{C-1}{i} P_D^{(i+1)} P_F^{(C-i-1)} + P_F^{(i+1)} P_D^{(C-i-1)} \right] + T P_F^\zeta \left[\sum_{i=0}^{C-\zeta} (\zeta+J+i) \binom{\zeta-2+i}{\zeta-2} P_D^i \right] \quad (4.20)$$

$$II_B = 1 - \sum_{i=0}^{\zeta-2} \binom{C-1}{i} [P_D^{i+1} P_F^{(C-i-1)} + P_F^{(i+1)} P_D^{(C-i-1)}] - P_F^\zeta \left[\sum_{i=0}^{C-\zeta} \binom{\zeta-2+i}{\zeta-2} P_D^i \right] \quad (4.21)$$

$$III_{\sigma_{\lambda C Q}^2} = \left\{ \frac{\sum_{i=0}^{C-\zeta} (\zeta+i) \binom{\zeta-2+i}{\zeta-2} P_F^i}{\sum_{i=0}^{C-\zeta} \binom{\zeta-2+i}{\zeta-2} P_F^i} \right\}^2 T^2 \quad (4.22)$$

$$IV_{\sigma_{\lambda C Q}^2} = \frac{IV_A}{IV_B} \quad (4.23)$$

$$IV_A = \left\{ -C(C-1) \sum_{i=0}^{\zeta-2} \binom{C-1}{i} [P_D^{i+1} P_F^{(C-i-1)} + P_F^{i+1} P_D^{(C-i-1)}] - P_F^\zeta \left[\sum_{i=0}^{C-\zeta} (\zeta+i)(\zeta+i-1) \binom{\zeta-2+i}{\zeta-2} P_D^i \right] \right\} T^2 \quad (4.24)$$

$$IV_B = II_B \quad (4.25)$$

$$V_{\sigma_{ACQ}^2} = \bar{T}_{ACQ} \quad (4.26)$$

It is important to emphasize that the expressions from equations (4.1) to equation (4.26) are important contributions of this thesis to the analytical study of the proposed scheme. The process of deriving these expressions involves the development of a suitable state transition diagram, followed by the detailed enumeration of possible cases leading to a particular event, and in no way is this a non trivial exercise.

4.2 Performance in a Rayleigh Fading Channel

In this section we derive expressions for the probability of detection P_D and probability of false alarm P_{FA} in a Rayleigh fading environment. The assumptions adopted in doing so are,

1. There exists only one sample corresponding to the correct phase.
2. All samples are independent from each other.
3. The length of the subcode is large enough so that the correlation of the received and receiver generated sequence yields zero when they are not in phase.
4. The entire length of the subcode is the uncertainty region.

The transmitted signal is a carrier biphase modulated by a PN sequence and therefore the received signal in the fading channel can be expressed as

$$r(t) = \sum_{k=-\infty}^{+\infty} \sqrt{2}x_k(t) \cos(\omega_0 t + c_k \pi) - \sqrt{2}y_k(t) \sin(\omega_0 t + c_k \pi) + n(t) \quad kT_c \leq t \leq (k+1)T_c \quad (4.27)$$

where $c_k \in \{0, 1\}$, $x_k(t)$ and $y_k(t)$ are independent zero mean stationary gaussian processes with variances,

$$E [x_k^2(t)] = E [y_k^2(t)] = \sigma_s^2. \quad (4.28)$$

The outputs of the I-Q branches of the I-Q matched filters are

$$Z_I = xT_c + N_I \quad (4.29)$$

$$Z_Q = yT_c + N_Q \quad (4.30)$$

where N_I , N_Q , x and y are independent zero mean gaussian random variables. The noise components N_I and N_Q have a variance of σ_n^2 . There are two cases of interest in defining the random variables x and y .

Case 1: Signal present (Hypothesis H_1): Referring to Figure 4.3, x and y are summations of ‘M’ zero mean Gaussian random variables that constitute the vectors (where M represents the length of each of the subcodes),

$$X^t = (x_1, x_2, x_3, \dots, x_M) \quad (4.31)$$

$$Y^t = (y_1, y_2, y_3, \dots, y_M) \quad (4.32)$$

therefore

$$E [x^2 | H_1] = M^2 \sigma_s^2 \quad (4.33)$$

$$E [y^2 | H_1] = M^2 \sigma_s^2 \quad (4.34)$$

Case 2: Signal absent (Hypothesis H_0) In this case the correlation of the received signal and the receiver generated sequence would represent approximately independent zero mean Gaussian random variables and hence x and y are summations of ‘M’ independent identically distributed Gaussian random variables each with variances of σ_s^2 , therefore

$$E [x^2 | H_0] = M \sigma_s^2 \quad (4.35)$$

$$E [y^2 | H_0] = M \sigma_s^2 \quad (4.36)$$

The outputs of the I-Q matched filters therefore follow Gaussian distributions. If $G(\mu, \sigma^2)$ represents a Gaussian distribution with a mean μ and variance σ^2 then,

$$Z_I|H_1 \sim G(0, \sigma_1^2) \quad (4.37)$$

$$Z_Q|H_1 \sim G(0, \sigma_1^2) \quad (4.38)$$

$$Z_I|H_0 \sim G(0, \sigma_0^2) \quad (4.39)$$

$$Z_Q|H_0 \sim G(0, \sigma_0^2) \quad (4.40)$$

where

$$\sigma_1^2 = M^2 \sigma_s^2 + \sigma_n^2 \quad (4.41)$$

$$\sigma_0^2 = M \sigma_s^2 + \sigma_n^2 \quad (4.42)$$

Referring to Figure 4.2, the sample 'W' follows a χ^2 distribution with two degrees of freedom, i.e.,

$$p_w(x|H_j) = \frac{1}{2\sigma_j^2} \exp\left(-\frac{x}{2\sigma_j^2}\right), \quad j = 0, 1 \quad (4.43)$$

Now the detection probability of the search can be expressed as

$$P_D = \int_0^\infty p_w(y|H_1) \left[\int_0^y p_w(x|H_0) dx \right]^{(NM/\Delta-1)} dy \quad (4.44)$$

Substituting equation (4.42) into equation (4.43) we have,

$$P_D = \int_0^\infty \frac{1}{2\sigma_1^2} \exp\left(\frac{-y}{2\sigma_1^2}\right) \left[\int_0^y \frac{1}{2\sigma_0^2} \exp\left(\frac{-x}{2\sigma_0^2}\right) dx \right]^{2NM-1} dy \quad (4.45)$$

where N represents the number of subcodes per Basic code (or the number of matched filters in the bank of filters). Simplifying the above expression we have

$$P_D = \frac{1}{2(1+M\alpha)} \int_0^\infty \exp\left(\frac{-x}{2(1+M\alpha)}\right) \left[1 - \exp\left(\frac{-x}{2(1+\alpha)}\right) \right]^{2NM-1} dx \quad (4.46)$$

where $\alpha = \frac{2\sigma_s^2 T_c}{N_0}$, and represents the SNR/chip, and also $P_D + P_F = 1$.

Performance analysis of the acquisition scheme is performed using numerical integration of equation (4.45) for evaluation of the probability of detection P_D along with the fact that $P_D + P_{FA} = 1$, and substituting these values into equations (4.11)-(4.25) for evaluating the mean and variance of the acquisition time for certain values of the system parameters CLIMIT and normalized threshold ζ .

4.2.1 Numerical Results and Discussion

- Figure 4.5 (page 92) is a plot of the mean acquisition time \bar{T}_{ACQ} as a function of the SNR/chip (in dB) for different values of the subcode lengths $M = 7, 15, 31, 63, 127, 255, 511$ chips, CLIMIT= 6, normalized threshold $\zeta = 3$. The number of subcodes per Basic code is 6. The chip rate of the PN sequence is 10^6 Chips/sec. As is clear from the figure, codes composed of subcodes of lengths $M= 511, 255, 127$ require lower time to be acquired as compared to codes composed of subcodes of length $M=7, 15, 31, 63$ chips. This reflects that larger number of search scenarios are required for the latter case as compared to the former case, and this tends to agree with the fact that more number of errors could occur in the process of detection (on the chip level) for user long codes composed of shorter subcodes as compared to codes composed to longer subcodes. Also it is seen that this difference between the sets of codes exists for high as well as low SNR/chip but the difference is more pronounced for low SNR/chip. In the case of $M=511, 255, 127$ chips the difference in the value of \bar{T}_{ACQ} tends to decrease with higher SNR/chip, and beyond SNR/chip = -12 dB, the curves almost have the same values. A low value of the mean acquisition time would reflect the fact that fewer search scenarios are required to acquire the codes as compared to a higher value.

- Figure 4.6 (page 93) is a plot similar to Figure 4.5 but represents the case for $CLIMIT=6$, $\zeta = 4$. The subcode lengths M shown are 127, 255, and 511 chips. As is observed earlier, the Basic code composed of longer subcodes tends to have a smaller value of the acquisition time at low values of SNR/chip. Also it is clear that for higher values of SNR/chip, the difference in the values of \bar{T}_{ACQ} for all three cases tends to decrease.
- Figure 4.7 (page 94) is a plot of \bar{T}_{ACQ} versus SNR/chip for $CLIMIT=6$, $\zeta = 6$ and $M=127, 255, 511$ chips. As noted earlier the value of \bar{T}_{ACQ} for $M=511$ chips is lower than for $M=127$, and 255 chips for low values of SNR/chip.
- Figure 4.8 (page 95) is a plot of the probability of detection P_D for a subcode versus the SNR/chip. The figure illustrates the fact that a longer subcode has a better probability of detection as compared to a shorter subcode.
- Figure 4.9 (page 96) is a plot of the mean acquisition time \bar{T}_{ACQ} versus the SNR/chip for subcode length $M=127$ chips, normalized threshold $\zeta = 3, 4$, and 6, and $CLIMIT=6$. The number of subcodes per user Basic code remains as 6. As is shown, higher values of the normalized threshold ζ require longer periods of time to be acquired. The tradeoff becomes clear when it is viewed in conjunction with Figure 4.10.
- Figure 4.10 (page 97) is a plot of the overall probability of detection $P_{D-Overall}$ as a function of the SNR/chip for subcode length $M=127$ chips and normalized threshold $\zeta =3, 4$, and 6, $CLIMIT=6$. As is seen, a larger value of the normalized threshold ζ has a higher value of overall probability of detection. Thus the probability of missing a search scenario or declaring a false alarm for higher threshold values is lower as compared to lower threshold values. The tradeoff involved is clear: higher values of ζ (normalized threshold) would have a better performance in terms of the Overall probability of detection $P_{D-Overall}$, but the price paid would be in terms of longer durations of acquisition \bar{T}_{ACQ} .

- Figure 4.11 (page 98) and Figure 4.12 (page 99) are the same set of plots as Figures 4.9 (page 96) and 4.10 (page 97), i.e., the mean acquisition time versus SNR/chip and the overall probability of detection versus SNR/chip, but for the difference that the plots are for the case of subcode length $M = 255$ chips, $CLIMIT=6$, $\zeta = 3, 4, 6$. As before, it is observed that higher values of the normalized threshold ζ , although longer periods of time for declaring acquisition are required, the usual tradeoff of better performance in terms of the overall probability of detection is observed.
- Figure 4.13 (page 100) and Figure 4.14 (page 101) are the final set of plots for mean acquisition time and overall probability of detection versus SNR/chip for subcode length $M=511$ chips, $CLIMIT=6$, $\zeta = 3, 4, 6$.
- Figure 4.15 (page 102) is the plot of the variance σ_{ACQ}^2 of the acquisition time as a function of the SNR/chip for subcode lengths $M= 127, 255, 511$ chips, $CLIMIT=6$, normalized threshold $\zeta = 3$. As is seen from the graphs, the variance of the acquisition time is smaller for the code composed of longer subcodes, and this difference is more marked for low values of the SNR/chip, although this difference remains even for high SNR/chip.
- Figure 4.16 (page 103) is the plot of the variance σ_{ACQ}^2 of the acquisition time as a function of the SNR/chip for subcode lengths $M= 127, 255, 511$, $CLIMIT = 6$, normalized threshold $\zeta = 4$. Again, it is clear that longer subcodes have a better performance as compared to shorter subcodes. One difference between Figures 4.15 and 4.16 is that at high values of SNR/chip, the value of σ_{ACQ}^2 for all the three cases tend to merge at around $-5dB$, and then spread apart, although the marked observation is that they all tend to have almost the same value of σ_{ACQ}^2 for higher SNR/chip.

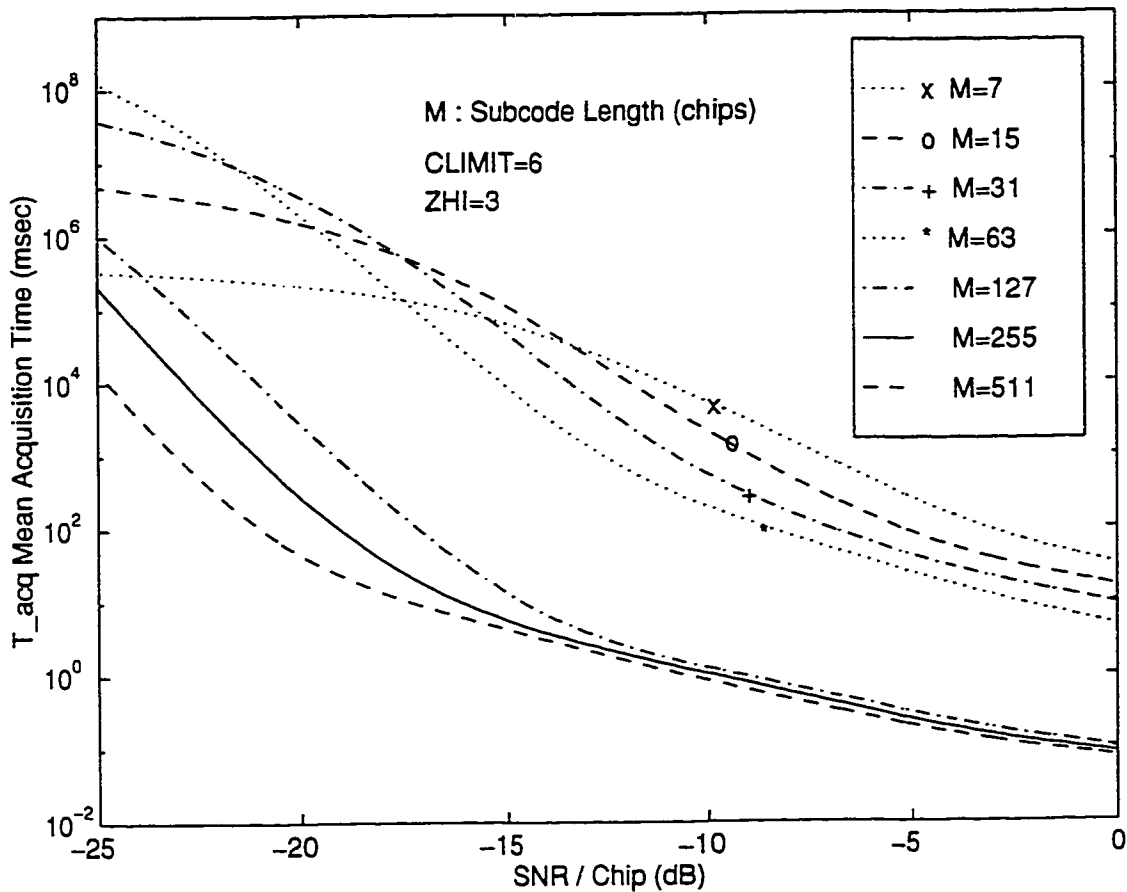


Figure 4.5: Mean Acquisition Time versus SNR/Chip (in dB) in a Rayleigh Fading channel for subcode lengths (M, in chips) 7, 15, 31, 63, 127, 255, 511, Normalized Threshold (ZHI) $\zeta = 3$, $CLIMIT = 6$. The number of subcodes per user Basic code is 6, Chip rate=1Mchips/sec

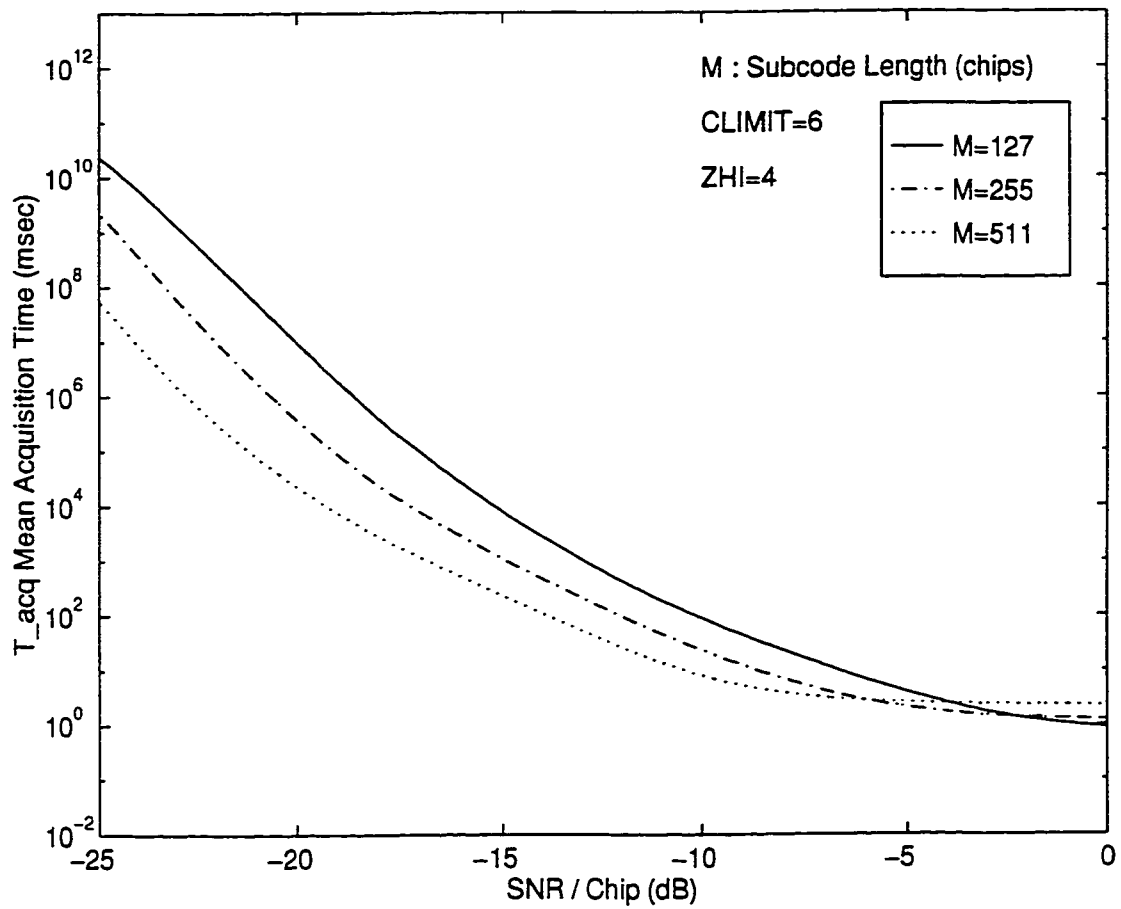


Figure 4.6: Mean Acquisition Time versus SNR/Chip (in dB) in a Rayleigh Fading channel for subcode lengths (M, in chips) 127, 255, 511, Normalized Threshold (ZHI) $\zeta = 4$, *CLIMIT* = 6. The number of subcodes per user Basic code is 6, Chip rate=1Mchips/sec

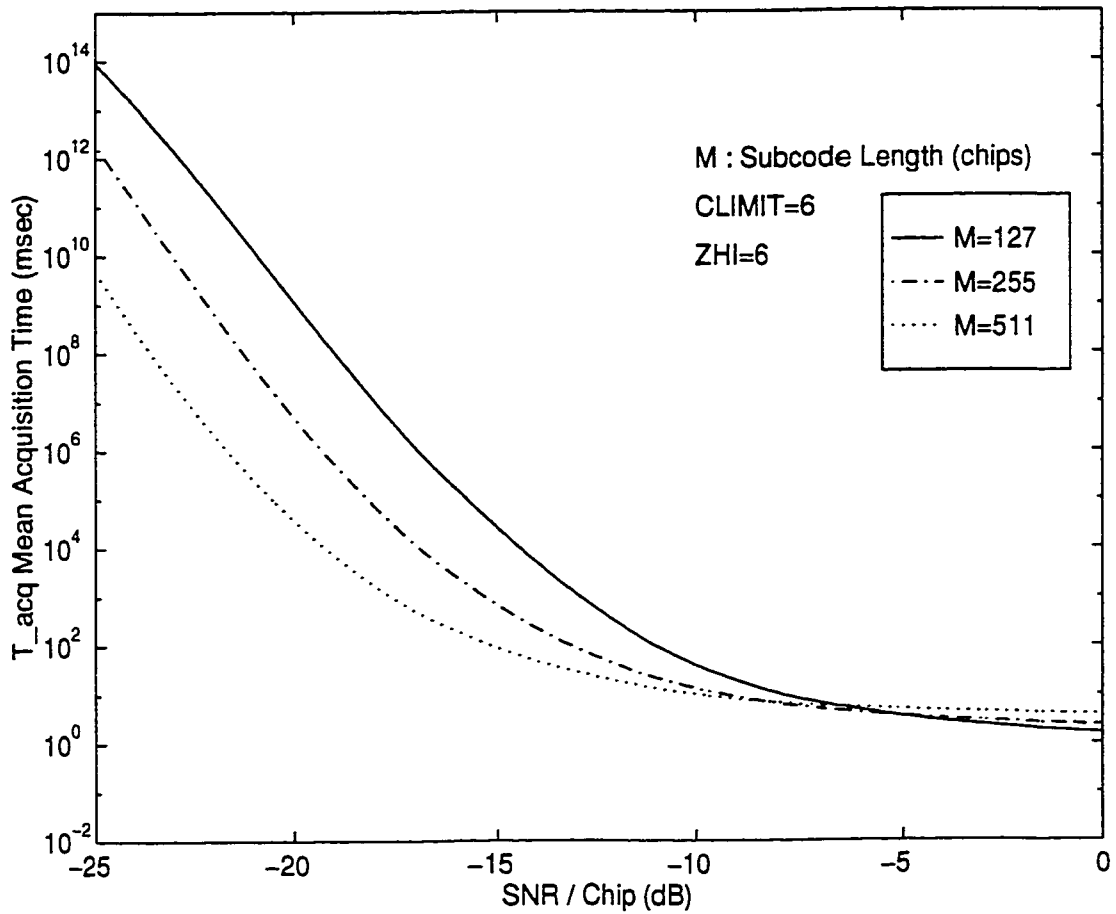


Figure 4.7: Mean Acquisition Time versus SNR/Chip (in dB) in a Rayleigh Fading channel for subcode lengths (M, in chips) 127, 255, 511, Normalized Threshold (ZHI) $\zeta = 6$, *CLIMIT* = 6. The number of subcodes per user Basic code is 6, Chip rate=1Mchips/sec

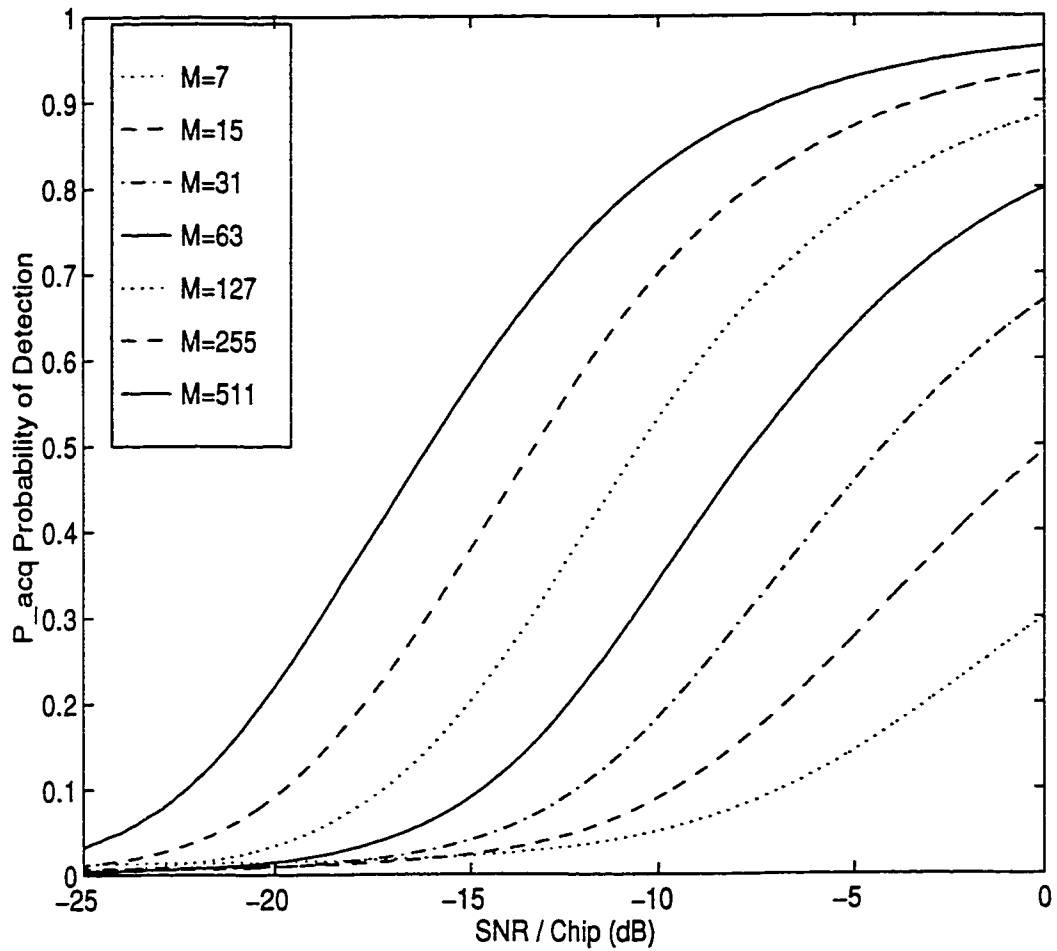


Figure 4.8: Probability of Detection of Subcode versus SNR/Chip (in dB) for Subcode length(in chips) $M=7, 15, 31, 63, 127, 255, 511$. The Chip rate =1M chips/sec.

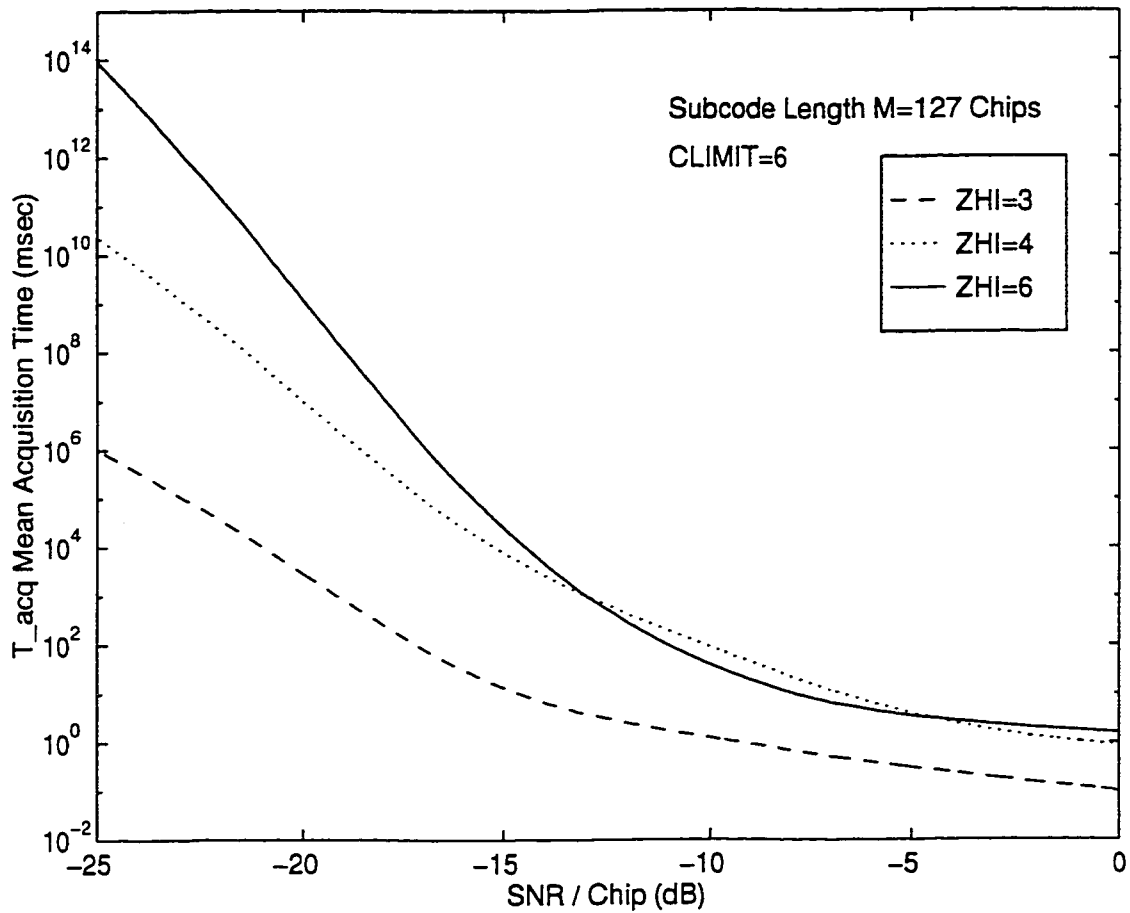


Figure 4.9: Mean Acquisition Time versus SNR/Chip (in dB) in a Rayleigh Fading channel for subcode lengths (M, in chips) 127, Normalized Threshold (ZHI) $\zeta = 3, 4, 6$, $CLIMIT = 6$. The number of subcodes per user Basic code is 6, Chip rate=1Mchips/sec

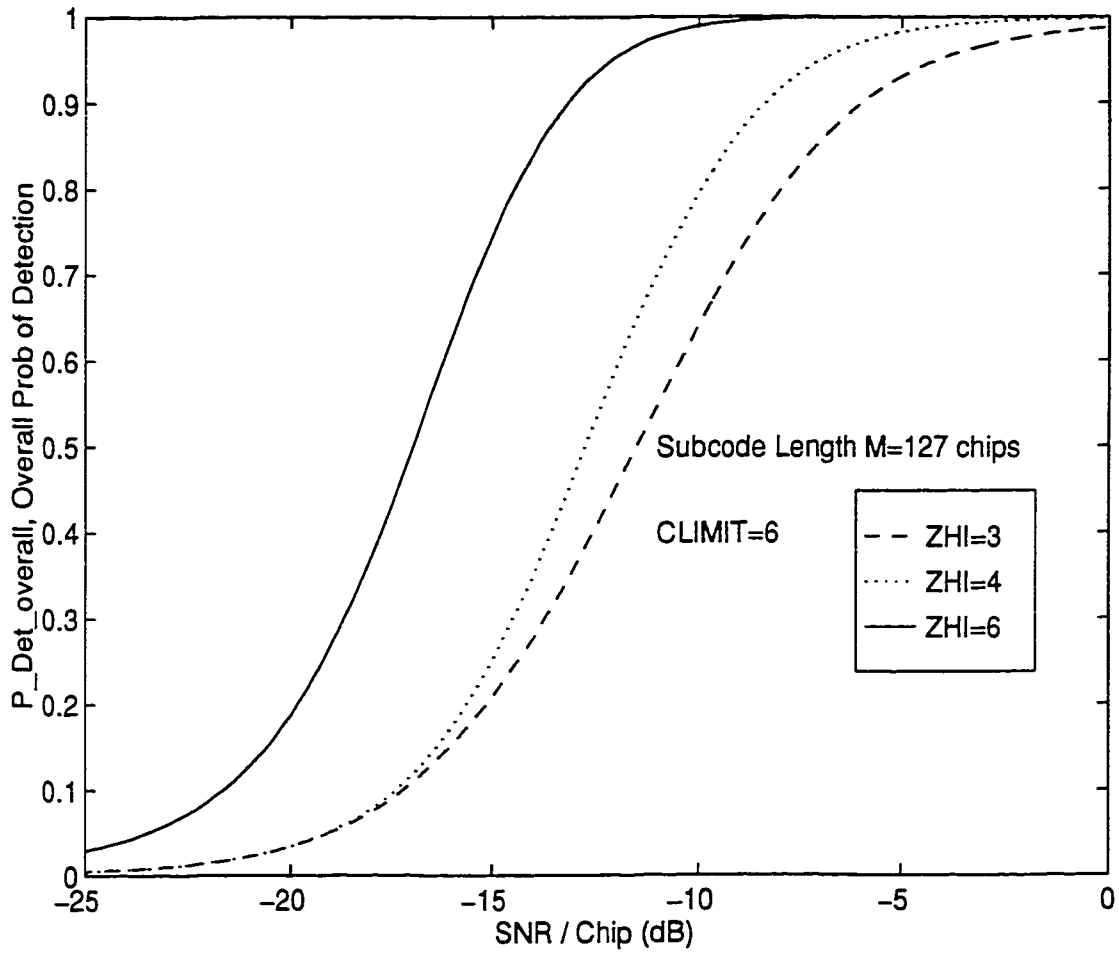


Figure 4.10: Overall Probability of Detection of user code versus SNR/Chip (in dB). The subcode length, $M = 127$ chips, Normalized Threshold $\zeta = 3, 4, 6$, CLIMIT= 6

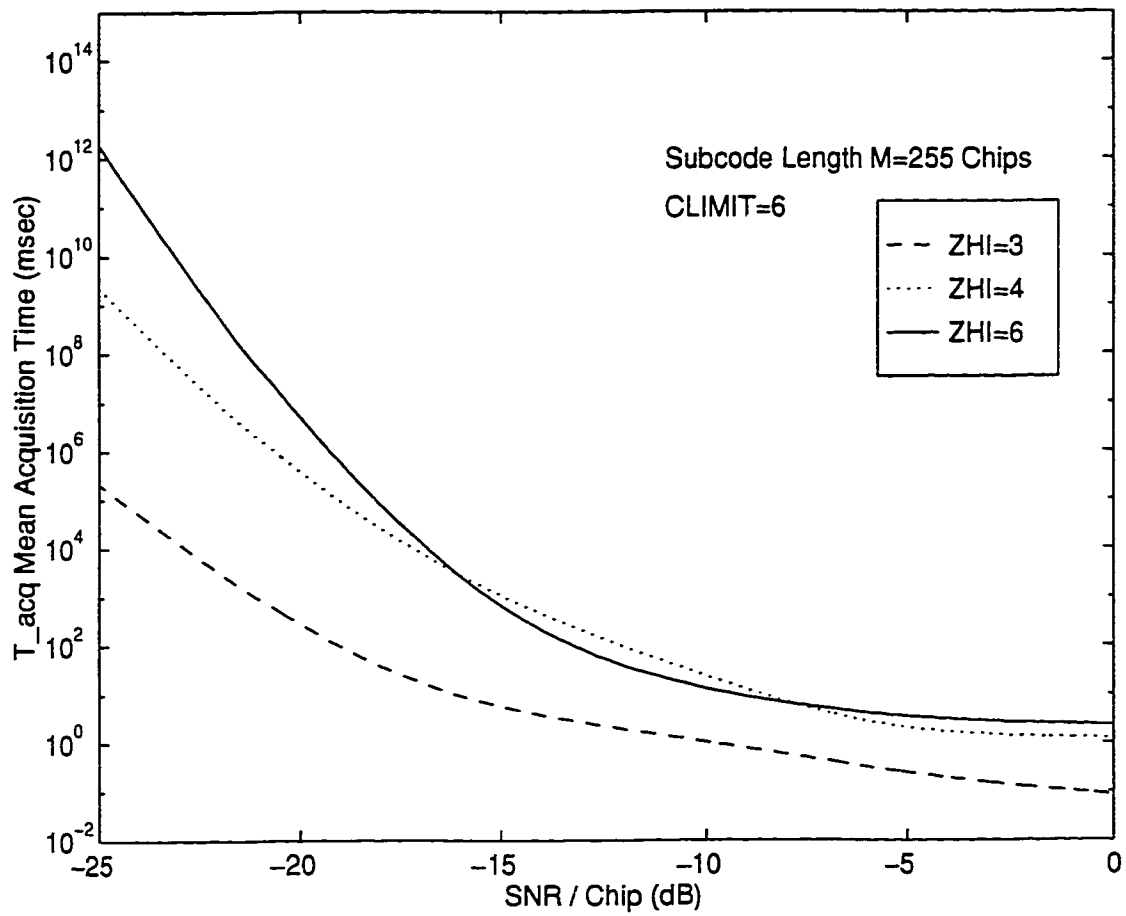


Figure 4.11: Mean Acquisition Time \bar{T}_{ACQ} versus SNR/Chip (in dB) for Normalized Threshold (ZHI) $\zeta = 3, 4, 6$. $CLIMIT = 6$, Subcode length M=255 chips

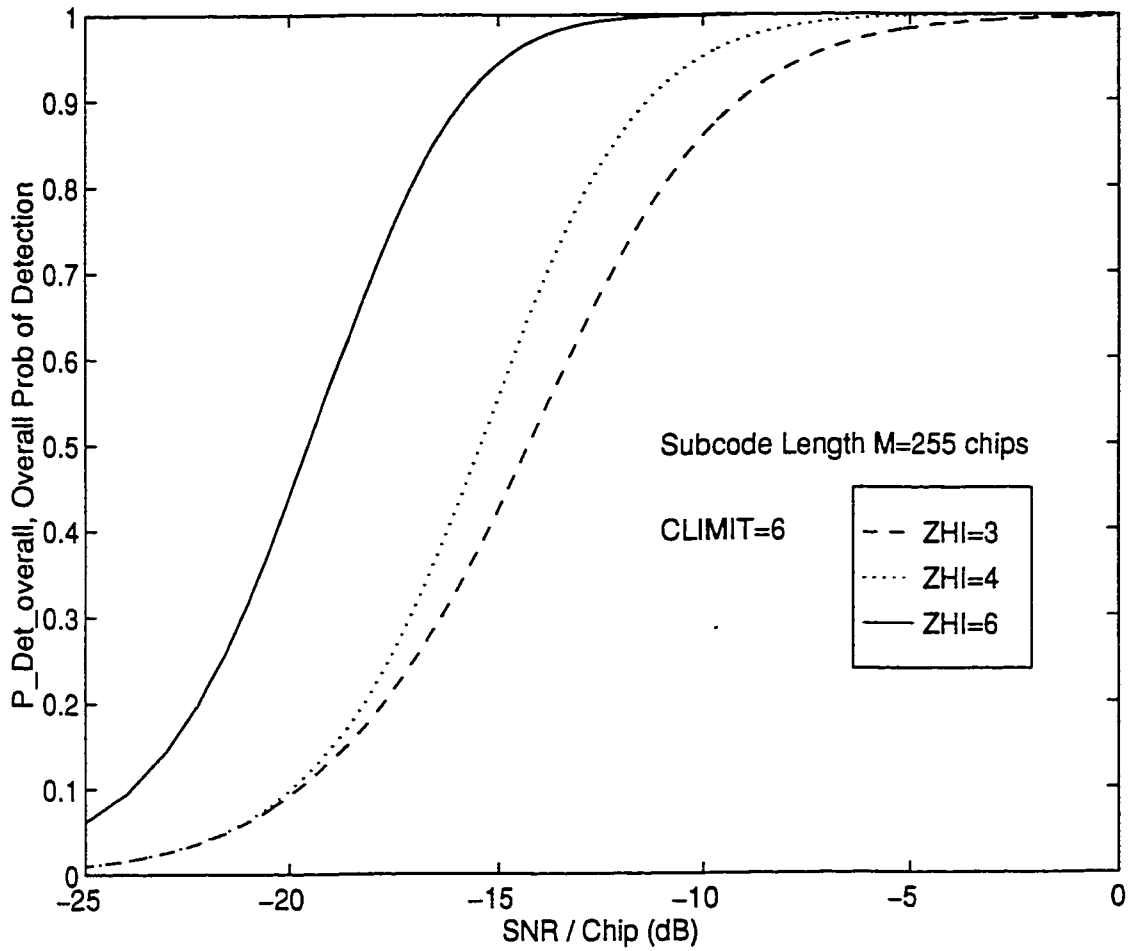


Figure 4.12: Overall Probability of Detection of user code versus SNR/Chip (in dB). The subcode length, $M = 255$ chips, Normalized Threshold $\zeta = 3, 4, 6$, CLIMIT= 6

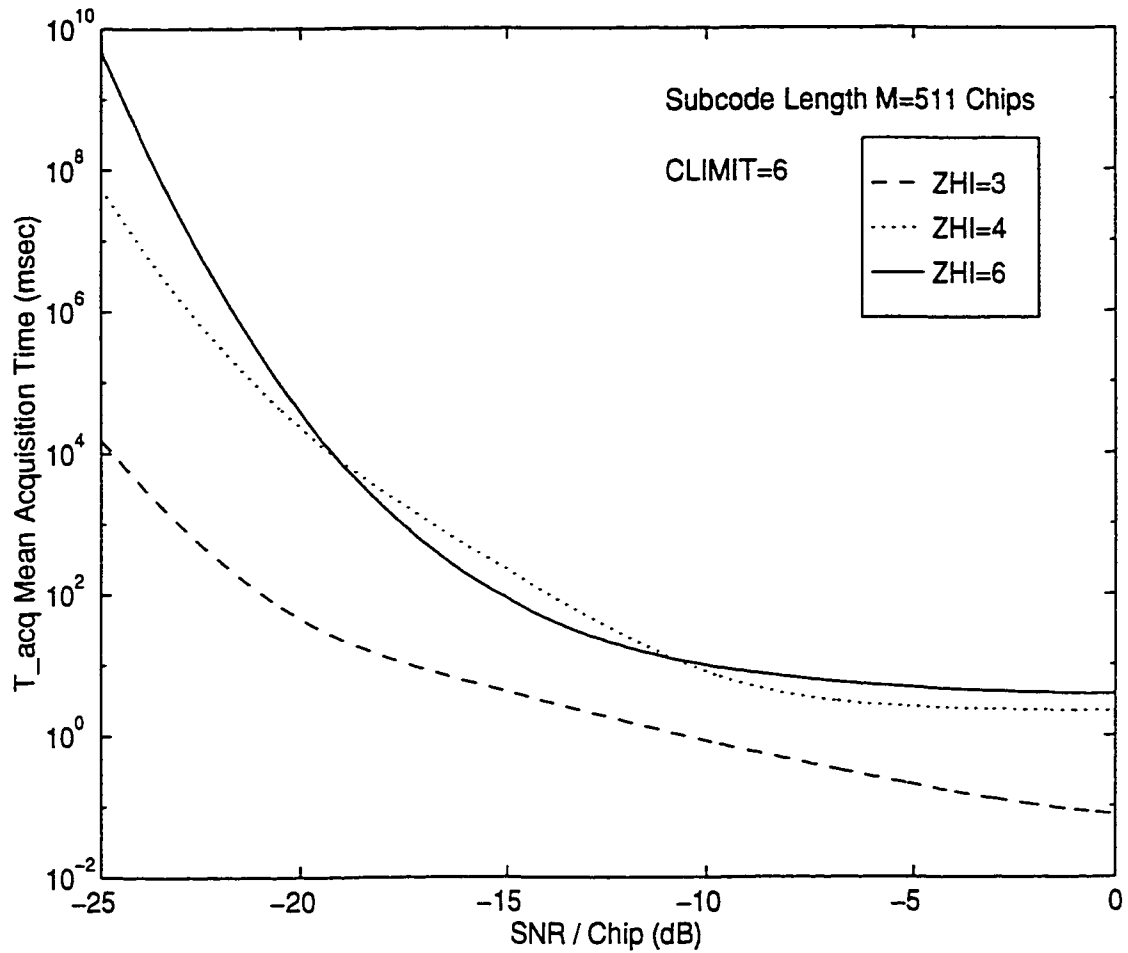


Figure 4.13: Mean Acquisition Time \bar{T}_{ACQ} versus SNR/Chip (in dB) for Normalized Threshold (ZHI) $\zeta = 3, 4, 6$. $CLIMIT = 6$, Subcode length M=511 chips

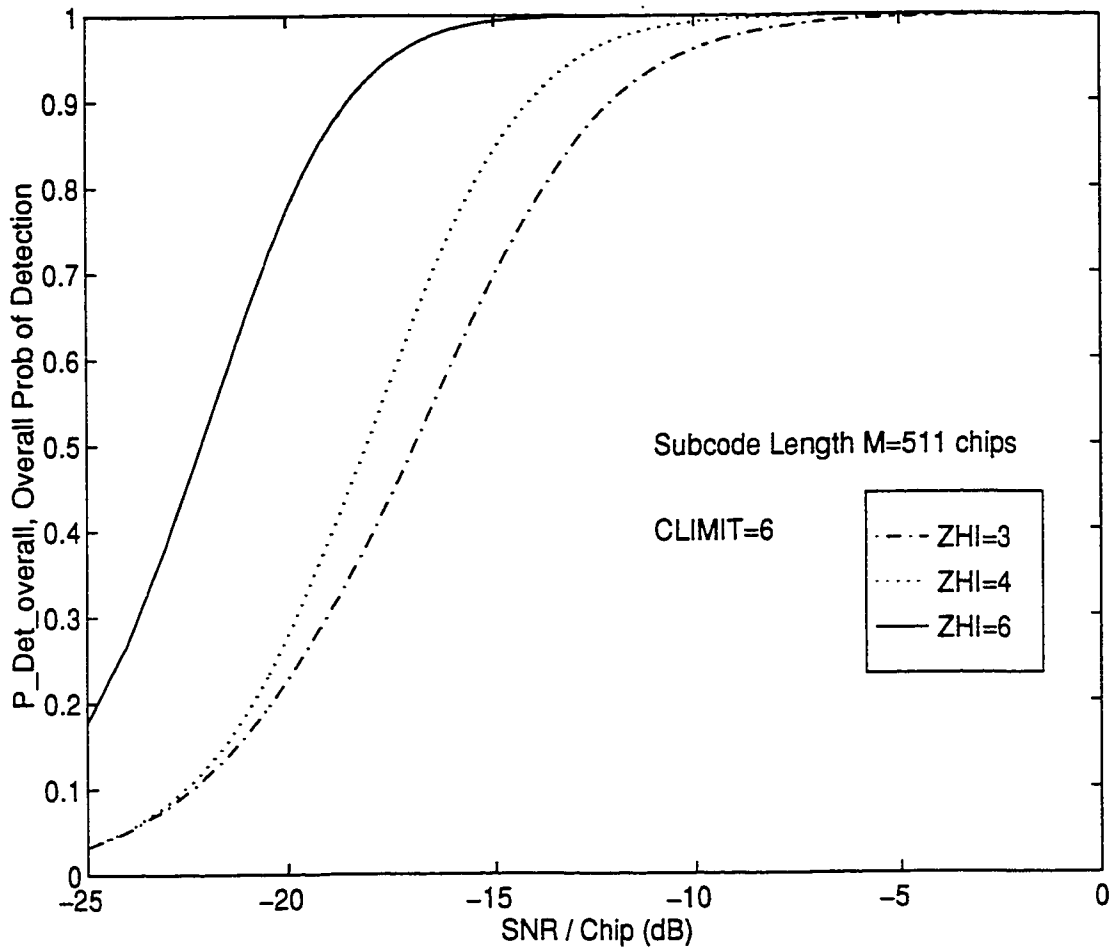


Figure 4.14: Overall Probability of Detection of user code versus SNR/Chip (in dB). The subcode length, $M = 511$ chips, Normalized Threshold $\zeta = 3, 4, 6$, CLIMIT= 6

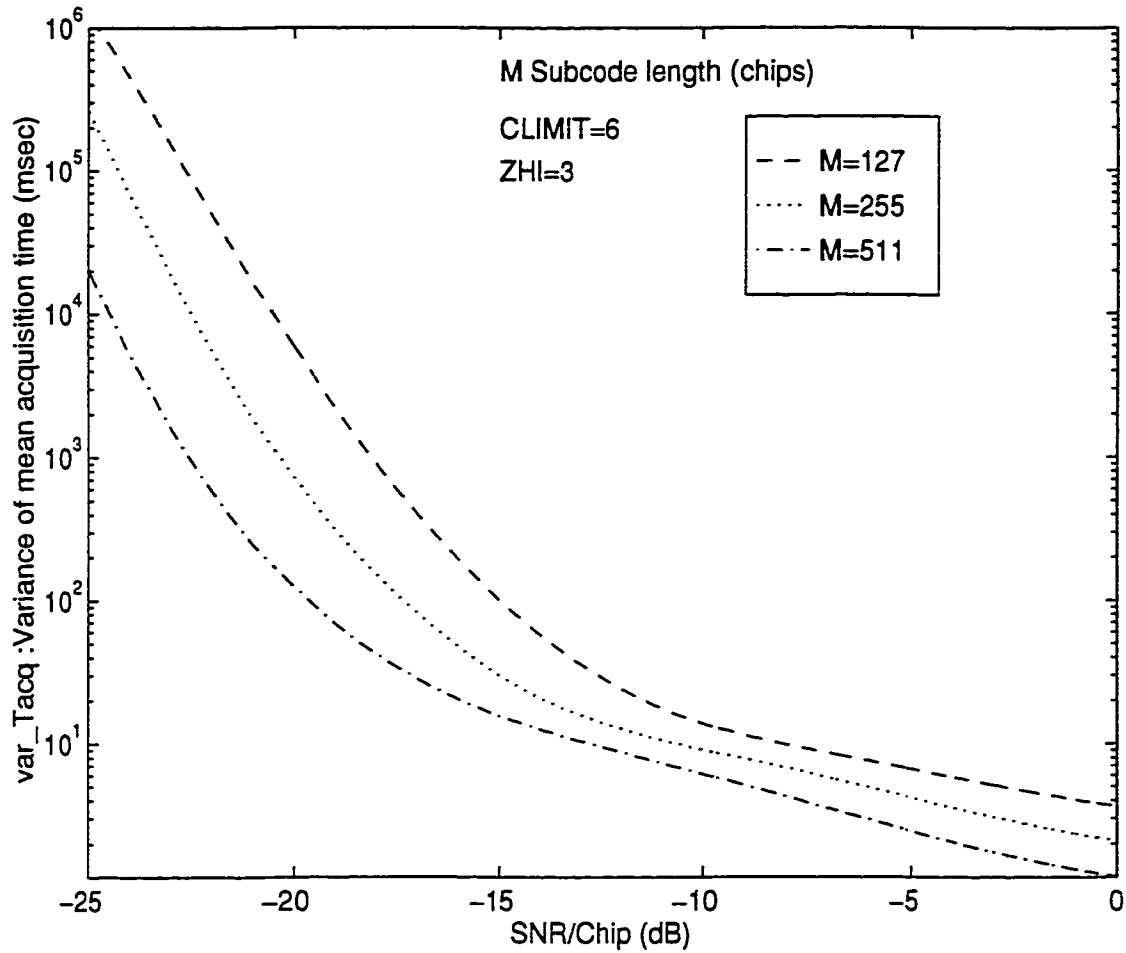


Figure 4.15: σ_{Acq} Variance of the Acquisition Time versus SNR/Chip (in dB) for subcode lengths $M=127, 255, 511$ chips, $CLIMIT = 6$, Normalized Threshold $(ZHI)\zeta = 3$ Chip rate=1M chips/sec.

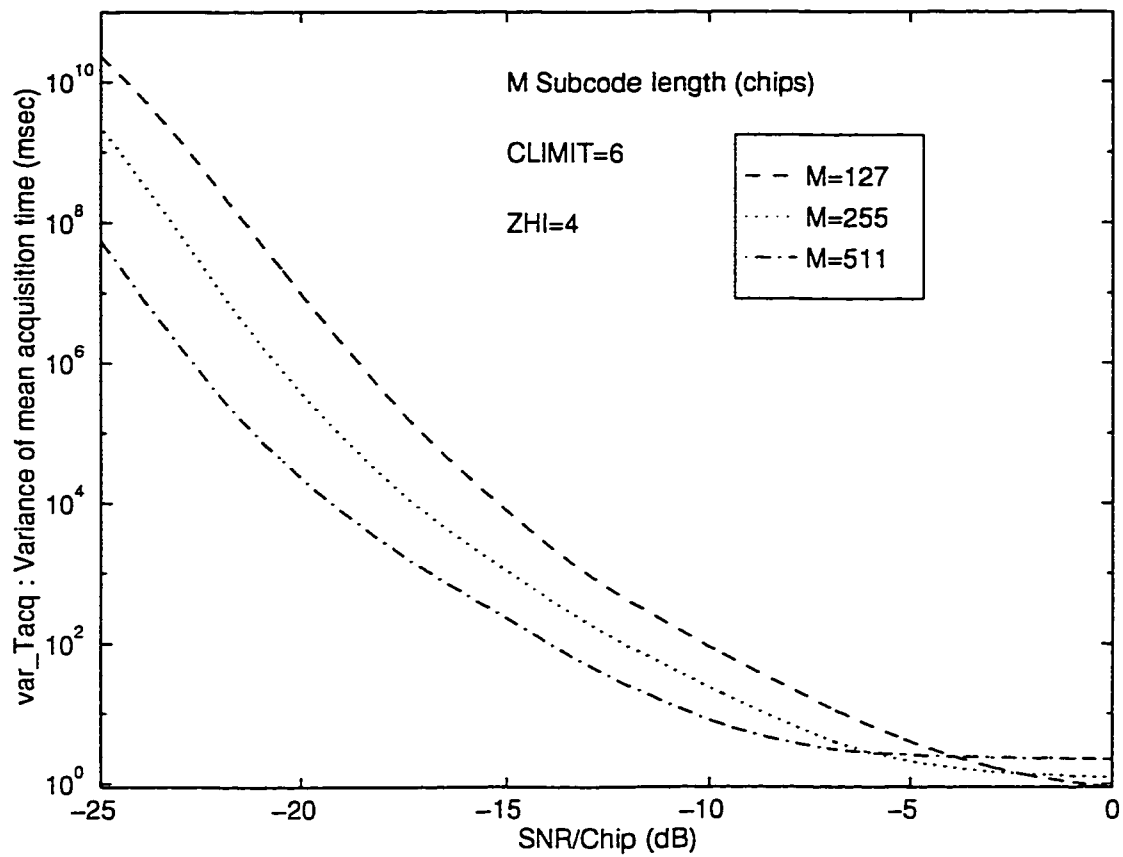


Figure 4.16: σ_{Acq} Variance of the Acquisition Time versus SNR/Chip (in dB) for subcode lengths $M=127, 255, 511$ chips, $CLIMIT = 6$, Normalized Threshold (ZHI) $\zeta = 4$ Chip rate=1M chips/sec.

Chapter 5

Summary and Conclusions

In this chapter we recount the salient features of the New Hybrid Acquisition scheme proposed as a part of the thesis along with the work presented in this thesis.

In chapter 3, we proposed a New Hybrid Acquisition Scheme for CDMA systems using short concatenated codes. A new concatenated coding scheme was introduced. A detailed description of the scheme and its various parameters was presented. The possible steps of the processing of the received signal were illustrated using diagrams. Certain salient aspects of the acquisition scheme were discussed in the end of chapter 3 and a few are recounted here as they reflect certain subtler aspects of the proposed scheme.

Brief summary of the Proposed Scheme

- Unlike conventional acquisition schemes, the proposed scheme is the process of accumulation of sufficient subcodes in sequence with a designated Pivot within a certain search scenario.
- The proposed new technique eliminates the penalty time associated with tracking, the latter being replaced by a sequential logic testing that takes less time and tolerates high multiple access interference.
- The proposed scheme is more robust than conventional acquisition schemes as

acquisition is declared based on a set of independent events. This is further reflected in the fact that upon the declaration of acquisition, the search scenario leading to this may contain a few subcodes that are not in sequence with the pivot.

- It is not necessary that the entire length of the user long code be searched to declare acquisition.

Simulation studies of the proposed scheme were performed in the presence of multiple access interference and additive white gaussian noise (AWGN). Two sets of detection schemes, the Soft decision detection and the Hard decision detection, were used. The scheme was studied for various values of the normalized threshold ζ , CLIMIT=6, and SNR's of 0dB, 4dB and 8dB. The mean acquisition time and overall probability of detection were evaluated as part of the performance evaluation of the scheme.

A set of conclusions based on the simulation studies of the scheme in a multiple access environment are noted here.

- Simulation studies clearly indicate that soft decision detection visibly performs better than the hard decision detection for all cases.
- Simulation studies show that the mean acquisition time tends to increase with an increase in the multiple access interference. This is accompanied with a corresponding decrease in the overall probability of detection.
- An engineering tradeoff was encountered with the observation that although higher values of the normalized threshold have a better performance in terms of the overall probability of detection, longer periods are required for acquiring the user code as compared to lower values of the normalized threshold. Therefore the value of the normalized threshold ζ to be fixed would depend upon the particular application at hand.

A simplified analytical model of the acquisition scheme proposed in chapter 3 was developed in chapter 4. The assumptions of fixed search scenario lengths and equal contributions of the subcodes detected within a search scenario to the accumulator value, although restricting the scope of the acquisition scheme, help make the analysis of the scheme simpler. This simplified scheme was studied in a Rayleigh fading channel. Analytical expressions for the mean (\bar{T}_{ACQ}) and variance (σ_{ACQ}^2) of the acquisition, and the probability of detection P_D were developed using state transition diagrams and standard signal flow reduction methods.

The performance of the scheme is studied for different values of subcode length 'M', threshold values ζ and different values of the SNR/chip. A set of observations made of the performance plots are summarized below.

- In a Rayleigh fading environment, codes composed of longer subcodes tend to have a lower acquisition time as compared to codes composed of shorter subcodes. This reflects the fact that the number of search scenarios required to declare acquisition for codes composed of longer subcodes is less as compared to codes composed of shorter subcodes.
- The difference in the mean acquisition time for subcodes of length 127, 255 and 511 chips tend to decrease at higher values of SNR/chip.
- As before a tradeoff is encountered between the mean acquisition time and the overall probability of detection for different values of the normalized threshold values ζ . Higher values of the normalized threshold ζ , although having a better performance in terms of the overall probability of detection, require longer periods of time to be acquired as compared to lower values of the normalized threshold.
- The variance of the acquisition time tends to decrease with an increase in the SNR/chip for a fixed value of CLIMIT and ζ . Also it was noted that the

difference between the value of σ_{ACQ}^2 for $M= 127, 255, 511$ tends to decrease with increasing SNR/chip.

- As with the mean acquisition time, the variance of the acquisition time also has a lower value for codes composed of longer subcodes.

Suggestions for future work

- Simulation studies of the scheme for different values of the subcode count limit CLIMIT and larger multiple access interference can be performed.
- Development of the analytical model of the acquisition scheme without the two assumptions we have made in our analysis of the model.
- Study of the analytical model of the acquisition scheme in a Rayleigh fading channel and in the presence of multiple access interference.
- Development and implementation of an acquisition scheme with dynamically varying parameters (normalized threshold ζ and subcode count limit CLIMIT). Information about the amount of multiple access interference could be transmitted in the signaling channel to the base station, which in turn could be used to fix the values of ζ and CLIMIT for a particular search scenario.

Bibliography

- [1] A. Salmasi and K. S. Gilhousen, "On the system design aspects of code division multiple access (cdma) applied to digital cellular and personal communications networks," *Proc. IEEE Veh. Technol. Conf.*, vol. 41, pp. 57–62, May 1991.
- [2] A. M. Viterbi and A. J. Viterbi, "Erlang capacity of a power controlled cdma system," *IEEE J. Selected Areas Commun.*, vol. 11, pp. 892–900, August 1993.
- [3] K. S. Gilhousen, I. M. Jacobs, R. Padovani, A. J. Viterbi, and L. A. Weaver, "On the capacity of a cellular cdma system," *IEEE Trans. Veh. Technol.*, vol. 40, pp. 303–312, May 1991.
- [4] Telecommunications Industry Association, Washington D.C, *TIA/EIA/IS-95 Interim Standard, Mobile Station-Base Station Compatibility Standard for Dual Mode Wideband Spread Spectrum Cellular System*, July 1993.
- [5] G. R. Cooper, R. W. Nettleton, and D. P. Grybos, "Cellular land-mobile radio-why spread spectrum ?," *IEEE Commun. Mag.*, vol. 17, pp. 17–24, March 1979.
- [6] A. J. Viterbi, A. M. Viterbi, and E. Zehavi, "Performance of power controlled wideband terrestrial digital communication," *IEEE Trans. Commun.*, vol. 41, pp. 559–569, April 1993.
- [7] J. W. Ketchum, "Down-link capacity of direct sequence cdma for application in cellular systems," *IEEE Symp. Spread Spectrum Tech. Appli.*, pp. 151–157, September 1990.

- [8] L. B. Milstein, J. Gevargiz, and P. K. Das, "Rapid acquisition for direct sequence spread-spectrum communications using parallel saw convolvers," *IEEE Trans. Commun.*, vol. COM-33, pp. 593–599, July 1985.
- [9] U. Cheng, "Performance of a class of parallel spread-spectrum code acquisition schemes in the presence of data modulation," *IEEE Transaction on Communications*, vol. 36, NO.5, pp. 596–604, May 1988.
- [10] V. M. Jovanovic, "On the distribution function of the spread spectrum code acquisition time," *IEEE Journal on Selected Areas in Communications*, vol. 10, NO 4, pp. 760–769, May 1992.
- [11] S. S. Rappaport and D. M. Grieco, "Spread spectrum signal acquisition: Methods and technology," *IEEE Communications Magazine*, vol. 22, NO 6, pp. 6–21, June 1984.
- [12] A. Polydoros and C. L. Weber, "A unified approach to serial search spread-spectrum code acquisition- part i: General theory," *IEEE Transactions on Communications*, vol. COM-32, NO 5, pp. 542–549, May 1984.
- [13] L. D. Davidsson and P. G. Flikkema, "Fast single-element pn acquisition for the TDRSS MA system," *IEEE Transactions on Communications*, vol. COM-36, NO 11, pp. 1226–1234, November 1988.
- [14] A. Weinberg, "Generalized analysis for the evaluation of search strategy effects on pn acquisition performance," *IEEE Transactions on Communications*, vol. COM-31, pp. 37–39, January 1983.
- [15] U. Cheng, W. J. Hurd, and J. I. Stratman, "Spread-spectrum code acquisition in the presence of doppler shift and data modulation," *IEEE Transactions on Communications*, vol. COM-38, pp. 241–250, February 1990.

- [16] S. M. Pan, D. E. Dodds, and S. Kumar, "Acquisition time distribution for spread spectrum receivers," *IEEE J. Selected Areas Commun*, vol. SAC-8, pp. 800–808, June 1990.
- [17] B. B. Ibrahim and A. H. Aghvami, "Direct sequence spread spectrum matched filter acquisition in frequency-selective rayleigh fading channels," *IEEE Journal on Selected Areas in Communications*, vol. 12, NO 5, pp. 885–890, June 1994.
- [18] J. K. Homes and C. C. Chen, "Acquisition time performance of pn spread spectrum systems," *IEEE Trans. Commun*, vol. COM-25, pp. 778–783, August 1977.
- [19] D. M. DiCarlo and C. L. Weber, "Statistical performance of single dwell serial synchronization systems," *IEEE Trans. Commun*, vol. COM-28, pp. 1382–1388, August 1980.
- [20] D. M. DiCarlo and C. L. Weber, "Multiple dwell serial search: Performance and applications to direct sequence code acquisition," *IEEE Trans. Commun*, vol. COM-31, No.5, pp. 650–659, May 1983.
- [21] P. M. Hopkins, "A unified analysis of pseudonoise synchronization by envelope correlation," *IEEE Trans. Commun*, vol. COM-25, pp. 770–777, August 1977.
- [22] R. B. Ward, "Acquisition of pseudonoise signals by sequential estimation," *IEEE Trans. Commun*, vol. COM-13, pp. 475–483, December 1965.
- [23] G. F. Sage, "Serial synchronization of pseudonoise systems," *IEEE Trans. Commun*, vol. COM-12, pp. 123–127, December 1964.
- [24] S. J. Mason, "Feedback theory—some properties of signal flow graphs," *Proc.IRE*, vol. 41, pp. 1144–1156, September 1953.
- [25] S. J. Mason, "Feedback theory—further properties of signal flow graphs," *Proc.IRE*, vol. 44, pp. 920–926, July 1956.

- [26] M. K. Simon, J. K. Omura, R. A. Scholtz, and B. K. Levitt, *Spread Spectrum Communications Handbook*. McGraw-Hill, Inc, 1994.
- [27] W. R. Braun, "Performance analysis for the expanding search pn acquisition algorithm," *IEEE Trans. Commun.*, vol. COM-30, pp. 424–435, March 1982.
- [28] D. V. Sarvate and M. B. Pursley, "Crosscorrelation properties of pseudorandom and related sequences," *Proc. IEEE*, vol. 68, pp. 593–619, May 1980.
- [29] V. Doradla and A. K. Elhakeem, "Hybrid acquisition schemes for cdma systems: A new perspective," Canadian Conference for Electrical and Computer Engineering, CCECE '97, May 1997.
- [30] V. Doradla and A. K. Elhakeem, "A new hybrid acquisition scheme for cdma systems employing short concatenated codes," 7th Virginia Tech/MPRG Symposium on Wireless Personal Communications, June 11-13 1997.
- [31] S. L. Maskara and J. Das, "Concatenated sequences for spread spectrum systems," *IEEE Transactions on Aerospace and Electronic Systems*, vol. Vol.ASE-17, pp. 342–349, May 1981.
- [32] E. Sourour and S. C. Gupta, "Direct sequence spread spectrum parallel acquisition in nonselective and frequency selective rician fading channels," *IEEE Journal on Selected Areas in Communications*, vol. 10, no.3, pp. 535–544, April 1992.
- [33] E. Sourour and S. C. Gupta, "Direct sequence spread spectrum parallel acquisition in a fading mobile channel," *IEEE Transactions on Communications*, vol. 38, no.7, pp. 992–998, July 1990.

Appendix

Here we include the matlab code that was written for the purpose of simulation of the scheme in a multiple access environment.

Program : Pivot test.m

```
% This function tests for whether there are any pivot
% subcodes from the previous tests.(basically the dd==0
% of dd==1 condition)
% y returns the value of dd(either 0 or 1), and x the
% position of the particular subcode.
function [y,x,LPIVT]=pivot_test(z)
for i=1:length(z)
    if z(2,i)==1
        LPIVT=i;
    end
end
for j=1:length(z)
    if z(2,j)==2
        y=1;x=j;
        break
    else
        y=0;
    end
end
end
```

Program: Newtestarea.m

```

%This program is the main program for simulation.
%The program calls many functions which have
%different roles to play.
clear AC AC_MEAN LP1 MAX N_FA N_acq PIVCT SUBCT
clear X c del del1 del2 del3 f i j info pivot_pos
clear pt pt2 tau
N1=3;
N2=4;
tau=0;
X=0;AC=0;SUBCT=0;N_FA=0;N_acq=0;N_miss_det=0;NR=0;
load gcode
load gcode1
load gcode2
j=0;info=[];
global pivot_pos f
f=5;
Thresh=55;c=0;pt2=0;
PIVCT=0;
pivot_pos=[];
while j<N1*N2
for i=1:N1*N2
    [MAX,LP1(1,i)]=gmain(t((i-1)*(2^7-1)+1+tau:i*(2^7-1)+tau));
    z1(1,i)=LP1(1,i);
    z1(2,i)=test2(LP1,i);
    pivot_pos=pivot(z1,i);
    if pivot_pos~=[]
        z1(2,pivot_pos)=2;
    end
end

```

```

z1(2,i)=test3(z1,i,pivot_pos);
z1;
MAX;
PIVCT;
  if MAX>=Thresh
    if z1(2,i)==0
      PIVCT=PIVCT+1;
    else
      c=c+1;
    end
    if PIVCT>CLIMIT
      PIVCT=0;
      X=0;AC=0;c=0;N_acq=0;N_FA=0;
      if f~=5
        f=2;
      else
        f=5;
      end
    end
  end
else
  PIVCT=PIVCT+1;
  if PIVCT>CLIMIT
    PIVCT=0;
    X=0;AC=0;c=0;N_acq=0;N_FA=0;
    if f~=5
      f=2;
    else
      f=5;
    end
  end
end

```

```

        end
    end
end
if (z1(2,i)==1)|(z1(2,i)==2)==1
    X=X+1;
    c=c+2*X;
else
    PIVCT=PIVCT+1;
end
SUBCT=SUBCT+1;
AC=AC+c;
AC_mean=round(AC/SUBCT);
if AC_mean>=zhi
    pt=final_test(z1(1,pivot_pos),pivot_pos);
    if pt==1
        if (z1(2,i)==1|z1(2,i)==2)==1
            N_acq=N_acq+1;
        else
            N_FA=N_FA+1;
        end
    elseif pt==0
        N_FA=N_FA+1;
    end
end
end
i;
j=j+1;
info(1,i)=AC_mean;
info(2,i)=N_acq;

```

```

info(3,i)=N_FA;
if ((info(1,i)>=zhi)&(pt==1))==1
    pt2=1;
    break
end %end of the if condition
end %end of the i loop.
if pt2==1
    break
end %end of the if condition
end %end of the j while loop.
z1
info;

```

Program :Pivot search function

```

%The function evaluates the value of f and decides what
% has to be done.
%f=3:Retain the previous pivot.
%f=5:didn't find a pivot yet.
%f=2:search for a new pivot from latest detected subcode.
%f=1:search for a pivot from the beginning.
function w=pivot_search(y,i)
global pivot_pos f
y;
f;
if f~=3
    if f~=5
        if f==0
            w=1;

```

```

    f=3;
    pivot_pos=1;
    y(2,i)=2;
end
if f==2
    for j=length(y):-1:1
        a=(y(1,j)==1)|(y(1,j)==2)|(y(1,j)==3)|(y(1,j)==4);
        if a==1
            break
        end
    end
    pivot_code=y(1,j);
    w=j;
    f=3;
    pivot_pos=j;
    y(2,i)=2;
end
if f==1
    for k=1:length(y)
        if ((y(1,k)==1)|(y(1,k)==2)|(y(1,k)==3)|(y(1,k)==4))==1
            break
        end
    end
    pivot_code=y(1,k);
    w=k;
    f=3;
    pivot_pos=k;
    y(2,i)=2;

```



```

        end
    elseif y(2,i)==1
        w=i;
        pivot_pos=i;
        y(2,i)=2;
        f=3;
    % end
    else
        break
    end
end
end
else
    w=pivot_pos;
end

```

Program : Pivot test function

```

function z1=pivottest(y,i)
%z(1,i)=y(1,i);
if ((y(1,i)==1)|(y(1,i)==2)|(y(1,i)==3)|(y(1,i)==4))==1
    if i==1
        z(1,i)=y(1,i);
        z(2,i)=2;
        z1=[z(1,i);2];
        pivot_pos=1
    end
end

if(i~=1)

```

```

for k=1:length(y)
    if ((y(1,k)==1)|(y(1,k)==2)|(y(1,k)==3)|(y(1,k)==4))==1
        break
    end
end
pivot_code=y(1,k);
pivot_pos=k
z(1,k)=y(1,k)
z(2,k)=2;
z1=[z(1,i);2]
end
if (y(2,i)==0)|(y(2,i)==1)==1
    z(1,i)=y(1,i);
z(2,i)=y(2,i);
z1=[z(1,i);z(2,i)]
end

```

Program :Sequential subcode detection

```

function y=pos_seq_det(x)
%This function returns the right sequential subcode
%position that would be required to decide.
%function takes as the input a number which is the
% pivot code position%returns a vector with the right
% positional sequence .
global pivot_pos f ;
pos_seq_matrix=[1 2 3 4];
d=x;
if x==1;

```

```

y=pos_seq_matrix;
else
y=[pos_seq_matrix(:,4-d+2:4),pos_seq_matrix(:,1:4-d+1)];
end

```

Program : Reassign Pivot Code

```

%this function reassigns the pivot code to the latest
% subcode we could also assign the pivot position to the
% correct subcode closest to the old pivot subcode.

```

```

function y=reassign_pivot_code(x)
global pivot_pos;
for i=1:length(x)
    if x(2,i)==-1
        break
    end
end
y=i;

```

Program : Sequential test function

```

% The function returns a matrix z with the second row
% of z indication whether the subcode detected is a
% pivotsubcode,correct sequential subcode or
% a subcode not belonging to the particular user.

```

```

function z=seq_test(x,i)
N2=4; %The number of subcodes in each code.
flag=0;
%z=□;

```

```

if((x(1,i)==1)|(x(1,i)==2)|(x(1,i)==3)|(x(1,i)==4))==0
    z(1,i)=x(1,i);
    z(2,i)=0;
end
if((x(1,i)==1)|(x(1,i)==2)|(x(1,i)==3)|(x(1,i)==4))==1
    for k=1:length(x)-1
        if((x(1,k)==1)|(x(1,k)==2)|(x(1,k)==3)|(x(1,k)==4))==1
            flag=1;
            break
        end
    end
    if flag==1
        z(1,i)=x(1,i);
        z(2,i)=1;
    else
        z(1,i)=x(1,i);
        z(2,i)=2;
    end
end
end
for l=1:length(z)
    if z(2,l)==2
        break
    end
    pivot_pos=l;
end
if rem((i-pivot_pos),N2)==0
    if z(1,i)==4;
        z(2,i)=1;
    end
end

```

```

else
    z(2,i)=0;
end
elseif rem((i-pivot_pos),N2)==1
    if x==1;
        z(2,i)=1;
    else
        z(2,i)=0;
    end
elseif rem((i-pivot_pos),N2)==2
    if z(1,i)==2
        z(2,i)=1;
    else
        z(2,i)=0;
    end
elseif rem((i-pivot_pos),N2)==3
    if z(1,i)==3
        z(2,i)=1;
    else
        z(2,i)=0;
    end
end
end

```

Program : Sequential test function

```

% The function takes as input a vector and returns a matrix
% the second row of the matrix gives information of the
% codes their position etc
function z=test2(y,i)

```

```

global pivot_pos f;
    if ((y(1,i)==1)|(y(1,i)==2)|(y(1,i)==3)|(y(1,i)==4))==0
        z=0;
    else
    if ((y(1,i)==1)|(y(1,i)==2)|(y(1,i)==3)|(y(1,i)==4))==1
        if i==1
            z=2;
            pivot_pos=1;
            f=0;
        elseif (f==5)  %|(f==2)|(f==3))==1
            z=1;
            % f=1;
        elseif f==2
            z=1;
        elseif f==3
            z=1;
        end
    end
end
end

```

Program : Test3.m

```

function z=test3(y,i,p)
global pivot_pos f ;
N2=4;
pivot_pos=p;
if y(2,i)==0
    z=0;
else

```

```

q=pos_seq_det(y(1,pivot_pos));
if ((pivot_pos==1)&(i==1))==0
  for j=pivot_pos:length(y)
    if j==pivot_pos
      z=2;
    elseif (rem(j-pivot_pos,N2)+1)==q(1)
      if y(1,j)==1;
        z=1;
      elseif((y(1,j)==2)|(y(1,j)==3)|(y(1,j)==4))==1
        z=-1;
      else
        z=0;
      end
    elseif (rem(j-pivot_pos,N2)+1)==q(2)
      if y(1,j)==2;
        z=1;
      elseif((y(1,j)==1)|(y(1,j)==3)|(y(1,j)==4))==1
        z=-1;
      else
        z=0;
      end
    elseif (rem(j-pivot_pos,N2)+1)==q(3)
      if y(1,j)==3
        z=1;
      elseif((y(1,j)==1)|(y(1,j)==2)|(y(1,j)==4))==1
        z=-1;
      else
        z=0;
      end
    end
  end
end

```

```

        end
    elseif (rem(j-pivot_pos,N2)+1)==q(4)
        if y(1,j)==4
            z=1;
        elseif((y(1,j)==1)|(y(1,j)==2)|(y(1,j)==3))==1
            z=-1;
        else
            z=0;
        end
    end
end
end
end
else
    z=2;
end
end
end

```

Program : Transmitter

```

function z=trans()
load gcode
load gcode1
load gcode2
t1=[g1 g2 g3 g4];
y=[t1 t1 t1 ];
z=[y y y y y y y y y y];

```

Program : Multiple access Interference

%The function receives the no of users and generates


```

random multiple access interference.
function z=multiaccess(x)
load gold_code
no_of_users=x;
rand('seed',sum(100*clock))
y1(1,:)=[1 2 3 4];
for i=2:no_of_users
    y1(i,:)=[round(50*rand(1,4))];
    y1(i,:)=check1(y1(i,:));
end
y=y1;
z1=check2(y);
[m,n]=size(z1);
for j=1:m
    z2(j,:)=[g(z1(j,1),:) g(z1(j,2),:) g(z1(j,3),:) g(z1(j,4),:)]];
    z3(j,:)=[z2(j,:) z2(j,:) z2(j,:)];
end
z=zeros(1,1524);
for k=1:m
    temp=z3(k,:);
    z=z+temp;
end

```

Program : Receiver with Bank of filters

```

% The function receives the signal and feeds it into bank
% of matched filters.
function [t1,t2]=gmain(z)
global gmax;

```

```

gmax=[];
thres=63.5;
randn('seed',sum(100*clock))
n=2*randn(1,127);
r=n+z;
for i=1:127
    if r(i)>0
        r(i)=1;
    else
        r(i)=-1;
    end
end
gmfil1(r);
gmfil2(r);
gmfil3(r);
gmfil4(r);
gmfil5(r);
gmfil6(r);
gmax;
fil_no=0;
max_fil_val=0;
for i=1:length(gmax)
    temp=gmax(i);
    if temp > max_fil_val
        max_fil_val=temp;
        fil_no=i;
    end
end
end

```

```

t1=max_fil_val;
t2=fil_no;
%if max_fil_val>thres
% Max_filter_value=t1
% Filtegmairn_No=t2
%end

```

Program :Funtion returns gold code of 127 chips

```

%gold.m%
function gc=gold(d)
%the function returns a gold code of length 127 chips.
load out
c1=out1;
c2=delay(d,out2);
z=xor(c1,c2);
gc=con(z);

```

Program :Example of a matched filter matched to a gold code of 127 chips

```

function max1=gmfilt1(r)
%matched filter
global gmax;
%clear gmax
gout1=
[ 1  -1  -1  -1  -1  -1   1   1   1   1  -1   1 ...
 -1   1   1  -1  -1  -1   1  -1  -1  -1  -1   1 ...
 -1  -1   1  -1   1  -1  -1  -1  -1   1   1   1 ...
  1   1  -1  -1  -1  -1   1  -1   1   1  -1   1 ...

```

```

-1 -1 -1 -1 -1 1 -1 -1 -1 1 1 -1 ...
 1 -1 -1 -1 -1 -1 1 1 1 1 1 1 ...
-1 -1 1 -1 1 -1 -1 1 1 -1 -1 1 ...
 1 -1 -1 -1 1 -1 1 -1 -1 1 -1 -1 ...
-1 1 -1 1 1 -1 -1 -1 1 -1 1 1 ...
 1 -1 1 -1 1 1 -1 -1 -1 1 1 -1 ...
 1 1 -1 1 -1 -1 1];

c=gout1;
a=zeros(127);
for m=length(c):-1:1
a(m,:)=[c(:,127-m+1:127),c(:,1:127-m)];
end
a;
thres=63.5;
%randn('seed',sum(100*clock));
%n=randn(1,127);
%r=n+z
%for i=1:127
% if r(i)>0
% r(i)=1;
% else
% r(i)=-1;
% end
%end
r1=r';
y1=zeros(1,127);
max=0;
max_ind=0;

```

```

for n=1:127
y1(n)=(a(n,:)*r1);
temp(n)=y1(n);
if temp(n)>max
    max=temp(n);
    max_ind=n;
end
end
y1;
max;
max_ind;
%if max>thres
    y2=a(max_ind,:);
    max1=max;
    gmax(1)=max1;
%end

```

Program : Hard Decision on each bit

```

function r=noise(z)
%function adds noise to the transmitted signal and makes a hard decision bit
% wise.
randn('seed',sum(100*clock));
n=randn(1,127);
r=n+z;
for i=1:127
    if r(i)>0
        r(i)=1;
    else

```

```
    r(i)=-1;
end
end
```

Program : Crosscorrelation function

```
function y=crosscorr(x1,x2)
%function evaluates the crosscorrelation of two codes that are input.

for i=1:length(x1)
% if (x1==x2)
    y(:,i)=delay(i,x1)*x2';
%end
end
```
